



UNIVERSITÀ  
DI SIENA  
1240

**UNIVERSITY OF SIENA**

DEPARTMENT OF MEDICAL BIOTECHNOLOGIES

**PhD COURSE IN MEDICAL BIOTECHNOLOGIES**

COORDINATOR: PROF. LORENZO LEONCINI

*XXXV CYCLE*

**Physicochemical and antigenic properties correlation in *Streptococcus gordonii* vaccine vectors and development of a *Streptococcus pneumoniae* intra-tracheal mouse model of pneumonia**

**Supervisor:**

Prof. Gianni Pozzi

**Co-supervisor:**

Prof. Francesco Iannelli

**PhD candidate:**

Samaneh Gholami

**Academic year 2021–2022**

# Table of Content

<b>ABSTRACT</b> .....	<b>3</b>
<b>Aim of the thesis</b> .....	<b>4</b>
<b>CHAPTER 1 Isoelectric of bacterial cells</b> .....	<b>5</b>
<b>Introduction</b> .....	<b>6</b>
DLVO theory to explain bacterial interaction .....	8
Surface charge of gram-positive and gram-negative bacteria .....	8
<b>Methods of Isoelectric point calculation in bacteria</b> .....	<b>11</b>
Differential staining.....	11
Cross-partitioning in dextran-polyethylene glycol two-phase .....	11
Electrophoretic mobility .....	12
Isoelectric focusing (IEF) .....	14
Capillary isoelectric focusing (CIEF) .....	14
Electrophoretic light scattering (ELS).....	15
<b>Application of bacterial isoelectric point</b> .....	<b>17</b>
Study of bacterial adhesion .....	17
Study of bacterial biofilm .....	18
Study of the influence of different methods of inactivation on bacterial surface .....	18
Using pI to control mechanisms of cell surface electric potential.....	19
Using pI to separate inclusion bodies of recombinant protein from host .....	20
Study of bacterial interaction with metals .....	20
Using pI to measure antibiotic activity on bacteria .....	20
Using pI to separate bacteria from complex medium .....	21
<b>Conclusion</b> .....	<b>28</b>
<b>CHAPTER 2 Correlation between bacterial surface charge (Zeta Potential) and the antigenicity and immunogenicity properties in recombinant Streptococcus gordonii vaccine vectors</b> .....	<b>35</b>
<b>CHAPTER 3 The human pathogen Streptococcus pneumoniae</b> .....	<b>66</b>
<b>Introduction</b> .....	<b>67</b>
<b>Pneumococcal virulence factors</b> .....	<b>68</b>
<b>Immunity</b> .....	<b>69</b>
<b>Prevention and vaccination</b> .....	<b>71</b>
<b>Research objective</b> .....	<b>71</b>
<b>Bibliography</b> .....	<b>73</b>
<b>CHAPTER 4 Immune memory after respiratory infection with Streptococcus pneumoniae is revealed by in vitro stimulation of murine splenocytes with inactivated pneumococcal whole cells: evidence of early recall responses by transcriptomic analysis</b> .....	<b>78</b>
<b>CHAPTER 5 Development of a Streptococcus pneumoniae, mouse model of pneumonia by intra-tracheal infection</b> .....	<b>93</b>
<b>CHAPTER 6. Conclusions</b> .....	<b>118</b>
<b>APPENDIX. Scientific Curriculum Vitae</b> .....	<b>120</b>

## ABSTRACT

In the present thesis, the correlation between the physicochemical and antigenic properties of different recombinant *Streptococcus gordonii* vaccine vectors was studied. Evaluation of vaccine efficacy, antigenicity and immunogenicity is a crucial step in developing vaccines, thus investigating a simple method to analyze vaccine efficacy besides other methods could be a major part of developing bacterial vaccine vectors. To approach this, isoelectric point measurements and zeta-potential titration as well as antigenicity and immunogenicity of *S.gordonii* vaccine vectors (with *fbpA*, *RPS*, *gtfg* genes mutations expressing H1 antigen) were used. These data showed that strains with more positive surface charge had higher heterologous antigen recognition and lower antibody responses in the serum of immunized mice. This correlation between surface charge and antigenicity and immunogenicity revealed the importance of using simple methods such as zeta potential titration and isoelectric point measurements to predict engineered vaccine vectors antigenicity and possible efficacy. In the second part of the thesis the immune recall in the days following *Streptococcus pneumoniae* lung infection by transcriptomic analysis was studied. *S. pneumoniae* is the most common bacterial cause of community-acquired pneumonia. Host-pathogen interaction is poorly understood, and factors that drive a more severe phenotype are unknown. One way to study host response to pathogen is using the stimulation of immune system cells with live or killed bacteria. We combined transcriptomic and cytokine level analysis on stimulated mouse splenocytes revealing the presence of a recall immune response involving both innate and adaptive immunity, stronger from the fourth day after infection. This model could analyze immune responses involved in pneumococcal infection as well as vaccine and experimental therapies efficacy in future studies. Finally, the development of a *S. pneumoniae* mouse model of pneumonia by intra-tracheal infection was set up. The nasopharynx of humans is the only natural reservoir for the pneumococci. To mimic human pneumonia, mice models are widely used. Bacteria can be administered to mice intranasally, intratracheally or as aerosols. Pneumococcal pneumonia was induced in mice by intra-tracheal inoculation with different doses of *S. pneumoniae* TIGR4. Data showed high colonization of bacteria in lung, liver and spleen starting 24 hours post-infection. Pneumonia mortalities were observed in all mice infected by  $10^8$  within 24 hours of infection. Further analysis should be done to investigate the host-pathogen interaction as well as vaccine and experimental therapies efficacy by using this model.

## **Aim of the thesis**

The aim of this thesis was to study i) the correlation between the physicochemical and antigenic properties of recombinant *Streptococcus gordonii* vaccine vectors, ii) the immune recall after *Streptococcus pneumoniae* lung infection by transcriptomic analysis, and iii) the development of an *S. pneumoniae* intra-tracheal mouse model of pneumonia. Chapter 1 is a review of the methods of calculation of isoelectric point in bacteria and its applications and it is meant to be an introduction. In Chapter 2 the correlation between the surface charge and the antigenic properties of recombinant *Streptococcus gordonii* vaccine vectors was reported. Chapter 3 is a brief introduction on the human pathogen *Streptococcus pneumoniae*. In Chapter 4, murine splenocytes collected after respiratory infection of mice were used to analyze the recall immune response using a transcriptomic approach. Finally, the development of a mouse model of pneumonia by *Streptococcus pneumoniae* intra-tracheal administration is reported in Chapter 5.

# CHAPTER 1

## Isoelectric point of bacterial cells

Samaneh Gholami, Francesco Iannelli, Antonio Vivi, and Gianni Pozzi

*Laboratory of Molecular Microbiology and Biotechnology, Department of Medical Biotechnologies,  
University of Siena, 53100 Siena, Italy*

Manuscript in preparation

## Introduction

Bacterial surface physicochemical properties such as isoelectric point (pI), charge and hydrophobicity mediates the interaction of bacteria with surrounding medium and host cells (Miorner et al., 1982). Bacteria as well as other biological particles possess a pH-dependent surface charge which is negative for most strains in physiological condition (Olsson & Glantz, 1977). However, at physiologic pH few strains shows a net positive charge such as *Streptococcus thermophilus* and *Stenotrophomonas maltophilia* (Malte Hermansson, 1999).

Bacteria are unicellular organisms and connecting with surrounding media is vital for bacterial homeostasis and survival. As a result, bacterial surface is highly dynamic interacting consistently to surrounding changes through different mechanisms such as adsorption or secretion of different macromolecules (Cowan et al., 1992). Since a layer of medium is formed at the surface of the bacteria, an electrical double layer (Helmholtz's double layer) is formed upon their surface. The double layer contains an inner region, called the Stern layer, where the ions are strongly bound and an outer region, so-called the diffuse layer, where they are less firmly attached. Within the diffuse layer there is a boundary inside which the ions and particles form a stable entity, called shear plane. Bacterial surface charge has often been described by the Zeta potential, an electrochemical property of the cell surface, which represents the potential at the shear plane of the diffuse layer. The schematic (Helmholtz's double layer) of bacteria is shown in Figure 1.

The knowledge of the electrical properties of Bacteria is of benefit in the electrokinetic formation of biofilms, aggregation and detection of physical changes of bacterial cells and is emerging as a modern diagnostic tool to determine bacterial phenotypical features (Kłodzińska et al., 2010).

Colloid particles are not stable in the range of  $\pm 15$  millivolt of zetapotential so-called critical potential. At this zone most particle form sedimentation or aggregation which also seen in bacteria (Olsson & Glantz, 1977). Alteration of Zeta potential may be correlated to the enhancement of membrane permeability and it was observed that beyond a critical point, it leads to cell death in both Gram-positive and Gram-negative bacteria (W. William Wilson et al., 2001). The bacterial surface charge originate from dissociation and protonation of charged groups and depends on pH (Poortinga et al., 2002). The isoelectric point (pI) of bacteria is the pH at which the anionic and cationic charged groups on the surface are in a balance. In other word, at pI the net charge or zeta potential of bacteria is zero.

Although isoelectric point of bacteria is a reflection of bacterial surface composition, many studies used pI to determine the ability of bacterial surface polymers to inhibit or promote bacterial adhesion, as inhibition or promotion are the result of repulsive steric interactions not electrostatic repulsions of DLVO theory (Rijnaarts et al., 1995). In this review we tried to summarize the importance and usage of isoelectric point as an important value in bacteriology which can give an idea about bacterial surface charge and composition at first glance.

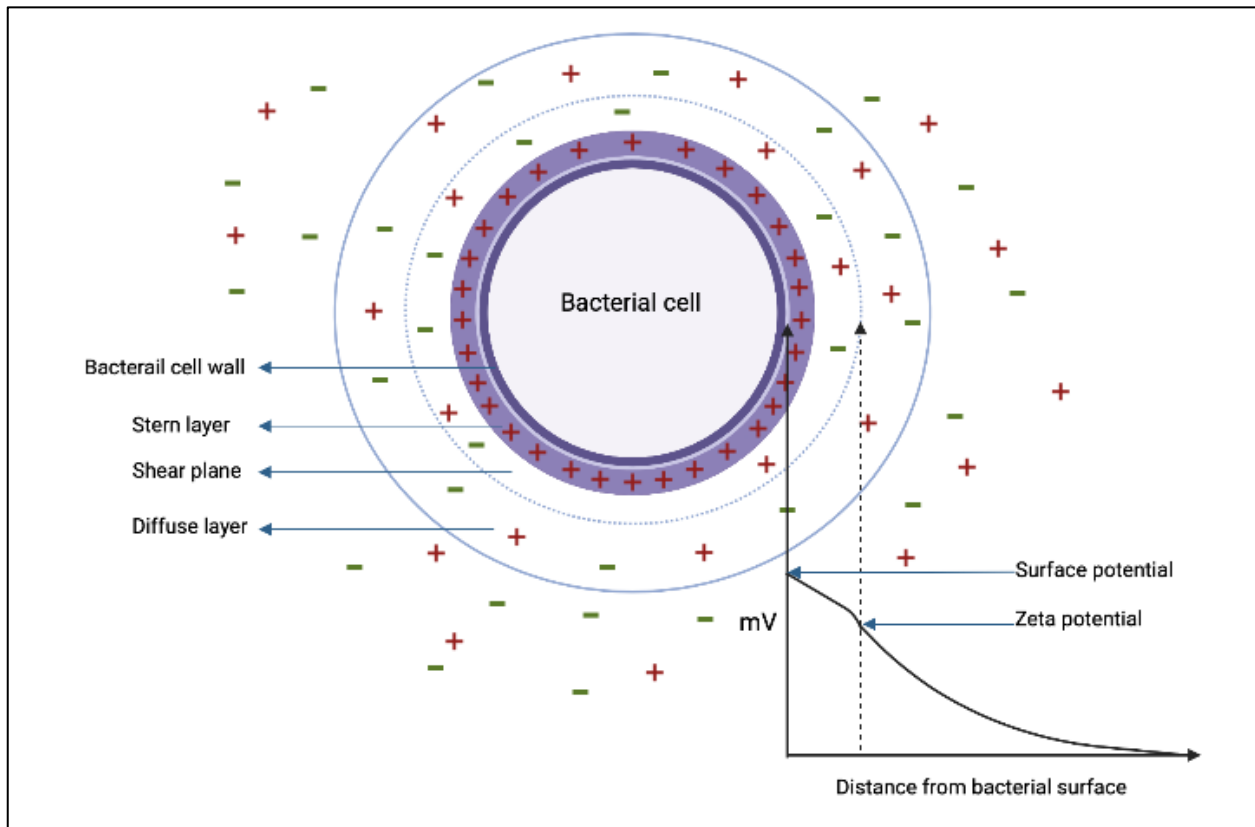


*Figure 1 Schematic representation of zeta potential. The liquid layer surrounding the particle exists as two parts; an inner region (Stern layer) where the ions are strongly bound and an outer (diffuse) region where they are less firmly associated. Within the diffuse layer there is a notional boundary inside which the ions and particles form a stable entity. When a particle moves (e.g. due to gravity), ions within the boundary move it. Those ions beyond the boundary stay with the bulk dispersant. The potential at this boundary (surface of hydrodynamic shear) is the zeta potential.*

## **DLVO theory to explain bacterial interaction**

Interactions between colloidal particles has been described by the DLVO theory (Derjaguin-Landau-Verwey-Overbeek), is also used to describe bacterial adhesion to surfaces (Marshall et al., 1971). The DLVO theory takes into consideration the contribution of van der Waals and electrostatic interactions (repulsive interactions which originate from interaction between charged group and is affected by the surrounding ionic strength) to predict the interaction free energy, as a function of distance (Malte Hermansson, 1999). Many studies showed that the DLVO theory cannot fully explain bacterial adhesion or stability of bacteria in suspension (Busscher & Elwing, 1999) as it has no explanation for bacterial surface moieties such as fibrils, fimbriae, flagella, and capsule. This theory assumes perfectly smooth surfaces which is not seen in bacteria, however, to conquer this Ohshima's "soft particle electrophoresis" theory present a presence of charged ion-penetrable layers around a core spherical particle. This theory was studied with bacterial cell mobility data, but for the first time it was applied for microorganisms by Sonohara et al. The differences in electrokinetic properties between Gram-positive (*S.aureus*) and Gram-negative bacteria (*E.coli*) were shown. It turned out that Gram-negative bacteria have a more negative charge than Gram-positive bacteria. They found that electrophoretic mobility measurement can be used to detect the difference in surface structure between Gram-positive and Gram-negative bacteria (Sonohara et al., 1995).

DLVO theory does not also able to explain and predict adhesion at high ionic strength solutions (Malte Hermansson, 1999). Therefore, extended DVLO (XDLVO) theory (Poortinga et al., 2002)(Smith et al., 2019) in addition to classical DLVO interactions, represent the Lewis acid-base or hydration interaction. The DLVO theory has also been applied to describe bacterial adhesion (M Hermansson, 1999; Rosan, 1981; Skvarla, 1993) on biomaterial implants (Harkes et al., 1991) and oral cavity (Satou et al., 1988).

## **Surface charge of gram-positive and gram-negative bacteria**

In many physiological conditions, bacterial cell surface conveys a net negative charge depends on the surface components involving ionized carboxylate (in protein, polysaccharide, peptidoglycan), phosphate (in teichoic acids, phospholipids) and amino groups (in proteins and peptidoglycan) (Busscher et al., 1990; Jucker et al., 1996). Upon changes in pH or ionic strength of suspension, these charged group may associate or dissociate from the bacterial membrane (Poortinga et al., 2002). The number of carboxyl and phosphate groups surpass the number of amino groups in physiological pH; therefore, most bacterial cell surfaces are negatively charged. Based on these



theories, changed in bacterial surface proteins (contains carboxyl and amino groups) may lead to alteration of bacterial charge distribution and isoelectric point.

The balance between bacterial surface charged anions and cations (acid/base) plus surface ions adsorption is determined as pI of bacteria. The most probable groups responsible for surface bacterial charge are summarized in Table 1 with their pKa. However, the interaction between charged groups results in a different pKa of an isolated group, for instance, pKa of an anion can be increased or decreased by anionic-anionic or anionic-cationic interactions respectively (Rijnaarts et al., 1995)(Poortinga et al., 2002).

*Table 1 pKa of possible charged groups on bacterial surface*

<b>Ionizable surface groups</b>	<b>pKa</b>	<b>Molecule and relative IEP</b>
$COOH \leftrightarrow COO^- + H^+$	4 - 5	Protein Peptidoglycan
$COOH \leftrightarrow COO^- + H^+$	2.8	Polysaccharide
$NH_3^+ \leftrightarrow NH_2 + H^+$	9 – 9.8	Protein Peptidoglycan
$H_2PO_4 \leftrightarrow HPO_4^- + H^+$	2.1	Teichoic Acid Phospholipid Phosphodiester bridge
$HPO^- \leftrightarrow PO^{2-} + H^+$	7.2	Protonated phosphate
$OH \leftrightarrow O^- + H^+$	8 - 12	Carbohydrate Protein Fatty acids

\*Sulfate groups are very rare on bacterial surface; thus, it was not mentioned here.

The Gram-positive bacterial cell wall contains thick layer of peptidoglycan on the top of cytoplasmic membrane. Instead, Gram-negative bacteria consist of a thin peptidoglycan layer between two phospholipid bilayer membrane, cytoplasmic and outer membrane. Besides, many surfaces structural accessories such as fibrils, flagella, fimbria, capsules, and slim layers are seen on bacterial surfaces affecting the total surface charge of bacteria. The isoelectric point of macromolecules on bacterial surface were summarized in Table 2.

As Gram-positive bacteria are negatively charged at neutral pH due to an excess of carboxyl and phosphate groups in addition to highly negatively charged teichoic acids, some strains show negative charge in all pH values with no isoelectric points (Olsson & Glantz, 1977).

In a study by Luo et al chitosan coated SMMPs (monodisperse starch magnetic micro- particles) were prepared to capture *Klebsiella pneumoniae*. They also used *Klebsiella pneumoniae* with different surface compositions (wild type as well as LPS or fimbriae mutant isoforms) to investigate the mechanisms of chitosan–bacteria interaction. Dense teichoic acids on Gram-positive bacterial surface containing polyol phosphates leads to a lower isoelectric point than Gram-negative bacteria. Therefore, the electrostatic absorption of Gram-negative bacteria onto chitosan-coated SMMPs is less than Gram-positive bacteria at a higher-pH environment. In addition, higher amount of chitosan was accumulated on Gram-positive bacterial surface compared to Gram-negative ones. The presence of higher chitosan molecules on the mutant isoforms shows the strong negative surface charge compared to wildtype which can be concluded LPS and fimbriae as well as surface charge play an important role in the bacterial defense mechanism by lowering the interaction and adhesion of positively charged antimicrobial agents such as chitosan (Luo et al., 2018).

*Table 2 Isoelectric point of macromolecules on bacterial surface*

<b>Macromolecule</b>	<b>IEP</b>	<b>Ionized groups</b>
Polysaccharide	$\leq 2.8$	Phosphate/Carboxyl
Peptidoglycan	Vary, $> 3.8$	1 $NH_3^+ / NH_2$ 3 $COOH / COO^-$
Proteins	Generally $> 4$	$NH_3^+ / NH_2$ $COOH / COO^-$

# **Methods of Isoelectric point calculation in bacteria**

## **Differential staining**

The first attempts to measure isoelectric point of bacteria was done in 1924 by Stearn and Stearn and others who have used differential staining at different pH levels. The isoelectric point was calculated as a pH in which bacterial cells obtained equal amount of acidic or basic dye.

However later studies showed no relation between staining and isoelectric point of bacteria, staining method had many defects to explain pI (HARDEN & HARRIS, 1953). Basic dyes stain cytoplasm and they cannot be a marker of charged molecules on the bacterial surface, as well as other factors influence electrical charge of bacteria. The staining procedure also depended on qualification judgement of investigator with no standard references.

In 1956 Kennedy et al. used a quantitative method for differential staining to calculate pI. They use micro-Kjeldahl analysis in which the amount of nitrogen was measured in bacterial cells before and after staining. They reported pI of 4.5 for E.coli in their experiment (KENNEDY & WOODHOUR, 1956).

## **Cross-partitioning in dextran-polyethylene glycol two-phase**

Briefly in liquid two-phase system bacteria were mixed at different pH in dextran-polyethylene glycol and the percentage of bacterial cells in the top phase was calculated and plotted against respective pH. (However, in another method bacteria can be partitioned at different pHs in dextran-polyethylene glycol phase systems containing two different salt compositions and two curves were obtained when partition coefficients were plotted against respective pH. These curves crossed close to the isoelectric point of the bacteria (Albertsson et al., 1970). Isoelectric point of 39 Streptococcus from groups A,C and G (pI=3.75) and 12 staphylococcus (pI<2) bacteria were determined by cross-partitioning in dextran-polyethylene glycol two-phase system (Miorner et al., 1982). The partition behavior of bacteria depends on the ionic composition of the system and the surface charge of the bacteria.(Albertsson et al., 1970). Miorner et al. also studied the effect of human serum proteins on these bacteria with incubation of them with human serum for 30 min to 1 hour in room temperature. Their result showed that treatments with human serum increase the pI of bacteria and it is significantly higher in streptococcus than staphylococcus. Binding of human serum protein to bacterial surface may mask the bacterial cell surface properties and leads to higher pI. No

differences of isoelectric point between laboratory maintained and freshly isolated strains were reported. However, the isoelectric point of heat-inactivated strains was significantly higher compared to other two groups both in streptococcus and staphylococcus. They also showed the ribitol teichoic acid less mutants of Staphylococcus had the  $pI < 2$ , concluded Teichoic acid had a minor effect on highly acidic cross-point staphylococcus. They suggest a positive correlation between the hydrophobicity of group A streptococcus and the density of specific receptor for human serum proteins (Miorner et al., 1982).

The reported isoelectric point of bacteria from different literature are summarized in Table 3, Table 4 and Table 5.

### **Electrophoretic mobility**

In an electric field charged particles such as bacteria tends to move towards the electrode of opposite charge. The velocity of a particle in an electric field is commonly referred to as its Electrophoretic mobility. Smoluchowski's formula is generally used to determine the zeta potential of colloidal particles:

$$\zeta = \frac{\mu\eta}{\epsilon_0\epsilon_r}$$

where  $Z$  is the viscosity of the electrolyte solution,  $\epsilon_0$  and  $\epsilon_r$  are the relative permittivity of the electrolyte solution and a vacuum, respectively (Kłodzińska et al., 2010).

For the first time in 1952 Harden et al. compared isoelectric points of gram-positive and gram-negative bacteria with microelectrophoresis in different pH. They used young growing bacteria in a dilute monovalent ions buffer with constant ionic strength ( $0.01\mu$ ) to reduce the influence of surrounding Ions in bacterial charge. They calculated isoelectric point through plotting electrophoretic mobility versus pH in which no movement of bacteria or movement in opposite direction were seen. They reported isoelectric point in a range of pH 1.75 to 4.15 for gram-positive bacteria and pH 2.07 to 3.65 for gram negative bacteria (HARDEN & HARRIS, 1953). Many factors affect electrophoretic mobility such as surrounding ions type and concentration, bacterial age, and growth condition and so on.

Another study in 1977 showed direct relation between the zeta potential of oral streptococcus and their adherence to surfaces. They used microelectrophoresis in different pH and different ionic buffers with adjusted conductivities of 1.7  $\mu\text{mhos/cm}$ . Most of streptococcus strains had negative surface charge till reach their isoelectric point and then gain positive charge as pH decreased. However, they did not observe any isoelectric point for some strains. All strains with negative charge have dominant carboxylic groups on the surface (pK value of carboxylic is 2.5) (carboxylic groups are in majority), they also expose amine groups as for positive charge in pH below pI. In this study anionic and monovalent cationic groups in bulk solution did not have any effect on zetapotential as well as isoelectric point. Although multivalent cations changed isoelectric point dramatically in different pH, aluminium showed contradiction effects in pH 3 and 5 which forms trivalent and four valent hydroxy complexes respectively (Olsson & Glantz, 1977).

Another study by Shi et al. utilized electrophoresis measurements with Lazer Zee Meter to calculate isoelectric point of BCG strains Tice and Glaxo). They performed average of ten reading with standard deviation of 5% and adjustment of pH with 0.005 mol/dm<sup>3</sup> Hydrochloric acid or sodium hydroxide solutions in the range of 2 to 10. They reported isoelectric point of 4.2 for BCG Tice, however they did not report isoelectric point of Glaxo strain in this pH rage, they estimated an isoelectric point around pH=2 for Glaxo BCG. They also studied the effect of washing with HCl or water on these strains with marked decrease of isoelectric point from approximately pH=4.2 to pH=3.1. They concluded with washing some loose adherent surface proteins (which also proved with transmission electron microscopy) may loose and consequently changes in isoelectric point were seen. The phosphate groups of phosphodiester linkages between peptidoglycan and arabinogalactan are responsible for the mycobacterium surface charge, as well as amino residues from surface proteins specially in lower pH. They also discussed that isoelectric point as well as surface charge which were result from different surface proteins can be related to immunological response against these vaccines (Shi M, Klegerman ME, 1989).

In 1992 Cowen et al. used electrophoretic mobility measurements by Lazer Zee Meter to calculate the surface bacterial charge. However, they did not mention isoelectric point directly, it can be extracted from zeta potential titration curves. Briefly, the mobility of bacterial cells in the applied electric field is calculated using a rotating prism with adjusting speed. *Porphyromonas gingivalis*, *Prevotella intermedia*, *Actinobacillus actinomycetemcomitans* as gram negative and *Peptostreptococcus micros* as gram positive bacteria were studied. The isoelectric point of 2 to 3 and

around 4 were reported for gram negative and gram positive respectively. They also studied the effect of higher-passage culture on *Peptostreptococcus micros*, which leads to higher isoelectric point. They discussed higher isoelectric point can be the result of fimbriae absence in higher-passage culture. Consequently, different degree of fimbriation, fimbriae length variation and amino acid composition leads to changes in surface charge and isoelectric point.

### **Isoelectric focusing (IEF)**

Jaspers et al. used isoelectric focusing with higher resolution than electrophoretic mobility to separate different bacteria in diverse soil bacterial community. *Chlorobium limicola*, *Pseudomonas stutzeri*, *Micrococcus luteus* with isoelectric point of 4.17, 3.80 and 3.38 respectively were reported.

The isoelectric point of *Chlorobium limicola*, *Pseudomonas stutzeri*, *Micrococcus luteus* did not show any changes with CaCl<sub>2</sub> or in the presence of Tween 20 (Jaspers et al., 1997).

### **Capillary isoelectric focusing (CIEF)**

Another well studied method to calculate isoelectric point is using capillary isoelectric focusing (CIEF) which is based on the principle of capillary gel electrophoresis (CGE) and separates particles according to their isoelectric point values. Ampholytes are used to form a pH gradient within the capillary, and the proteins to be separated migrate (or are focused) through the ampholyte medium until they become uncharged at their isoelectric point values (Otter, 2003).

Horka et al. used combination of capillary isoelectric focusing (CIEF) with matrix-assisted laser desorption/ionization time-of-flight mass spectrometry (MALDI-TOF MS) to identify probiotic bacteria in cow's milk. CIEF of *Lactobacillus* as reference and milk probiotics were optimized and isoelectric point of bacteria were calculated from migration times of the pI markers. Their result demonstrated that the combination of CIEF with MALDI-TOF MS is an efficient approach for identification of the bacteria in cow's milk (Marie Horká et al., 2013).

CIEF is a high-resolution technique, but the capillaries used in this method should be modified for different bacteria to prevent their adsorption (M. Horká et al., 2007).

### **Electrophoretic light scattering (ELS)**

One of the most rapid, non-invasive and direct methods procedures used widely to calculate isoelectric points of is represented by the hydrodynamic methods involving Electrophoretic light scattering (ELS) (Jachimska et al., 2008). An electric field is applied, and the electrophoretic mobility of the particles is measured by Electrophoretic light scattering (ELS): The mobile particles during electrophoresis scatter an incident laser. As the particles are mobile the scattered light has a different frequency than the original laser and the frequency shift is proportional to the speed of the particles (Doppler shift) (Bhattacharjee, 2016). The instrumentation used for this technique is shown in Figure 2. In short, the laser beam is split into two and while one beam is directed towards the sample the other one is used as a reference beam. The scattered light from the sample is combined or optically mixed with the reference beam to determine the Doppler shift. The magnitude of particle velocity (V) is deduced from the Doppler shift converts to Zeta potential values allowed to determine the isoelectric point through pH titration too.

The first use of Electrophoretic light scattering (ELS) to measure bacterial isoelectric point in different ionic strength of 10 mM or 40 mM potassium phosphate buffers at different pH ranging from 2 to 7 was reported by Van der Mei in 1994. They used *Streptococcus mitis*, *Streptococcus salivarius* and *Acinetobacter calcoaceticus* with reporting isoelectric point of 4,3 and 2 respectively. Although they did not discussed the reasons of different isoelectric point, they mentioned the possible collapsed surface structure at pH 2 than at pH 7 because of the electrostatic repulsion reduction in lower pH as well as the more fragile cell wall in Gram-negative bacteria (Van der Mei et al., 1994).

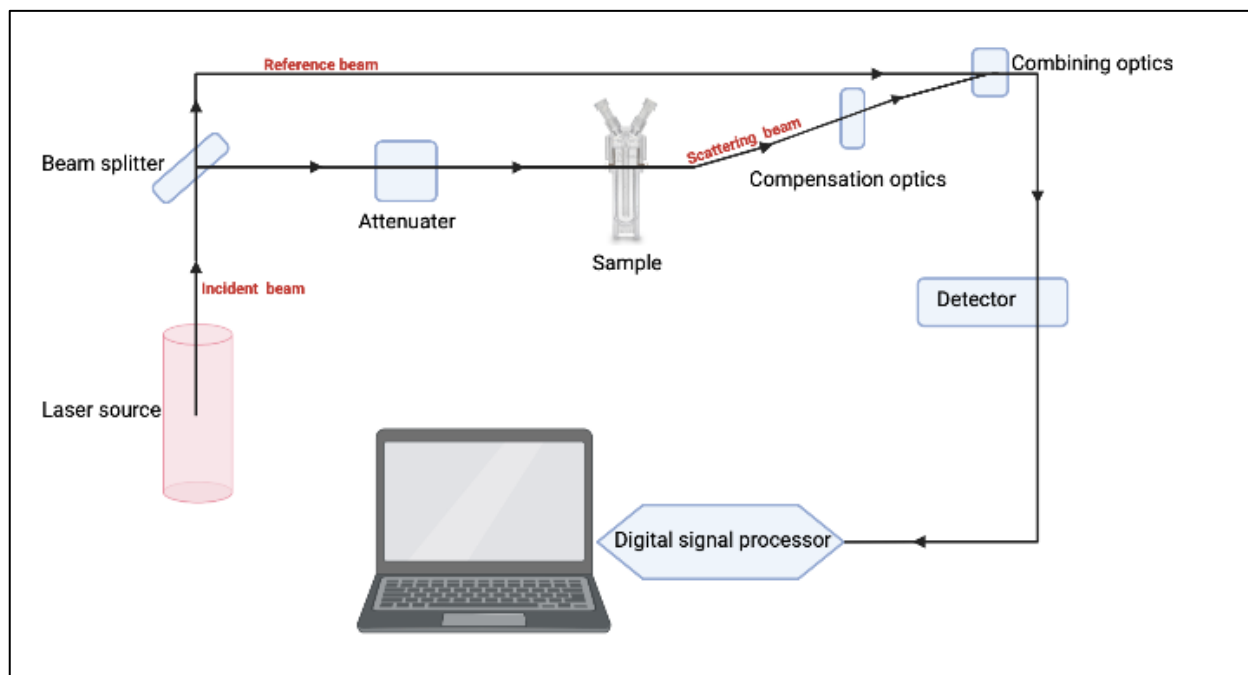


Figure 2 Schematic showing the instrumentation of zeta potential measurement by electrophoretic light scattering.



# Application of bacterial isoelectric point

## Study of bacterial adhesion

Bacterial adhesion is the initial step in colonization and biofilm formation (Katsikogianni et al., 2004). Bacterial adhesion to different surfaces contains two fundamental steps, reversible adhesion, and irreversible adhesion. The first reversible step is directed by physical and chemical integration between bacterial cell and the surface, thus surface charge as well as electrolyte concentration can affect this step. The correlation between surface charge and adhesion is not clearly understandable as many factors affect it directly and indirectly (Malte Hermansson, 1999).

In a review article of bacterial adhesion in 2004, Katsikogianni discussed that bacterial adhesion to hydrophobic surfaces occurs at pH between 2.2 to 4, at the range of isoelectric point, when bacterial bacteria are zero (Katsikogianni et al., 2004). Thus, isoelectric point can be studied to predict the adhesion of bacterial cell to hydrophobic surface which are negatively charged.

Rijnaarts et al. studied isoelectric point using electrophoretic mobilities of bacteria at 0.01 M ionic strength as well as bacterial adhesion to glass and Teflon using light microscopy. The correlation between bacterial isoelectric point and their adhesion showed a lower adhesion for bacteria with isoelectric point less than 3 to glass and isoelectric point less than 2.8 to Teflon. Bacteria with isoelectric point less than 2.8 probably have surface polymers inhibiting cell adhesion by steric hinderance. isoelectric point less than 2.8 is a result of phosphate groups of teichoic acid in highly hydrophobic strains. However, phosphate groups in phosphodiester bridge of mycolic-acid and arabinogalactan cause higher isoelectric point seen in coryneform or mycobacterium. These phosphate groups probably located deeper in bacterial cell wall than teichoic acid phosphate groups, thus they have less contribution in isoelectric point. In general, isoelectric point less than 2.8 indicate the presence of dominant polysaccharide and glucuronic acids containing phosphate and carboxylic acid with  $pK_a \leq 2.8$  or lipopolysaccharide (LPS) of gram-negative bacteria. Although  $pI \geq 3.2$  is difficult to interrupt, it reflects combination of charged groups such as proteins, peptidoglycan and others and has been detected in strains without significant anionic polysaccharides to inhibit adhesion (Rijnaarts et al., 1995). Based on this result it can be concluded that at high ionic strength, cell surface hydrophobicity as well as isoelectric point could improve prediction of bacterial adhesion on different surfaces. (this one and (Van der Mei et al., 1994), (Rijnaarts et al., 1995).

However, others believed that prediction of bacterial surface interactions and adhesions through hydrophobicity, electrostatic interactions and Gibb's energy does not provide a comprehensive explanation, which may be related to heterogeneity of bacterial surface. Variety of cell surface structure such as appendages, pili and capsules, as well as dynamic cell surface alteration via gene expression changes could be the reasons of these heterogeneity (Gallardo-Moreno et al., 2011).

In other studies Yuan et al have shown the super-hydrophilic substrate with negative zeta potential exhibited limited bacterial binding, due to the reduced hydrophobic interaction and possible repulsive interaction between bacteria and surface, however they did not work on isoelectric point directly. These findings and similar studies can be utilized for an effective surface design to inhibit bacterial adhesion as an alternative solution to use antibiotics (Yuan et al., 2017).

### **Study of bacterial biofilm**

The concentrations and characterization of charged groups (carboxylic, phosphoric, hydroxyl and amine) on the bacterial surface plays an important role in bacterial biofilm formation and precipitations, as they are responsible for the surface binding capacity. In 2005 By the means of electrophoretic mobility through Zetasizer zetapotential and isoelectric point of picocyanobacteria, gram negative bacteria in soil and freshwater were calculated. They also used potentiometric titration to describe the numbers, concentration and thermodynamic properties of ionizable functional groups on bacterial surface (Dittrich & Sibling, 2005).

### **Study of the influence of different methods of inactivation on bacterial surface**

Microorganism inactivation without damaging structure and integrity can be advantageous for the identification and isolation of high-risk pathogens.

Isoelectric points of native and modified chemically and physically inactivated *E.coli* and *Staphylococcus epidermidis* were calculated. isoelectric point of *E.coli*, *Staphylococcus epidermidis* biofilm negative and *Staphylococcus epidermidis* biofilm positive were reported at pH 4.6, 2.3 and 2.6 respectively. The isoelectric point were changed in inactivated bacteria with different methods. For *E.coli* thermal inactivation at 100c for 1 hour cause surface damage, however small group of bacteria with isoelectric point around 5 were detected. Inactivation of bacteria with EtOH 70%, formaldehyde 4% and peroxyacetic acid for 30 min leads to complete damage of bacterial cells and consequently no isoelectric point were detected in any strains (M. Horká et al., 2007).

Tan et al. studied the mechanism of multivalent interactions at the graphene–pathogen interface as Graphene and its derivatives have recently attracted much attention for inhibiting microorganisms. Interactions between such zwitterionic systems and bacteria could even be controlled to some extent through their isoelectric point (pI). Although they mainly focused on isoelectric point of Graphene and its derivatives but they also used bacterial pI to trap and release them from Graphene by changing pH to lower and higher than their pI (Tan et al., 2018)

### **Using pI to control mechanisms of cell surface electric potential**

Martinez et al. studied the control mechanisms of cell surface electric potential and proton/hydroxyl adsorption through zeta potential and acid-base titration of active, inactive, and dead cyanobacteria. Bacterial net surface charge can be determined by zeta potential measurement which is the electrical potential differences at the hydrodynamic slip plane, the interface between the aqueous fluid and the stationary layer of fluid attached to bacterial cell. They combined high resolution zeta potential measurements and potentiometric acid-base titration to determine which metabolic process can control bacterial surface electric potential as well as adsorption of proton or hydroxyl on their surface. Similar isoelectric point was detected between different strains of cyanobacteria (*Synechococcus* and *Planothrix*) suggested the similarities in cell wall of those strains. Previous studies showed similar isoelectric point between live and dead autotrophic bacteria and concluded the zeta potential of these bacteria are only controlled by chemical components of slim layer and are not influenced by metabolic activity. However, isoelectric point differences between dead and live cyanobacteria showed that bacterial electric charge are controlled by a combination of metabolic and structural based factors (Martinez et al., 2008).

In another study by Bardavid et al. the mechanisms of bacterial osmolarity balance to live in hypersaline environment was studied. They predicted the isoelectric point of *Halobacterium* proteomics through metagenomic data analysis using the programs in the Galaxy platform (Elevi Bardavid & Oren, 2012), however the experimental data on these kind of research still should be studied to have a general conclusion. Further investigation was done Cabello-Yeves in 2019, where they compared the predicted proteome isoelectric point of bacteria in freshwater and salt water. They have found major differences at the level of the predicted metaproteomes of marine and freshwater habitats with more acidic values of the isoelectric points (pI) in marine microbes. However more experimental data should be done and maybe bacterial IEP measurements can explain the adaptation of bacteria to live in marine or freshwater environments (Cabello-Yeves & Rodriguez-Valera, 2019).

### **Using pI to separate inclusion bodies of recombinant protein from host**

Another important application of studying isoelectric point is in electrophoretic deposition of inclusion body separation from host bacteria. Novak et al utilized the differences in isoelectric point of *E.coli* and the recombinant protein to separate inclusion body of this protein from *E.coli*. At pI=3.8, *E.coli* surface charge is zero and they are not expected to migrate in electrophoretic deposition (electrophoresis-based method), thus at this pH the zeta potential of selected recombinant protein is negative and they could migrate towards the positive electrode (deposition) (Novak et al., 2009).

### **Study of bacterial interaction with metals**

Physicochemical properties of bacterial surface are essential in different interactions with surrounding medium and metals. The concentration and type of functional group such as proton active carboxylic, phosphoric, phosphodiester, hydroxyl and amine on bacterial surface play a major role in this surface binding, adhesion, and interactions. To compare copper sensitivity of cyanobacteria, Hadjoudja et al calculated zetapotential from electrophoresis of bacteria. Acid-Base titration and electrophoretic mobility measurements were done in constant ionic strength of 0.1 M. They reported highly negative surface charge for Cyanobacteria with isoelectric point 2.2 to 2.9 for *Microcystis* and *Chlorella* respectively which explain their potential high copper affinity. By combination of zeta potential measurements, potentiometric titration and infrared spectroscopy, they reported higher total concentration of functional groups specially carboxyl groups on the surface of *Microcystis* than *Chlorella* which confirm the higher sensitivity of *Microcystis* to copper (Hadjoudja et al., 2010).

### **Using pI to measure antibiotic activity on bacteria**

Detection and quantification of antibiotics and bacteria in human samples is essential for disease diagnosis therefore CIEF based on different isoelectric point can be used as a fast and specific method for the possibility of microorganisms separation directly from some biological fluids (Marie Horká et al., 2014). It is also discussed isoelectric point of bacteria and antibacterial agent are key parameters to estimate the persistence and toxicity of antimicrobials (Lim et al., 2013).

In 2014, Cell surface changes of *Staphylococcus epidermidis* under tetracycline treatments were studied by CIEF. The whole human blood samples with vancomycin and *S.epidermidis* was directly separated with CIEF too. Although the *S.epidermidis* isoelectric point was reported around 2.3, the

interaction of bacteria with different concentration of antibiotics changed bacterial isoelectric point in the range of pH 5.3 to 6.4 (Marie Horká et al., 2014).

A very recent study showed the presence of a highly negatively charged, hydrophilic, thickened capsular outer layer (TCOL) on a small proportion of the rifampicin surviving population (RSP) after exposure of *Mycobacterium tuberculosis* to bactericidal concentrations of rifampicin in vitro. They reported high negative surface charge on rifampicin surviving population which inspired to determine the ionic properties of cell surface in different population. They calculated and compared isoelectric point of rifampicin surviving population, mid-log phase and killing phase through zeta potential pH-titration. All populations showed similar isoelectric point between pH 4.0 and pH 6.0, with the value being closer to pH 4.0 which indicate that the nature of the negatively charged molecules might not have changed on the cell surface during the transition from the killing phase to the rifampicin surviving population and to the regrowth phase. However, rifampicin surviving population showed higher negative zeta potential value at higher pH, unlike other examined population, which indicate higher negative cell surface charge (Sebastian et al., 2020).

### **Using pI to separate bacteria from complex medium**

Identification and separation of different microorganisms such as bacteria from complex media is crucial in diagnosis in various field of medicine, biotechnology, food industry, marine biology and so on (Marie Horká et al., 2013)(Marie Horká et al., 2017). Thus, separation of different bacteria from complicated matrix is the first important step especially for uncultured bacteria or with very low growth rate. For this purpose, electrophoresis is very useful as they are easy and fast procedure and among them, capillary isoelectric focusing (CIEF) is potentially a suitable technique to separate bacteria based on their isoelectric point.

Using CIEF, isoelectric points found for the examined cells were 1.8 for *Micrococcus luteus* (Gram-positive bacteria), 3.5 for *Dietzia* sp. (Gram-positive bacteria), and 4.7 for *Rhodotorula mucilaginosa* (Yeast-like cells). The separation was done between the isoelectric point of different strains by CIEF (Marie Horká et al., 2017).

They have shown in different studies that isoelectric focusing (IEF) specially CIEF certainly belong among potentially suitable electrophoretic techniques for the separation of different bacteria based on their isoelectric point.

A study in 2018 represented a new method for simultaneous identification of urinary tract pathogens in the case of poly-bacterial urinary tract infections using IEF in a cellulose-based separation medium with a MALDI-TOF MS analysis. Bacteria can be separated and concentrated by isoelectric focusing analytes according to their different isoelectric points during focusing. They successfully reported the use of IEF for both purification and separation of bacteria, *Escherichia coli* (pI 4.6) and *Staphylococcus aureus* (pI 3.4), in urine samples. This method can be useful to separate bacteria from polymicrobial infections where most of current methods fail to detect them (Šalplachta et al., 2018). More investigation for the identification of urinary tract pathogens in urine specimens in the case of the high concentration of Human Serum Albumin were done by the same group in 2019. Using Cellulose-based preparative isoelectric focusing method (which is based on isoelectric point separation) they were able to successfully separate *E.coli* with isoelectric point around 4.6 from urine with high concentration of Albumin which has isoelectric point of 4.8 very close to isoelectric point of *E.coli* (Marie Horká et al., 2019).

Table 3 Isoelectric point of Gram-Positive bacteria from literature

<b>Bacteria</b>	<b>IEP</b>	<b>Method</b>	<b>Ref</b>
<i>Mycobacterium tuberculosis</i>	4.15	Electrophoretic mobility in acetate-HCl buffer	(HARDEN & HARRIS, 1953)
<i>Bacillus sphaericus</i>	3.99	Electrophoretic mobility in acetate-HCl buffer	(HARDEN & HARRIS, 1953)
<i>Bacillus terminalis</i>	3.57	Electrophoretic mobility in acetate-HCl buffer	(HARDEN & HARRIS, 1953)
<i>Bacillus cereus</i>	3.55	Electrophoretic mobility in acetate-HCl buffer	(HARDEN & HARRIS, 1953)
<i>Rhodospirillum rubrum</i>	3.46	Electrophoretic mobility in acetate-HCl buffer	(HARDEN & HARRIS, 1953)
<i>Bacillus brevis</i>	3.2	Electrophoretic mobility in acetate-HCl buffer	(HARDEN & HARRIS, 1953)
<i>Bacillus polymyxa</i>	3.12	Electrophoretic mobility in acetate-HCl buffer	(HARDEN & HARRIS, 1953)
<i>Erysipelothrix rhusiopathiae</i>	2.91	Electrophoretic mobility in acetate-HCl buffer	(HARDEN & HARRIS, 1953)
<i>Clostridium sporogenes</i>	2.75	Electrophoretic mobility in acetate-HCl buffer	(HARDEN & HARRIS, 1953)
<i>Lactobacillus casei, strain 9595</i>	2.45	Electrophoretic mobility in acetate-HCl buffer	(HARDEN & HARRIS, 1953)
<i>Leuconostoc mesenteroides, strain 8042</i>	2.25	Electrophoretic mobility in acetate-HCl buffer	(HARDEN & HARRIS, 1953)
<i>Sarcina lutea</i>	2.20	Electrophoretic mobility in acetate-HCl buffer	(HARDEN & HARRIS, 1953)
<i>Bacillus subtilis</i>	2.19	Electrophoretic mobility in acetate-HCl buffer	(HARDEN & HARRIS, 1953)
<i>Micrococcus citreus</i>	1.90	Electrophoretic mobility in acetate-HCl buffer	(HARDEN & HARRIS, 1953)
<i>Streptococcus faecalis, strain 9790</i>	1.90	Electrophoretic mobility in acetate-HCl buffer	(HARDEN & HARRIS, 1953)
<i>Bacillus alvei</i>	1.85	Electrophoretic mobility in acetate-HCl buffer	(HARDEN & HARRIS, 1953)
<i>Bacillus megaterium, strain 8245</i>	1.80	Electrophoretic mobility in acetate-HCl buffer	(HARDEN & HARRIS, 1953)
<i>Bacillus pumilis</i>	1.75	Electrophoretic mobility in acetate-HCl buffer	(HARDEN & HARRIS, 1953)
<i>Diplococcus pneumoniae</i>	3.5 to 4.7	?	Thompson(1932)
<i>Bacillus subtilis</i>	3.6	?	Yamaha and Abe(1934)
<i>Staphylococcus aureus</i>	3.4	?	Yamaha and Abe(1934)
<i>Bacillus anthracis</i>	3.1	?	Yamaha and Abe(1934)
<i>Bacillus cereus</i>	3	?	Winslow, Falk, and Caulfield(1923)
<i>Diplococcus pneumoniae</i>	2.7 to 3.3	?	Falk and Jacobson(1926)
<i>Sarcina lutea</i>	2.6	?	Yamaha and Abe(1934)
<i>Clostridium flabelliferum</i>	2.5	?	Winslow and Upton(1926)
<i>Lactobacillus acidophilus</i>	2.5	?	Winslow and Upton(1926)
<i>Mycobacterium smegmatis</i>	2.5	?	Winslow and Upton(1926)
<i>Mycobacterium leprae(R)</i>	2.2	?	Reed and Gardiner(1932)
<i>Diplococcus pneumoniae</i>	2 to 3	?	Mudd(1933)
<i>Bacillus pseudodiphtheriae</i>	1.8	?	Yamaha and Abe(1934)
<i>Mycobacterium leprae(S)</i>	1.2	?	Yamaha and Abe(1934)
<i>Staphylococcus sp</i>	0.7	?	Verwey and Frobisher(1940)
<i>Streptococcus from group A</i>	3.67 ± 0.15	Two phase cross partitioning (Dextran-PEG)	(Miorner et al., 1982)
<i>Streptococcus from group C</i>	3.8 ± 0.12	Two phase cross partitioning	(Miorner et al., 1982)

		(Dextran-PEG)	
<i>Streptococcus from group G</i>	3.80 ± 0.16	Two phase cross partitioning (Dextran-PEG)	(Miorner et al., 1982)
<i>Staphylococcus</i>	1.95 ± 0.16	Two phase cross partitioning (Dextran-PEG)	(Miorner et al., 1982)
<i>Streptococcus mitis</i>	4	Electrophoretic mobility	(Van der Mei et al., 1994)
<i>Streptococcus salivarius</i>	3	Electrophoretic mobility	(Van der Mei et al., 1994)
<i>Arthrobacter sp. DSM 6687</i>	1.7	Electrophoretic mobility	(Rijnaarts et al., 1995)
<i>Coryneform DSM 6685</i>	2.6	Electrophoretic mobility	(Rijnaarts et al., 1995)
<i>Rhodococcus sp. C 125</i>	3	Electrophoretic mobility	(Rijnaarts et al., 1995)
<i>Rhodococcus erythropolis A177</i>	2.8	Electrophoretic mobility	(Rijnaarts et al., 1995)
<i>Corynebacterium sp. DSM 6688</i>	3.2	Electrophoretic mobility	(Rijnaarts et al., 1995)
<i>Corynebacterium sp. DSM 44016</i>	3.8	Electrophoretic mobility	(Rijnaarts et al., 1995)
<i>Gordona sp. 1775/15</i>	3.3	Electrophoretic mobility	(Rijnaarts et al., 1995)
<i>Gordona sp. DSM 44015</i>	3.4	Electrophoretic mobility	(Rijnaarts et al., 1995)
<i>Micrococcus luteus</i>	3.38	Isoelectric focusing	(Jaspers et al., 1997)
<i>Staphylococcus epidermidis (biofilm negative)</i>	2.3	Capillary electrophoretic focusing	(M. Horká et al., 2007)
<i>Staphylococcus epidermidis (biofilm positive)</i>	2.6	Capillary electrophoretic focusing	(M. Horká et al., 2007)
<i>Lactobacillus casei</i>	3.2	Capillary isoelectric focusing	(Marie Horká et al., 2013)
<i>Lactobacillus delbrueckii</i>	2	Capillary isoelectric focusing	(Marie Horká et al., 2013)
<i>Lactobacillus acidophilus</i>	2.5	Capillary isoelectric focusing	(Marie Horká et al., 2013)
<i>Lactobacillus salivarius</i>	3.3	Capillary isoelectric focusing	(Marie Horká et al., 2013)
<i>Lactobacillus plantarum</i>	3.8	Capillary isoelectric focusing	(Marie Horká et al., 2013)
<i>Lactobacillus gasseri</i>	4	Capillary isoelectric focusing	(Marie Horká et al., 2013)
<i>Lactobacillus rhamnosus</i>	3.6	Capillary isoelectric focusing	(Marie Horká et al., 2013)
<i>Staphylococcus epidermidis</i>	2.3	Capillary isoelectric focusing	(Marie Horká et al., 2014)
<i>Micrococcus luteus</i>	1.8	Capillary isoelectric focusing	(Marie Horká et al., 2017)
<i>Dietzia sp.</i>	3.5	Capillary isoelectric focusing	(Marie Horká et al., 2017)
<i>Staphylococcus aureus</i>	3.4	Cellulose-based preparative isoelectric focusing	(Šalplachta et al., 2018)



Table 4 Isoelectric point of Gram-Negative bacteria from literature

<b>Bacteria</b>	<b>IEP</b>	<b>Method</b>	<b>Ref</b>
<i>Mycoplana bulata</i> ,strain4278	3.65	Electrophoretic mobility in acetate-HCl buffer	(HARDEN & HARRIS, 1953)
<i>Moraxella bovis</i>	3.47	Electrophoretic mobility in acetate-HCl buffer	(HARDEN & HARRIS, 1953)
<i>Alkaligenes faecalis</i> ,strain8749	3.28	Electrophoretic mobility in acetate-HCl buffer	(HARDEN & HARRIS, 1953)
<i>Pseudomonas cyanogenes</i> , strain795	3.25	Electrophoretic mobility in acetate-HCl buffer	(HARDEN & HARRIS, 1953)
<i>Erwinia carotovora</i> ,strain495	2.99	Electrophoretic mobility in acetate-HCl buffer	(HARDEN & HARRIS, 1953)
<i>Pseudomonas convexa</i>	2.95	Electrophoretic mobility in acetate-HCl buffer	(HARDEN & HARRIS, 1953)
<i>Proteus vulgaris</i>	2.67	Electrophoretic mobility in acetate-HCl buffer	(HARDEN & HARRIS, 1953)
<i>Klebsiella pneumoniae</i>	2.48	Electrophoretic mobility in acetate-HCl buffer	(HARDEN & HARRIS, 1953)
<i>Aerobacter aerogenes</i>	2.42	Electrophoretic mobility in acetate-HCl buffer	(HARDEN & HARRIS, 1953)
<i>Serratia marcescens</i>	2.17	Electrophoretic mobility in acetate-HCl buffer	(HARDEN & HARRIS, 1953)
<i>Pseudomonas aeruginosa</i>	2.17	Electrophoretic mobility in acetate-HCl buffer	(HARDEN & HARRIS, 1953)
<i>Salmonella pullorum</i>	2.12	Electrophoretic mobility in acetate-HCl buffer	(HARDEN & HARRIS, 1953)
<i>Azotobacter chroococcum</i>	2.07	Electrophoretic mobility in acetate-HCl buffer	(HARDEN & HARRIS, 1953)
<i>Hemophilus influenzae</i>	3 to 4	Electrophoretic mobility	Mudd(1933)
<i>Brucella abortus</i>	3 to 4	Electrophoretic mobility	Mudd(1934)
<i>Bacillus caryocyaneus</i>	3.5	Electrophoretic mobility	Lasseur,Dupaix-Lasseur,andFribourg (1933)
<i>Phytomonas stewartii</i>	3.5	Electrophoretic mobility	Frampton and Hildebrand(1944)
<i>Erwinia amylovora</i>	3.3	Electrophoretic mobility	
<i>Bacillus pyocyaneus</i>	3.1	Electrophoretic mobility	Yamaha and Abe(1934)
<i>Pseudomonas pyocyaneus</i>	2.5	Electrophoretic mobility	Winslow and Upton(1926)
<i>Bacterium coli</i>	2.5	Electrophoretic mobility	
<i>Diplococcus gonorrhoeae</i>	2.5	Electrophoretic mobility	Yamaha and Abe(1934)
<i>Bacillus pertusis</i>	2.5	Electrophoretic mobility	
<i>Brucella abortus</i>	2.3 to 3.3	Electrophoretic mobility	Stearns and Roepke(1941)
<i>Bacillus proteus</i>	2.1	Electrophoretic mobility	Yamaha and Abe(1934)
<i>E.coli</i>	4.5	quantitative method for differential staining	(KENNEDY & WOODHOUR, 1956)
<i>Acinetobacter calcoaceticus</i>	2	dynamic light scattering (DLS)	(Van der Mei et al., 1994)
<i>Pseudomonas oleovorans</i> ATCC 29347	1.7	Electrophoretic mobility	(Rijnaarts et al., 1995)
<i>Pseudomonas fluorescens</i> p62	3.6	Electrophoretic mobility	(Rijnaarts et al., 1995)
<i>Pseudomonas sp. strain B13</i>	2.2	Electrophoretic mobility	(Rijnaarts et al., 1995)
<i>Pseudomonas putida</i> mt2	3.2	Electrophoretic mobility	(Rijnaarts et al., 1995)
<i>Chlorobium limicola</i>	4.17	isoelectric focusing	(Jaspers et al., 1997)
<i>Pseudomonas stutzeri</i>	3.80	isoelectric focusing	(Jaspers et al., 1997)

<i>Pycocyanobacteria</i> <i>Synechococcus-type strain</i>	5	Electrophoretic mobility by Zetasizer	(Dittrich & Sibling, 2005)
<i>E.coli</i>	5	Capillary electrophoretic focusing	(M. Horká et al., 2007)
<i>Synechococcus</i> ( <i>Cyanobacteria</i> )	2.5 – 2.8	Electrophoretic mobility	(Martinez et al., 2008)
<i>Planktothrix</i> ( <i>Cyanobacteria</i> )	Nothing observed	Electrophoretic mobility	(Martinez et al., 2008)
<i>E.coli</i>	3.8	Zeta potential - titration	(Novak et al., 2009)
<i>E.coli</i> K12 DSM 498	3.5	Zeta potential - titration	(Schwegmann et al., 2010)
<i>Microcystis aeruginosa</i>	2.2	Zeta potential - titration	(Hadjoudja et al., 2010)
<i>Chlorella vulgaris</i>	2.9	Zeta potential - titration	(Hadjoudja et al., 2010)
<i>E.coli</i>	4.6	Cellulose-based preparative isoelectric focusing	(Šalplachta et al., 2018)(Marie Horká et al., 2019)

Table 5 Isoelectric point of Acid-fast bacteria from literature

<b>Bacteria</b>	<b>IEP</b>	<b>Method</b>	<b>Ref</b>
<i>Mycobacterium (BCG vaccine Tice)</i>	4.2	Electrophoresis (ELS)	(Shi M, Klegerman ME, 1989)
<i>Mycobacterium (BCG vaccine Glaxo)</i>	$\cong 2$	Electrophoresis (ELS)	(Shi M, Klegerman ME, 1989)

## Conclusion

To understand the bacterial cell function and behavior in different physiological conditions, determination of surface charge and the effect of hydrophobicity, zeta potential and isoelectric point are important parameters. Moreover, the zeta potential titration analysis and isoelectric point calculation can be used as a helpful analysis besides other analysis in bacterial research to study physicochemical profiles.

The cell surface components such as phosphate groups in phosphodiester bridge of teichoic acids or at the end of phospholipids, carboxyl group in proteins or peptidoglycan and ammonium groups in peptidoglycan as well as other chemical components are related to different value of isoelectric point (Rijnaarts et al., 1995). At isoelectric point, the particles are less stable and can easily aggregate (Salgın et al., 2012). The negative charge of polysaccharides in gram negative bacteria, determined by phosphate and carboxyl groups, gives the  $pI < 2.8$  (Mozes & Rouxhet, 1987)(Busscher et al., 1990). In gram positive bacteria the ammonium and carboxyl groups give  $pI > 3.8$ , however, the interaction of ammonium and carboxyl groups in different ways may decrease the isoelectric point in these bacteria (Rijnaarts et al., 1995). The differences in the isoelectric point values are also caused by different ionic strength, pH and ion type of the solution (Salgın et al., 2012), as a result there are different values of isoelectric point for the same bacteria in previous studies.

Although there is no direct method to calculate isoelectric point, an indirect zeta potential measurement though pH titration has proven to be useful. Between existing methods to calculate this, Electrophoretic light scattering (ELS) provides an accurate, fast and easy method. Isoelectric point of bacteria as a simple method can be utilized in different field of study as described earlier.

## Bibliography

- Albertsson, P. Å., Sasakawa, S., & Walter, H. (1970). Cross Partition and Isoelectric Points of Proteins. *Undefined*, 228(5278), 1329–1330. <https://doi.org/10.1038/2281329A0>
- Bhattacharjee, S. (2016). DLS and zeta potential - What they are and what they are not? *Journal of Controlled Release : Official Journal of the Controlled Release Society*, 235, 337–351. <https://doi.org/10.1016/J.JCONREL.2016.06.017>
- Busscher, H. J., Bellonfontaine, M. N., Mozes, N., Vandermei, H. C., Sjollem, J., Leonard, A. J., Rouxhet, P. G., & Cerf, O. (1990). An Interlaboratory Comparison of Physicochemical Methods for Studying the Surface-Properties of Microorganisms - Application to Streptococcus-Thermophilus and Leuconostoc-Mesenteroides. *Journal of Microbiological Methods*, 12(2), 101–115. [https://doi.org/Doi 10.1016/0167-7012\(90\)90020-7](https://doi.org/Doi 10.1016/0167-7012(90)90020-7)
- Busscher, H. J., & Elwing, H. (1999). Special issue: Self assembled monolayers and gradient surfaces. *Colloids and Surfaces B-Biointerfaces*, 15(1), 1.
- Cabello-Yeves, P. J., & Rodriguez-Valera, F. (2019). Marine-freshwater prokaryotic transitions require extensive changes in the predicted proteome. *Microbiome*, 7(1), 1–12. <https://doi.org/10.1186/S40168-019-0731-5/FIGURES/6>
- Cowan, M. M., Van der Mei, H. C., Stokroos, I., & Busscher, H. J. (1992). Heterogeneity of surfaces of subgingival bacteria as detected by zeta potential measurements. *Journal of Dental Research*, 71(11), 1803–1806. <https://doi.org/10.1177/00220345920710110701>
- Dittrich, M., & Sibling, S. (2005). Cell surface groups of two picocyanobacteria strains studied by zeta potential investigations, potentiometric titration, and infrared spectroscopy. *Journal of Colloid and Interface Science*, 286(2), 487–495. <https://doi.org/10.1016/J.JCIS.2005.01.029>
- Elevi Bardavid, R., & Oren, A. (2012). Acid-shifted isoelectric point profiles of the proteins in a hypersaline microbial mat: an adaptation to life at high salt concentrations? *Extremophiles : Life under Extreme Conditions*, 16(5), 787–792. <https://doi.org/10.1007/S00792-012-0476-6>
- Gallardo-Moreno, A. M., Navarro-Pérez, M. L., Vadillo-Rodríguez, V., Bruque, J. M., & González-Martín, M. L. (2011). Insights into bacterial contact angles: difficulties in defining hydrophobicity and surface Gibbs energy. *Colloids and Surfaces. B, Biointerfaces*, 88(1), 373–380. <https://doi.org/10.1016/J.COLSURFB.2011.07.016>
- Hadjoudja, S., Deluchat, V., & Baudu, M. (2010). Cell surface characterisation of *Microcystis aeruginosa* and *Chlorella vulgaris*. *Journal of Colloid and Interface Science*, 342(2), 293–299.

<https://doi.org/10.1016/J.JCIS.2009.10.078>

HARDEN, V. P., & HARRIS, J. O. (1953). The isoelectric point of bacterial cells. *Journal of Bacteriology*, 65(2), 198–202. <https://doi.org/10.1128/JB.65.2.198-202.1953/ASSET/26DD6905-5436-4F66-B85F-F8760A70EAF5/ASSETS/JB.65.2.198-202.1953.FP.PNG>

Harkes, G., Feijen, J., & Dankert, J. (1991). Adhesion of Escherichia-Coli on to a Series of Poly(Methacrylates) Differing in Charge and Hydrophobicity. *Biomaterials*, 12(9), 853–860. [https://doi.org/Doi 10.1016/0142-9612\(91\)90074-K](https://doi.org/Doi 10.1016/0142-9612(91)90074-K)

Hermansson, M. (1999). The DLVO theory in microbial adhesion. *Colloids and Surfaces B-Biointerfaces*, 14(1–4), 105–119. [https://doi.org/Doi 10.1016/S0927-7765\(99\)00029-6](https://doi.org/Doi 10.1016/S0927-7765(99)00029-6)

Hermansson, Malte. (1999). The DLVO theory in microbial adhesion. *Colloids and Surfaces B: Biointerfaces*, 14, 105–119. [www.elsevier.nl/locate/colsurfb](http://www.elsevier.nl/locate/colsurfb)

Horká, M., Kubiček, O., Růžička, F., Holá, V., Malinovská, I., & Šlais, K. (2007). Capillary isoelectric focusing of native and inactivated microorganisms. *Journal of Chromatography A*, 1155(2), 164–171. [https://www.academia.edu/18446359/Capillary\\_isoelectric\\_focusing\\_of\\_native\\_and\\_inactivated\\_microorganisms](https://www.academia.edu/18446359/Capillary_isoelectric_focusing_of_native_and_inactivated_microorganisms)

Horká, Marie, Karásek, P., Šalplachta, J., Růžička, F., Vykydalová, M., Kubesová, A., Dráb, V., Roth, M., & Šlais, K. (2013). Capillary isoelectric focusing of probiotic bacteria from cow's milk in tapered fused silica capillary with off-line matrix-assisted laser desorption/ionization time-of-flight mass spectrometry identification. *Analytica Chimica Acta*, 788, 193–199. <https://doi.org/10.1016/J.ACA.2013.05.059>

Horká, Marie, Šalplachta, J., Růžička, F., & Šlais, K. (2019). Utilization of Red Nonionogenic Tenside Labeling, Isoelectric Focusing, and Matrix-Assisted Laser Desorption/Ionization Time-of-Flight Mass Spectrometry in the Identification of Uropathogens in the Presence of a High Level of Albumin. *Undefined*, 5(8), 1348–1356. <https://doi.org/10.1021/ACSINFECDIS.9B00045>

Horká, Marie, Šlais, K., Šalplachta, J., & Růžička, F. (2017). Preparative isoelectric focusing of microorganisms in cellulose-based separation medium and subsequent analysis by CIEF and MALDI-TOF MS. *Analytica Chimica Acta*, 990, 185–193. <https://doi.org/10.1016/J.ACA.2017.08.046>

Horká, Marie, Vykydalová, M., Růžička, F., Šalplachta, J., Holá, V., Dvořáčková, M., Kubesová, A., & Šlais, K. (2014). CIEF separation, UV detection, and quantification of ampholytic

- antibiotics and bacteria from different matrices. *Analytical and Bioanalytical Chemistry*, 406(25), 6285–6296. <https://doi.org/10.1007/S00216-014-8053-8>
- Jachimska, B., Wasilewska, M., & Adamczyk, Z. (2008). Characterization of Globular Protein Solutions by Dynamic Light Scattering, Electrophoretic Mobility, and Viscosity Measurements. *Langmuir*, 24(13), 6867–6872. <https://doi.org/10.1021/LA800548P>
- Jaspers, E., Jo, J., & Overmann, J. (1997). Separation of Bacterial Cells by Isoelectric Focusing, a New Method for Analysis of Complex Microbial Communities. *APPLIED AND ENVIRONMENTAL MICROBIOLOGY*, 63(8), 3176–3181. <https://journals.asm.org/journal/aem>
- Jucker, B. A., Harms, H., & Zehnder, A. J. B. (1996). Adhesion of the positively charged bacterium *Stenotrophomonas (Xanthomonas) maltophilia* 70401 to glass and teflon. *Journal of Bacteriology*, 178(18), 5472–5479. <https://doi.org/DOI 10.1128/jb.178.18.5472-5479.1996>
- Katsikogianni, M., Missirlis, Y. F., Harris, L., & Douglas, J. (2004). Concise review of mechanisms of bacterial adhesion to biomaterials and of techniques used in estimating bacteria-material interactions. *European Cells & Materials*, 8, 37–57. <https://doi.org/10.22203/ECM.V008A05>
- KENNEDY, E. R., & WOODHOUR, A. F. (1956). QUANTITATIVE STUDIES OF DIFFERENTIAL STAINING REACTIONS I. : The Effect of pH on the Quantity of Dye Retained by Bacteria and the Apparent Isoelectric Point1. *Journal of Bacteriology*, 72(4), 447. <https://doi.org/10.1128/JB.72.4.447-450.1956>
- Kłodzińska, E., Szumski, M., Dziubakiewicz, E., Hrynkiewicz, K., Skwarek, E., Janusz, W., & Buszewski, B. (2010). Effect of zeta potential value on bacterial behavior during electrophoretic separation. *Electrophoresis*, 31(9), 1590–1596. <https://doi.org/10.1002/elps.200900559>
- Lim, S. J., Jang, E., Lee, S. H., Yoo, B. H., Kim, S. K., & Kim, T. H. (2013). Antibiotic resistance in bacteria isolated from freshwater aquacultures and prediction of the persistence and toxicity of antimicrobials in the aquatic environment. *Journal of Environmental Science and Health. Part. B, Pesticides, Food Contaminants, and Agricultural Wastes*, 48(6), 495–504. <https://doi.org/10.1080/03601234.2013.761911>
- Luo, K., Jeong, K. B., You, S. M., Lee, D. H., Jung, J. Y., & Kim, Y. R. (2018). Surface-Engineered Starch Magnetic Microparticles for Highly Effective Separation of a Broad Range of Bacteria. *ACS Sustainable Chemistry and Engineering*, 6(10), 13524–13531. <https://doi.org/10.1021/acssuschemeng.8b03611>
- Marshall, K. C., Stout, R., & Mitchell, R. (1971). Mechanism of the Initial Events in the Sorption of Marine Bacteria to Surfaces. *Microbiology*, 68(3), 337–348. <https://doi.org/10.1099/00221287->

- Martinez, R. E., Pokrovsky, O. S., Schott, J., & Oelkers, E. H. (2008). Surface charge and zeta-potential of metabolically active and dead cyanobacteria. *Journal of Colloid and Interface Science*, 323(2), 317–325. <https://doi.org/10.1016/J.JCIS.2008.04.041>
- Miorner, H., Albertsson, P. A., & Kronvall, G. (1982). Isoelectric points and surface hydrophobicity of gram-positive cocci as determined by cross-partition and hydrophobic affinity partition in aqueous two-phase systems. *Infection and Immunity*, 36(1), 227–234. <https://doi.org/10.1128/iai.36.1.227-234.1982>
- Mozes, N., & Rouxhet, P. G. (1987). Methods for Measuring Hydrophobicity of Microorganisms. *Journal of Microbiological Methods*, 6(2), 99–112. [https://doi.org/Doi.10.1016/0167-7012\(87\)90058-3](https://doi.org/Doi.10.1016/0167-7012(87)90058-3)
- Novak, S., Maver, U., Peternel, Š., Venturini, P., Bele, M., & Gaberšček, M. (2009). Electrophoretic deposition as a tool for separation of protein inclusion bodies from host bacteria in suspension. *Colloids and Surfaces A: Physicochemical and Engineering Aspects*, 340(1–3), 155–160. <https://doi.org/10.1016/J.COLSURFA.2009.03.023>
- Oh, J. K., Yegin, Y., Yang, F., Zhang, M., Li, J., Huang, S., Verkhoturov, S. V., Schweikert, E. A., Perez-Lewis, K., Scholar, E. A., Taylor, T. M., Castillo, A., Cisneros-Zevallos, L., Min, Y., & Akbulut, M. (2018). The influence of surface chemistry on the kinetics and thermodynamics of bacterial adhesion. *Scientific Reports*, 8(1). <https://doi.org/10.1038/s41598-018-35343-1>
- Olsson, J., & Glantz, P. O. (1977). Effect of pH and counter ions on the zeta-potential of oral streptococci. *Archives of Oral Biology*, 22(8–9), 461–466. [https://doi.org/10.1016/0003-9969\(77\)90038-3](https://doi.org/10.1016/0003-9969(77)90038-3)
- Otter, D. (2003). PROTEIN | Determination and Characterization. *Encyclopedia of Food Sciences and Nutrition*, 4824–4830. <https://doi.org/10.1016/B0-12-227055-X/00980-9>
- Poortinga, A. T., Bos, R., Norde, W., & Busscher, H. J. (2002). Electric double layer interactions in bacterial adhesion to surfaces. *Surface Science Reports*, 47(1), 1–32. [https://doi.org/10.1016/S0167-5729\(02\)00032-8](https://doi.org/10.1016/S0167-5729(02)00032-8)
- Rijnaarts, H. H. M., Norde, W., Lyklema, J., & Zehnder, A. J. B. (1995). The isoelectric point of bacteria as an indicator for the presence of cell surface polymers that inhibit adhesion. *Colloids and Surfaces B: Biointerfaces*, 4(4), 191–197. [https://doi.org/10.1016/0927-7765\(94\)01164-Z](https://doi.org/10.1016/0927-7765(94)01164-Z)
- Rosan, B. (1981). Microbial adhesion to surfaces. *Science*, 214(4523), 902–903. <https://doi.org/10.1126/science.214.4523.902-a>
- Salgın, S., Salgın, U., & Bahadır, S. (2012). Zeta Potentials and Isoelectric Points of Biomolecules:



- The Effects of Ion Types and Ionic Strengths. *Int. J. Electrochem. Sci*, 7, 12404–12414.  
[www.electrochemsci.org](http://www.electrochemsci.org)
- Šalplachta, J., Horká, M., Růžička, F., & Šlais, K. (2018). Identification of bacterial uropathogens by preparative isoelectric focusing and matrix-assisted laser desorption/ionization time-of-flight mass spectrometry. *Journal of Chromatography. A*, 1532, 232–237.  
<https://doi.org/10.1016/J.CHROMA.2017.11.072>
- Satou, N., Fukunaga, A., & Shintani, H. (1988). Studies on the Adherence of Oral Streptococci on Solid-Surface. *Journal of Dental Research*, 67(4), 736.
- Sebastian, J., Nair, R. R., Swaminath, S., & Ajitkumar, P. (2020). Mycobacterium tuberculosis Cells Surviving in the Continued Presence of Bactericidal Concentrations of Rifampicin in vitro Develop Negatively Charged Thickened Capsular Outer Layer That Restricts Permeability to the Antibiotic. *Frontiers in Microbiology*, 11(December), 1–20.  
<https://doi.org/10.3389/fmicb.2020.554795>
- Shi M, Klegerman ME, G. M. (1989). The effect of washing on the surface charge of Mycobacterium bovis BCG vaccine, Tice substrain. *Microbios*, 60(243), 97–101.
- Skvarla, J. (1993). A Physicochemical Model of Microbial Adhesion. *Journal of the Chemical Society-Faraday Transactions*, 89(15), 2913–2921. <https://doi.org/DOI 10.1039/ft9938902913>
- Smith, D. E., Dhinojwala, A., & Moore, F. B. G. (2019). Effect of Substrate and Bacterial Zeta Potential on Adhesion of Mycobacterium smegmatis. *Langmuir*, 35(21), 7035–7042.  
<https://doi.org/10.1021/acs.langmuir.8b03920>
- Sonohara, R., Muramatsu, N., Ohshima, H., & Kondo, T. (1995). Difference in surface properties between Escherichia coli and Staphylococcus aureus as revealed by electrophoretic mobility measurements. *Biophysical Chemistry*, 55(3), 273–277. [https://doi.org/10.1016/0301-4622\(95\)00004-H](https://doi.org/10.1016/0301-4622(95)00004-H)
- Tan, K. H., Sattari, S., Donskyi, I. S., Cuellar-Camacho, J. L., Cheng, C., Schwibbert, K., Lippitz, A., Unger, W. E. S., Gorbushina, A., Adeli, M., & Haag, R. (2018). Functionalized 2D nanomaterials with switchable binding to investigate graphene-bacteria interactions. *Nanoscale*, 10(20), 9525–9537. <https://doi.org/10.1039/C8NR01347K>
- Tuson, H. H., & Weibel, D. B. (2013). Bacteria-surface interactions. In *Soft Matter* (Vol. 9, Issue 17). <https://doi.org/10.1039/c3sm27705d>
- Van der Mei, H. C., Meinders, J. M., & Busscher, H. J. (1994). The influence of ionic strength and pH on diffusion of micro-organisms with different structural surface features. *Microbiology*, 140(12), 3413–3419. <https://doi.org/10.1099/13500872-140-12-3413>

- Vasudevan, R., Kennedy, A. J., Merritt, M., Crocker, F. H., & Baney, R. H. (2014). Microscale patterned surfaces reduce bacterial fouling-microscopic and theoretical analysis. *Colloids and Surfaces B: Biointerfaces*, 117. <https://doi.org/10.1016/j.colsurfb.2014.02.037>
- Wilson, W. William, Wade, M. M., Holman, S. C., & Champlin, F. R. (2001). Status of methods for assessing bacterial cell surface charge properties based on zeta potential measurements. *Journal of Microbiological Methods*, 43(3), 153–164. [https://doi.org/10.1016/S0167-7012\(00\)00224-4](https://doi.org/10.1016/S0167-7012(00)00224-4)
- Wilson, W W, Wade, M. M., Holman, S. C., & Champlin, F. R. (2001). Status of methods for assessing bacterial cell surface charge properties based on zeta potential measurements. *Journal of Microbiological Methods*, 43(3), 153–164. [https://doi.org/Doi 10.1016/S0167-7012\(00\)00224-4](https://doi.org/Doi%2010.1016/S0167-7012(00)00224-4)
- Yuan, Y., Hays, M. P., Hardwidge, P. R., & Kim, J. (2017). Surface characteristics influencing bacterial adhesion to polymeric substrates. *RSC Advances*, 7(23), 14254–14261. <https://doi.org/10.1039/C7RA01571B>

## CHAPTER 2

### **Correlation between bacterial surface charge (Zeta Potential) and the antigenicity and immunogenicity properties of recombinant *Streptococcus gordonii* vaccine vectors**

Samaneh Gholami, Francesco Iannelli, Antonio Vivi, Riccardo Arrigucci, Karolin  
Hijazi, and Gianni Pozzi

*Laboratory of Molecular Microbiology and Biotechnology, Department of Medical Biotechnologies,  
University of Siena, 53100 Siena, Italy*

Manuscript in preparation

## Abstract

The surface electrical changes, isoelectric point and zeta potential evaluation along with antigenicity and immunogenicity assessments of vaccine vectors are fundamental in vaccine development, microbiology and biotechnology field. The aim of the present work is to study the physicochemical properties of recombinant *Streptococcus gordonii* vaccine vector expressing a heterologous antigen as well as their antigenicity and immunogenicity. To study this we measured isoelectric point and zeta potential of the engineered strains followed by analysis through similarity models, as well as antigenicity by the means of flow cytometry. To evaluate immunogenicity of these bacterial vectors, serum of immunized Balb/c mice were assessed. Zeta potential and isoelectric points measurement showed direct correlation with surface changes. Mutation and deletion of a negative charge protein, RPS, resulted in more positive surface charge. Flow cytometric analysis of the different mutant bacterial strains showed that the absence of the RPS molecule allows a higher heterologous antigen recognition, while the removal of other components do not alter the exposure of H1. The analysis of the H1-specific antibody response in the serum of immunized mice showed that the response induced by the mutant strains for FbpA and GtfG is similar to the non-mutant strain responses. This results indicate that the assessment of physicochemical properties of bacterial vectors can help to understand many complexities of their adhesions, pathogenesis and immunogenicity

## Introduction

The interface between the outer cell layer and the extracellular environment plays a particularly essential role in their overall physiology (Wilson et al., 2001). The outer cell surface mediates exchange and adhesive processes, while also affecting interactions with immunological factors and participating in cell growth and division (Mozes & Rouxhet, 1987).

Interactions between colloidal particles has been described by the DLVO theory, but is also used to describe bacterial adhesion to surfaces. Many studies showed that the DLVO theory cannot fully explain bacterial adhesion or stability of bacteria in suspension (Busscher & Elwing, 1999). Therefore, extended DLVO (XDLVO) theory (Poortinga et al., 2002) in addition to classical DLVO interactions, represent the Lewis acid-base or hydration interaction. The DLVO theory has also been applied to describe bacterial adhesion (Hermansson, 1999; Rosan, 1981; Skvarla, 1993) on biomaterial implants (Harkes et al., 1991) and oral cavity (Satou et al., 1988). In many physiological

conditions, bacterial cell surface conveys a net negative charge depends on the surface components involving ionized carboxylate (in protein, polysaccharide, peptidoglycan), phosphate (in teichoic acids, phospholipids) and amino groups (in proteins and peptidoglycan) (Busscher et al., 1990; Jucker et al., 1996). Upon changes in pH or ionic strength of suspension, these charged group may associate or dissociate from the bacterial membrane (Poortinga et al., 2002). The number of carboxyl and phosphate groups surpass the number of amino groups in physiological pH; therefore, most bacterial cell surfaces are negatively charged. Based on these theories, changed in bacterial surface proteins (contains carboxyl and amino groups) may lead to alteration of bacterial charge distribution.

Many methods are used to characterize bacterial cell surface including proton titration, dielectric spectroscopy and particulate micro-electrophoresis. Particulate micro-electrophoresis reveals the electrokinetic potential (zeta potential) and electrokinetic charge of the bacteria and is the most frequently used method.

The zeta potential is defined as the electric potential at the hydrodynamic plane of shear, the slip plane. The slip plane is the hypothetical interface between a stagnant liquid layer adjacent to the particle surface and the liquid moving relative to the surface during electrophoresis (Lyklema, 1994). Based on morphological heterogeneity of bacterial surface, it is difficult to define the location of the slip plane. Therefore, the zeta potential is often assumed to be equal to the diffuse double layer potential and net cell surface charge can be assessed on the basis of Zeta potential which is the electrical potential of the interfacial surface and the aqueous environment (Saito et al., 1997). While many existing studies have involved the effect of bacterial cell surface properties on the bacterial biofilm and bacterial adhesion to various surface or in different media (Oh et al., 2018; Tuson & Weibel, 2013; Vasudevan et al., 2014; Wilson et al., 2001) there are very few studies done about the how alteration of surface properties in bacteria itself can change the charge distribution on their surface and if these changes are related to different bacterial antigenicity and immunogenicity. The alteration of surface properties in bacteria changes the charge distribution on their surface. To investigate how changes in the bacterial cell surface could possibly alter the bacterial cell surface charge distribution and bacterial immunogenicity, we evaluate the bacterial surface electrical changes as well as antigenicity and immunogenicity of modified strains of *S.gordonii* as bacterial vaccine vectors. Human commensal streptococci, such as *S.gordonii* (human commensal bacterium generally found in the oral cavity and in early dental plaque (Pozzi et al., 1992) and it is likewise a

critical etiologic agent of infectious endocarditis (Douglas et al., 1993; Watanakunakorn & Pantelakis, 1993)), express a large number of surface proteins that allow it to colonize the substrates present in their natural environment within the human organism. The adhesion capacity, therefore, allows interacting with the surface of the epithelial cells, the proteins of the extracellular matrix (EMP) and the surface of other bacterial species (Jenkinson & Lamont, 1997; Kolenbrander & London, 1993; Tanzer et al., 2003) . EMPs are complex proteins that have multiple at functional sites. These sites interact with the cellular component of the tissue, regulating its biological activity and at the same time acting as cell receptors for bacteria that colonize the host. The tissue components that mediate streptococcal adhesion include both extracellular matrix proteins such as laminin (Sommer et al., 1992; Switalski et al., 1987; Vercellotti et al., 1985) , fibronectin, collagen, elastin, vitronectin, decorin, and proteoglycans, and blood proteins such as fibrinogen (Beg et al., 2002; Vaccasmith et al., 1994). The numerous types of interaction involved in the adhesion of *S.gordonii* to EMP determine its success in the colonization in hard and soft tissues (Giomarelli et al., 2006). Microbial adhesins that bind extracellular matrix are collectively known as microbial surface components recognizing adhesive matrix molecules (MSCRAMMs)(Giomarelli et al., 2006; Takahashi et al., 2004; Zhang et al., 2005) including fibronectin-binding protein (FbpA), the polysaccharide of the wall bacterial (RPS) and glucosyltransferases (GtfG):

(i) FpbA has been identified as the second fibronectin binding protein in *S.gordonii*. FbpA falls into the category of atypical proteins binding the fibronectin expressed by streptococci. These proteins contain a conventional sequence composed of regions dedicated to secretion, anchoring, and fibronectin binding. FbpA, like CshA (surface associated protein), binds only to the immobilized form of fibronectin (Lowrance et al., 1990). Inactivation of the FpbA gene has been associated with a significant reduction of adhesion to fibronectin and of the hydrophobicity of the cell surface of *S.gordonii* (Christie et al., 2002).

(ii) The polysaccharide on the *S.gordonii* bacterial wall have the receptor function for bacterial co-aggregation by recognizing the surface adhesins of the other members of oral microbial community. The structural characterization of the RPS results in the identification of 6 different types of RPS (Reddy et al., 1994) recognized as receptors by adhesives binding the galactose or N-Acetyl-galactose arranged on the surface of other bacteria (Cisar et al., 1995). RPS also is closely associated with the antigenicity of the polysaccharide (Cisar et al., 1997; McIntire et al., 1988).

(iii) Glucosyltransferases are enzymes that hydrolyze sucrose and polymerize the glucose fraction to produce glucan. Glucosyltransferase production has been associated with the ability of *S.gordonii* to adhere to hydroxyapatite and therefore glucosyl-transferase plays a role in its colonization at the tooth surface (Vickerman et al., 1995, 1996; Vickerman & Clewell, 1997).

In this study *S.gordonii* mutants of the genes FbpA, RPS, GtfG which expressing on the surface the heterologous antigen H1 of Mycobacterium tuberculosis as well as wild type were studied through the surface electrical changes, antigenicity and immunogenicity to find any possible relation between the cell surface physicochemical properties with antigenicity of these modified strains.

## Material and Methods

### Recombinant strains of *S.gordonii* modified in surface composition

The strains of *S.gordonii* used are summarized in Table 6. Briefly, the surface components FbpA, RPS, GtfG, were deleted by gene inactivation by PCR Gene SOEing on *S.gordonii* V288 (Iannelli & Pozzi, 2004). These mutants were used for the surface expression of the H1 heterologous protein, consisting of the merger of Ag85B and ESAT-6, two antigenic proteins of *M.tuberculosis*. The mutant strains were transformed to express the H1 antigen. The new recombinant strains are selected based on the loss of antibiotic resistance residing in *S.gordonii* and the acquisition of a new resistance, acquired from the donor plasmid (Figure 3). The final structure of vectors was confirmed by PCR and DNA sequence analysis.

Table 6 *S.gordonii* strains and relevant properties.

Strain	Mutated gene(s)	Surface antigen expressed	Inserted cassette (antibiotic resistance)
V288	-	-	-
GP1413	$\Delta$ RPS a	-	
GP1441	-	H1	EM
GP1458	$\Delta$ FbpA,CshA b	H1	SM/EM
GP1459	$\Delta$ RPS	H1	SPC/EM
GP1460	$\Delta$ gtfG c	H1	KM/EM

<sup>a</sup> RPS locus (12662-bp deletion, from nt 983559 to 996221, GenBank acc, TIGR 29390, contig 4353)

<sup>b</sup> FbpA cshA (9255 bp deletion, from nt 646-9900, GenBank acc. no. X65164).

<sup>c</sup> GtfG (4368-bp deletion, from nt 67 to 4434 nt, GenBank acc. no. U12643).



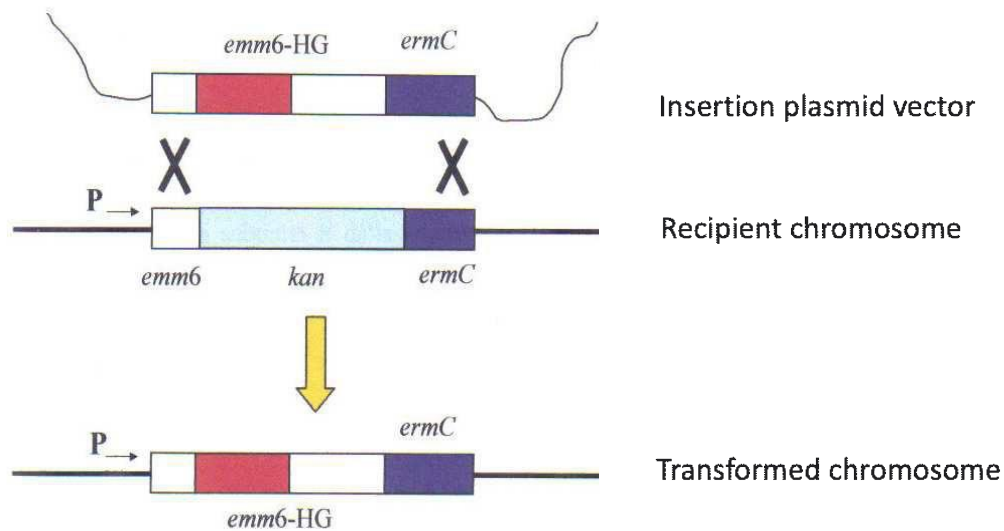


Figure 3 General diagram of the chromosomal integration of an *E. coli* plasmid vector into the *S. gordonii* chromosome. The *E. coli* recombinant plasmid vector contains an antibiotic resistance gene (*ermC*, which confers resistance to erythromycin; in purple) and the fusion between the *emm6* gene (in white) and the gene encoding a heterologous protein (HG; in red). In the recipient strain, two regions of homology with the insertion vector flank the kanamycin antibiotic resistance gene (*kan*, in blue), different from that present in the plasmid. Plasmid DNA is linearized during the transformation process. If gene recombination occurs via a double "cross-over" mechanism, the transformants have the gene fusion and the *ermC* gene integrated into the chromosome and simultaneously lose the *kan* gene. The *emm6*\HG gene fusion is therefore inserted at the chromosomal level downstream of a strong promoter.

### ***Streptococcus gordonii* strains and culture methods**

The bacteria obtained were subcultured on TSA plates (TSB with addition of 1.5% Agar) and 3% horse blood (Liofilchem) over night at 37°C with 5% CO<sub>2</sub>. The isolated bacteria were grown in TSB at 37°C (Tryptic Soy Broth, Becton Dickinson, France) medium, containing suitable antibiotics at the following concentration based on Table 6; Erythromycin at 1 µg/mL, Kanamycin at 500 µg/mL, Streptomycin at 500 µg/mL and Spectinomycin at 100 µg/mL. The culture starters were taken at an optical density at 590 nm (OD<sub>590</sub>) ranging from 0.2 to 0.3 and were stored at -70°C with the addition of 10% glycerol. Bacteria was inoculated 1:100 from starter culture in 50 mL of TSB containing appropriate antibiotics. The growth was carried at 37°C and OD<sub>590</sub> every 30 minutes.

### **Preparation of bacterial solution for zeta potential measurement**

For zeta potential analysis, the Bacteria was inoculated 1:100 from starter in 100 ml TSB without antibiotics. The culture was taken at an optical density 0.5 to 0.6 at 590 nm. Bacterial cell Cultures were centrifuged at 3000g for 15 minutes at room temperature, the supernatant was removed, and pellets were resuspended in appropriate solution, dH<sub>2</sub>O (14MΩ/cm) and different concentration of

Saline solution (0.010, 0.050 and 0.150 M). The optical density of bacterial suspension was set to 0.3 at 590 nm which indicate  $10^6$  CfU/ml of bacteria.

### **Measurement of Zeta potential - Titration**

Zeta potential measurement was carried out by Zetasizer Nano ZS90 instrument (Malvern Instruments Ltd). The zeta potential with pH titration was done on bacterial cell prepared in different concentration of salts. The sample was prepared in dH<sub>2</sub>O as the 0mM concentration and subsequently in 10mM, 50mM and 150mM of Saline. ZEN1010 cell was placed in the Malvern instrument connected to MPT2 titrator. The pH electrode was calibrated in three different pH buffers, 4.01, 7.00 and 9.20. All the zeta potential data were analysed by using the methods such as protein charge and  $f(\kappa a)$  calculator, scattering function tool, SLS Debye Plot and DLS Debye Plot. The data were plotted with R functions.

### **Similarity modelling**

To understand the differences between two curves, selecting the appropriate distance measures is crucial. We designed a statistical similarity model with R software, in which the differences between zeta potential curves of two bacteria were calculated at the same pH. The starting pH of strains solutions were not the same in all bacteria, therefore, we used a statistical fitting model to alienate the zeta potential points. Predicted zeta potential value in fixed pH with interval with step of 0.25 pH unit was calculated with loess (local estimated scatterplot smoothing) which represent local polynomial regression fitting (Shirkhorshidi et al., 2015). Then zeta potential similarities of two bacteria was plotted on a graph with a highlighted 45-degree line.

### **Flow cytometric analysis of recombinant bacterial strains**

The expression of the H1 antigen on the surface of the different *S.gordonii* mutant strains was evaluated by flow cytometric analysis. The bacterial strains were grown in TSB up to the exponential phase and approximately  $1 \times 10^7$  CFU of bacteria were used for each strain. The samples were washed in PBS and centrifuged at 3800g for 5 minutes. The pellet obtained was resuspended in PBS with 1% bovine serum albumin (Sigma, St. Luis, USA), for 30 minutes at 37°C under stirring. The bacteria were again centrifuged and resuspended with 100µl of anti H1 mouse serum (1:300 produced in this laboratory) and incubated for 1 hour at 4°C. After washing with 1% PBS/BSA, the samples were incubated 30 minutes at 37°C with the secondary anti-mouse antibody, conjugated

with fluorescein isothiocyanate (FITC) (Sigma, diluted 1:64). After washing, bacteria were resuspended in 300µl of filtered PBS and analyzed on a flow cytometer (FACScan, Becton Dickinson).

### **Immunization of animals**

Six-week-old female BALB/c mice (Charles River, Italia S.p.A, Lecco) were used for the immunization experiments. Animal maintained in the animal facilities at the University of Siena under specific pathogen free conditions. All animal procedures were in accordance with institutional guidelines. The animals were divided into groups of 6 mice each and inoculated with the strains GP1441, GP1458, GP1459, GP1460 (Table 1). Subcutaneous inoculations were performed at weeks 0, 3 and 6 with 100µl of suspension containing 10<sup>9</sup>CFU of bacteria. Blood was collected at weeks 3, 5 and 8 and serum was stored at -80°C.

### **ELISA assay**

The presence of anti-H1 in mice sera was measured by ELISA. High binding affinity plates (Greiner, Frikenhausen, Germany), were coated with 100µl/well of H1 antigen (0.5µg/ml, Staten Serum Institute) overnight at 4°C. The plates were washed three times and the non-specific sites were blocked by adding 200µl/well of 1% PBS/BSA for 2 hours at 37°C. Individual serum samples were diluted 1:20 in duplicate. After incubating for 3 hours at 37°C, 100µl/well of a solution containing the secondary antibodies, anti-IgG1, IgG2a, IgG2b of mouse (each diluted 1: 1500, Immucor Italia S.r.l.), labelled with alkaline phosphatase, were added. The plates were incubated at 37°C for 2 hours, then 200µl/well of p-nitrophenyl phosphate (Sigma, Phosphatase substrate 1mg/ml), diluted in 10% diethanolamine at pH 10, was added. The plates were read using an ELISA 340 ATC reader at 405 nm (SLT, Lab instruments Germany, Austria).

### **ELISPOT essay**

The production of INF-γ by spleen cells of immunized mice was evaluated using the ELISPOT technique. After disrupting the spleens, cells were centrifuged for 10 minutes at 250g. Red blood cell lysis was performed in 10ml of cold 0.15M NH<sub>4</sub>Cl. Cells were counted in Burker's chamber by 0.1% Trypan Blue (Sigma-Aldrich) dye. For the ELISPOT assay, 96-well Millipore plates incubated with 100µl of anti-INF-γ (Becton-Dickinson, PharMingen) diluted in carbonate buffer to a final

concentration of 10µg/ml. After incubation overnight, 150µl/well of RPMI medium containing 10% fetal bovine serum (SFB) was added for 1 hour at 37°C. Cells were added in triplicate at four different concentrations (3x10<sup>6</sup>, 1x10<sup>6</sup>, 3x10<sup>5</sup> and 1x10<sup>5</sup>). Cell stimulation was carried out with the H1 antigen at a concentration of 20µg/ml. The negative control was set up by distributing only the cells in the wells. The platelet was incubated 24 hours at 37°C with 5% CO<sub>2</sub>. After washing in PBS and Tween20 (BDH, Italy) the cells were discarded, and the biotinylated secondary anti-INF-γ antibody (Becton-Dickinson, PharMingen) was added in PBS and 0.5% BSA at a final concentration of 2µg/ml. After 2 hours incubation the cells were washed with PBS/Tween20 then streptavidin perox (Becton-Dickinson, PharMingen) diluted 1:1000 in 0.05% PBS and Tween20 was added. The plates were incubated for 1 hour at room temperature and washed 3 times with PBS/Tween20 and with PBS alone. DAB substrate [3, 3'- Diaminobenzidine, (Sigma)] was added at a concentration of 1mg/ml dissolved in distilled water. After 15 minutes the membranes were washed 3 times with distilled water. The development of spots was observed with a stereomicroscope (Laica) at a magnification of 20X.

### **THP-1 cell stimulation with *S.gordonii* mutant strains**

The human monocytic THP-1 line, (ATCC number TIB-202(52)) was obtained from the Experimental Zoo prophylactic Institute of Lombardy and Emilia (Brescia). Cells were incubated at 37°C with 5% CO<sub>2</sub> and cell growth was observed daily under a light microscope (Nikon, Eclipse TS100) until maximum cell density (1x10<sup>6</sup> cells/ml) was reached. THP-1 cells were distributed in 96-well round-bottom cell culture plate (SARSTED) at a concentration of 2x10<sup>5</sup> per well in RPMI 1640 medium with L-Glutamine and 10% SFB without addition of antibiotics. Cells were incubated with different doses (100, 30, 10, 3, 1 and 0.3 bacteria/cell) of strains GP1441, GP1458, GP1459, GP1460, at 37°C, with 5% CO<sub>2</sub>, for 18 hours. CD54 surface expression was evaluated by flow cytometric analysis using phycoerythrin (PE) labelled anti-human CD54 monoclonal antibody (20µl /10<sup>6</sup> cells) (PharMingen, BD), incubated at 4°C for 30 minutes. The samples were resuspended in 300 µl of filtered PBS and analyzed on a flow cytometer.

### **Data analysis**

The evaluation of the anti-H1 antibody titer and the expression of the CD54 receptor were performed using the student t-Test. The significance level was set to  $P \leq 0.05$ .

## Results

**The absence of RPS molecule shows a greater exposure of the heterologous antigen on *S.gordonii* surface, while other surface component do not alter the expression of H1.**

The different mutant strains of *S.gordonii* expressing the H1 fusion protein, composed of Ag85B and ESAT-6 of *M. tuberculosis*, were analyzed by the flow cytometer to assess whether the removal of the different surface components changed the recognition of the H1 antigen. The mutant strains were compared with a strain of *S.gordonii* expressing H1 (GP1441) without any mutations, showing a mean fluorescence intensity (MFI) of 35 (Figure 4A). Single deletion of *fbpA* and *gtfG* genes did not induce changes with respect to non-mutant strain GP1441 (Figure 4B). The deletion of the gene coding for RPS has instead led to a substantial increase in MFI (131) with about 90% of the positive population (Figure 4B).

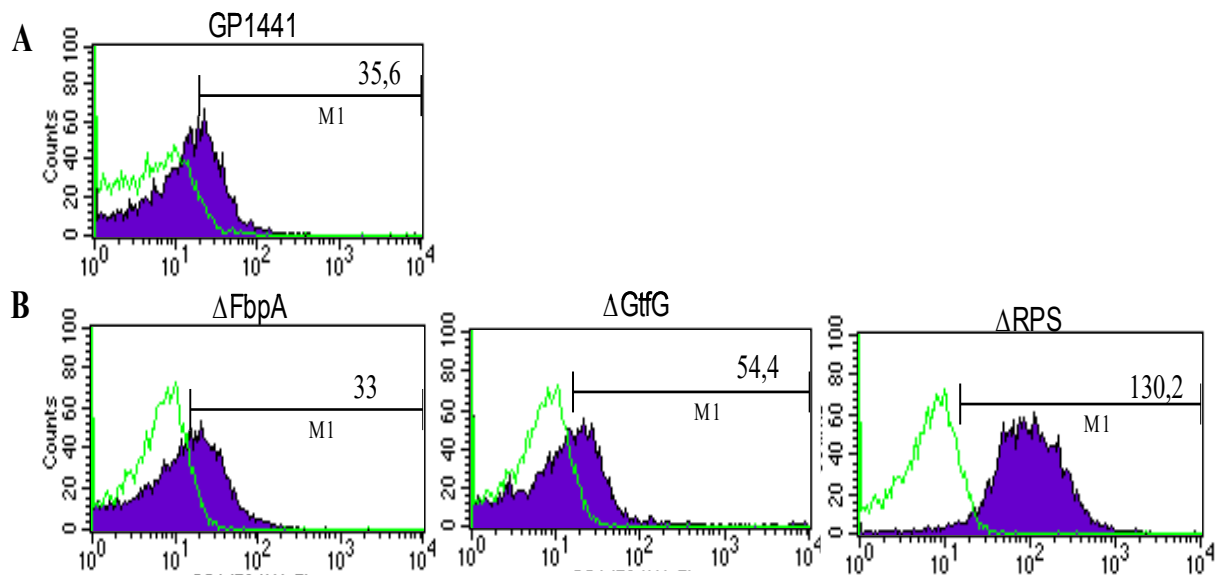


Figure 4 Flow cytometric analysis of *S.gordonii* mutant strains. The different *S.gordonii* mutant strains were analyzed on a flow cytometer to evaluate the expression of the H1 protein. The bacteria were incubated with the anti-H1 polyclonal antibody (diluted 1: 100) and the FITC-conjugated secondary anti-mouse antibody (1:64). The green histogram represents the negative control GP1435 not expressing H1, while the purple histogram represents the expression of the H1 antigen on the surface of the recombinant strains GP1441 (which does not carry surface mutations) (A), GP1458 ( $\Delta FbpA$ ), GP1459 ( $\Delta RPS$ ), GP1460 ( $\Delta GtfG$ ) (B). The value of MFI is reported inside each graph.

## **Removal of surface polysaccharide reduces both the humoral and cellular responses to the H1 antigen expressed on the bacterium.**

To assess whether changes in the surface composition affect the immunogenicity of *S.gordonii*, the presence of H1-specific IgG was evaluated in sera from the immunized mice. The GP1441 expressing H1 strain without gene deletions induced the production of H1-specific serum IgG with increasing titres of  $40 + 9.54$ ,  $320 + 125$  and  $640 + 160$  respectively after the first, second and third immunizations (Figure 5A). These values agree with those observed with recombinant strains expressing different heterologous antigens (32.45.36). The deletions of *fbpA* and *gtfG* did not significantly affect the antibody response, compared to that induced by the GP1441 strain. A significant reduction of the antibody titer was instead observed in the strains with deletion of the RPS molecule. After two immunizations the antibody titer was  $30 + 3.3$  in mice immunized with RPS deletion, compared at the value of 320 induced by the GP1441 strain ( $P < 0.05$ ). Following the third immunization, the antibody titer observed in mice immunized with RPS mutants was  $100 + 24.5$  compared to about 640 of the GP1441 strain ( $P < 0.01$ ).

The induction of a cellular response following subcutaneous immunization was evaluated with the IFN- $\gamma$  assay by ELISPOT technique in spleen cells of mice immunized with *S.gordonii* mutant and non-mutant (GP1441) strains expressing H1 on surface. No significant difference was observed in the H1-specific cellular response induced by *FbpA*, *GtfG* or RPS mutant strains compared to the non-mutant GP1441 strain (Figure 5B), however *fbpA* and *gtfG* deletion showed a reduction in IFN- $\gamma$  production compared to GP1441.

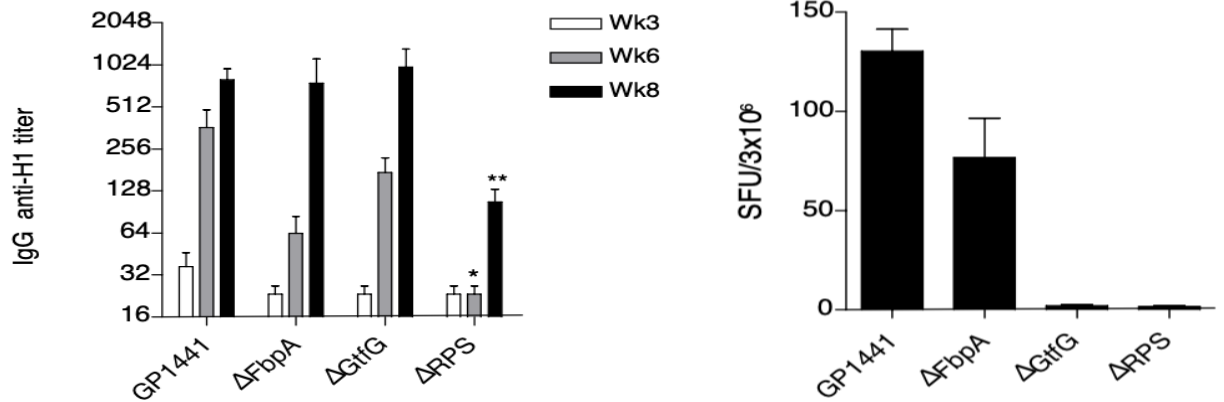


Figure 5 Analysis of serum anti-H1 IgG and production of  $INF-\gamma$  following subcutaneous immunization with *S.gordonii* mutant strains. (A) Six weeks old BALB/c mice were inoculated with the mutant strains GP1458 ( $\Delta FbpA$ ), GP1459 ( $\Delta RPS$ ), GP1460 ( $\Delta GtfG$ ) expressing the H1 protein on the cell surface. The non-mutant strain GP1441 expressing H1 was used as a control. The presence of H1-specific IgG was evaluated by ELISA in single sera collected from mice of each group at weeks 3, 5 and 8 after inoculation. The antibody titer was expressed as the reciprocal of the highest dilution, which, subtracted from the blank value, from an optical density value  $\geq 0.2$ . The values are reported as the geometric mean  $\pm$  SEM of the individual sera for group. \*,  $P \leq 0.05$  and \*\*,  $P \leq 0.01$  compared to the GP1441 control group. (B) Spleen cells obtained from mice immunized subcutaneously with the mutant strains GP1458 ( $\Delta FbpA$ ), GP1459 ( $\Delta RPS$ ), GP1460 ( $\Delta GtfG$ ) and with the non-mutated control strain GP1441, they were stimulated with the H1 antigen. Data are reported as spot-forming unit (SFU)/ $3 \times 10^6$  cell counts obtained by subtracting the value of the non-stimulated cells from that of the stimulated cells.



### **Expression of CD54 does not influenced by the removal of *S.gordonii* surface components.**

In order to assess whether the removal of bacterial surface components influences the expression of the CD54 adhesion molecule (ICAM-1), THP-1 human monocyte line cells have been treated with different doses of the mutant bacterial strains. The intercellular adhesion molecule ICAM-1 is a cell surface transmembrane molecule belonging to the super family of immunoglobulins which allows the initiation of a process called "rolling" that allows the lymphocytes to adhere to the endothelium cells near the sites of inflammation (KINASHI, 2019; Kishimoto et al., 1989). ICAM-1 also plays an important role in presenting antigen to T cells (KINASHI, 2019). Viruses and bacteria are able to induce the expression of the ICAM-1 receptor. Streptococcal interaction studies such as *S.pneumoniae* (Thornton & McDaniel, 2005), *S.suis* serotype 2 (Al-Numani et al., 2003) and *S.gordonii* (Corinti et al., 2000) with monocytic cells of the THP-1 line have demonstrated the induction of ICAM-1 on the cell surface. M. tuberculosis is also able to induce an increase in ICAM-1 expression in THP-1 monocytic line cells (Kishimoto et al., 1989).

The expression of the CD54 surface molecule was evaluated in the human monocytic cell line THP-1 stimulated for 18 and 48 hours with the bacterial strains of *S.gordonii* mutants, at the doses of 100, 30, 10, 3, 1 bacteria cell. The non-mutated strain (GP1441) was used as a control. All the bacterial strains used induced the expression of CD54 at the doses of 100, 30, 10, 3, 1 bacteria per cell, without showing significant differences compared to the non-mutated bacteria (Figure 6). In cells stimulated for 48 hours, no changes in CD54 receptor expression were observed compared to 18 hours (data not shown). These data confirm what reported in the literature regarding the ability of *S.gordonii* to induce the expression of CD54 on human monocytic line THF-1 cells (Al-Numani et al., 2003; Corinti et al., 1999; Thornton & McDaniel, 2005) and show that the expression of this adhesion molecule does not influenced by the removal of the surface components we studied.

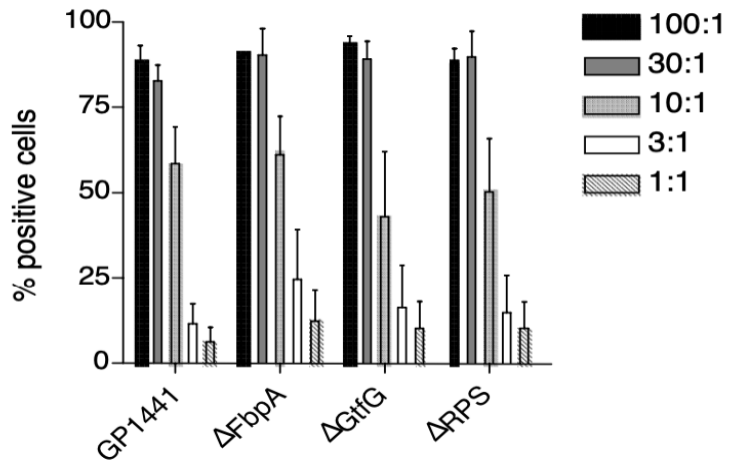


Figure 6 Expression of the CD54 receptor in THP-1 lineage cells. Expression of the CD54 receptor on the surface of THP-1 cells at 18 hours, stimulated with different doses of *S.gordonii* mutant strains and with a non-mutant strain (GP1441). The cells were labeled with the anti-human CD54 monoclonal antibody ( $20\mu\text{l}/10^6$  cells) labeled with phycoerythrin (PE). For doses 100:1, 30:1 and 10:1 the data represent the mean  $\pm$  SD of two independent experiments. Results are reported as a percentage of positive cells.

**The alteration of surface properties in *S.gordonii* changes the charge distribution on their surface.**

Zeta potential measurements were determined as a function of pH in different ionic strength (NaCl concentration; Sodium and Chloride are among common electrolytes in human body). The pH range of 1.5 to 7 for ionic strength of 0 to 150 mM NaCl were examined.

A decrease in pH solution resulted in a decrease in the negative surface charge of bacteria in all ionic strains. However, this reduction was more evident at 0 mM NaCl. With increasing ionic strength (higher NaCl concentration) a significant decline of zeta potential which led to less negative bacterial surface charge is seen, besides the flattening of the titration curve is remarkable in all strains (Figure 7).

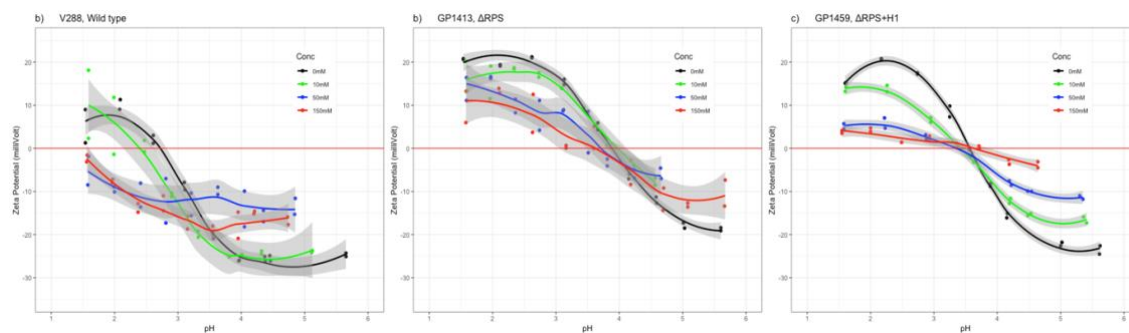


Figure 7 Zeta potential of wild type (A) and modified strains, (B) GP1413, *S.gordonii* with RPS mutation and (C) Zeta potential of GP1459, *S.gordonii* with RPS mutation and insertion of H1, as a function of pH in four different (0, 10, 50, 150 mM) NaCl concentrations. The zeta potential trends become flatten with increasing the ionic strength, also wild type strain V288, loses its isoelectric points. The RPS mutant of *S.gordonii* with expressing H1 antigen GP1459 shows the similar zeta potential trend compared to RPS mutant without expressing heterologous antigen, GP1413, the isoelectric point is detectable in high salt concentration.

In Figure 8 the zeta potential titration of GP1413, *S.gordonii* with RPS mutation, and GP1441, without mutation expressing H1, is shown compared to wildtype in 0 and 150mM salt concentration. Both mutants have more positive surface charge compared to wild type, however, this trend changes at pH more than 4 for GP1441. In higher NaCl concentration, the flattening of the titration curve is remarkable in both strains. In GP1413 the graph still shows positive surface charge at pH less than 4 and negative surface charge distribution at pH more than 4. However, in GP1435 the charge distribution becomes negative and independent of pH.

The correlation similarities compared with wild type in both salt concentrations are shown which indicate GP1441 is more similar to wild type than GP1413. Based on these data, adding H1 protein on the bacterial surface has less effect on changing zeta potential than RPS mutation.

The zeta potential titration of mutants *S.gordonii* expressing H1 compared to wild type were studied and the result were shown in Figure 9, Figure 10 and Figure 11 for GP1458 ( $\Delta$ FbpA), GP1459 ( $\Delta$ RPS) and GP1460 ( $\Delta$ GtfG), respectively. The correlation similarities compared with wild type are shown on the right side of the graphs as well.

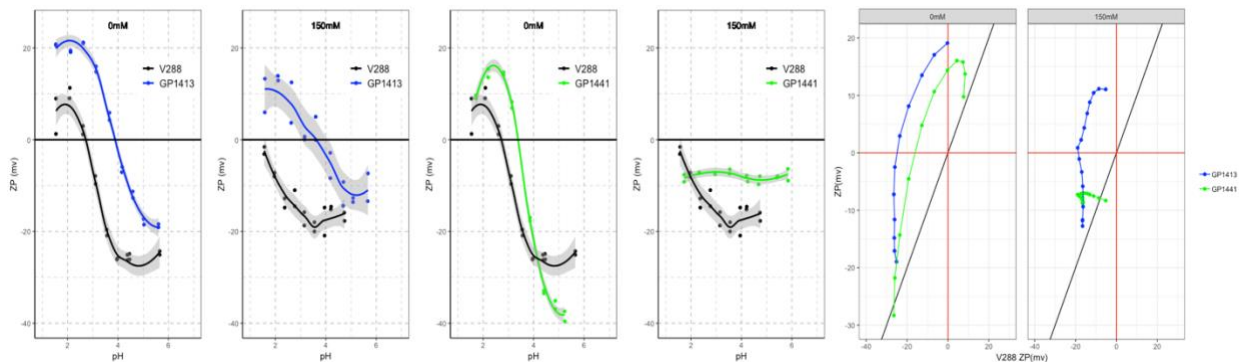


Figure 8 Zeta potential titration *S. gordonii* modified strains. (A) and (B) show the zeta potential titration curve of GP1413 ( $\Delta$ RPS) mutants compared with wild type in 0 and 150mM salt concentration, respectively. In both concentrations, the deletion of RPS make the surface charge of bacteria more positive than wild type. With increasing the ionic strength, the titration curve becomes flatten and more positive. (C) and (D) show the same conditions for GP1441, *S.gordonii* without mutation expressing H1. In 0 mM salt concentration the curve shows more positive surface charge than wild type at pH less than 4 and this trend changes at pH more than 4. With increasing salt concentration, the mutant strain shows more positive surface charge compared with wild type, however, the surface charge is negative and pH independent. (E) and (F) show the similarity models of these strains compared to wild type.

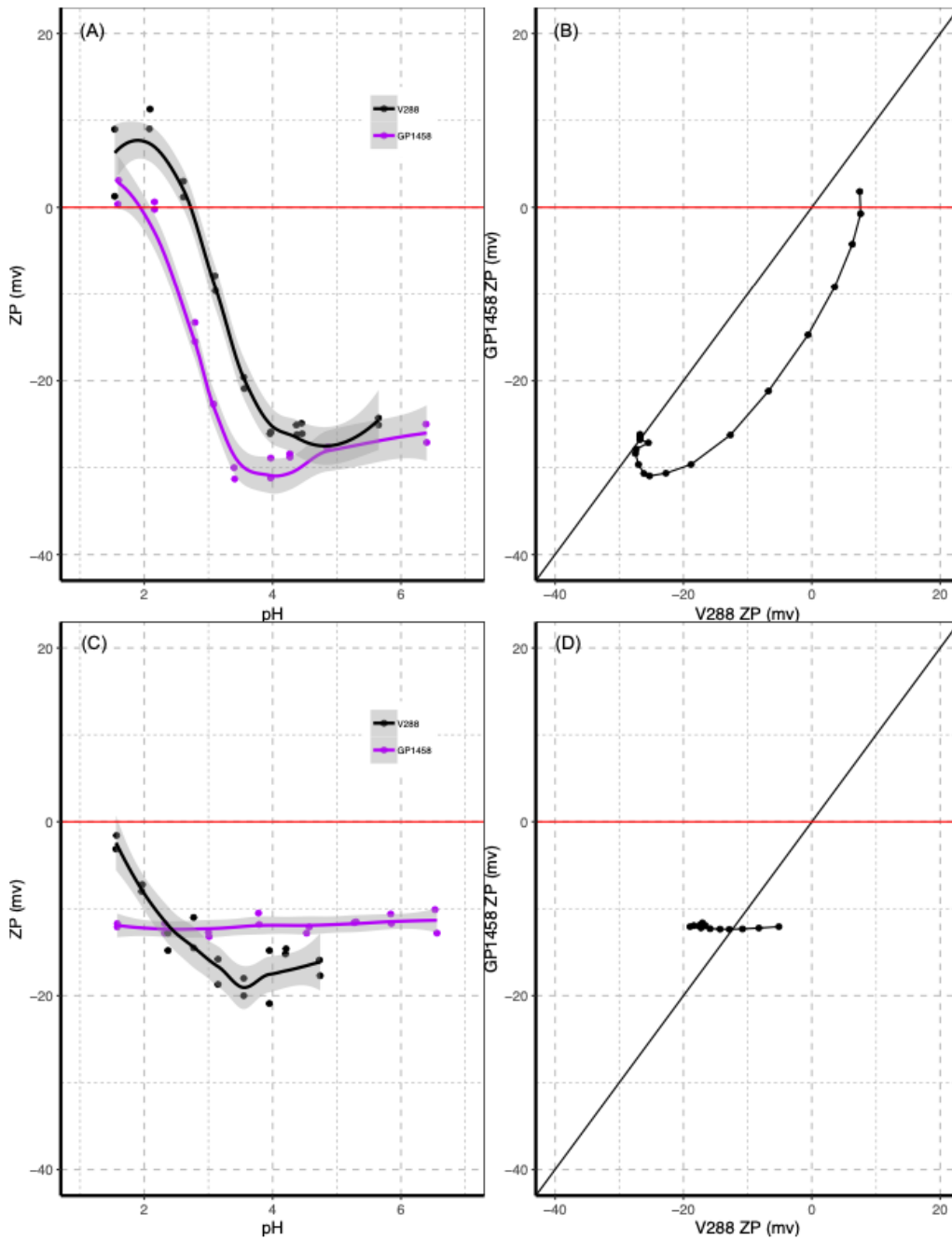


Figure 9 Zeta potential titration and similarity models in GPI1458 *S.gordonii* with *FbpA* mutation expressing HI (purple line) with wild type V288 (black line) in different NaCl concentration. Panel (A) and (C) shows the analysis in 0 mM and 150 mM NaCl concentration respectively. The strain shows more negative surface charge than V288 in lower pH. The positive surface charge distribution is notable in 150 mM NaCl concentration.

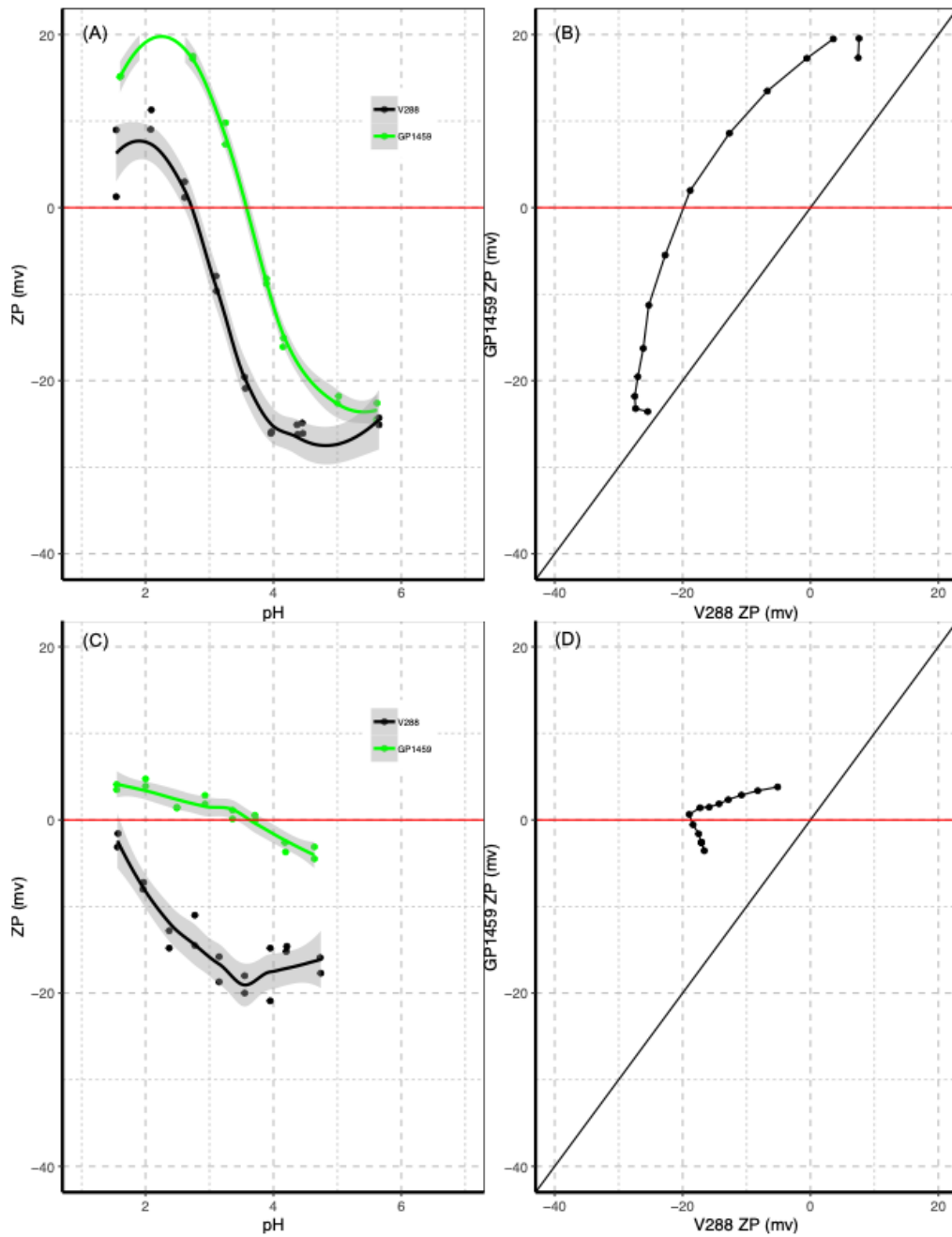


Figure 10 Zeta potential titration analysis in GP1459, *S.gordonii* with  $\Delta$ RPS plus H1 insertion, and V288, wild type *S.gordonii*, with their relative similarity models. Panel (A) and (C) demonstrate V288 (black line) and GP1459 (green line) zeta potential titration curve in two different salt concentration of 0 and 150 mM respectively. Their relative similarity curve is shown in panel (B) and (D). GP1459 shows more positive surface charge than wild type in all salt concentration (data for 10 and 50 mM are not shown). In 0mM concentration the zeta potential titration curve shows the similar trend as wild type curve at pH more than 6 and the similarity graph tend to reach 45-degree line in lower zeta potentials.

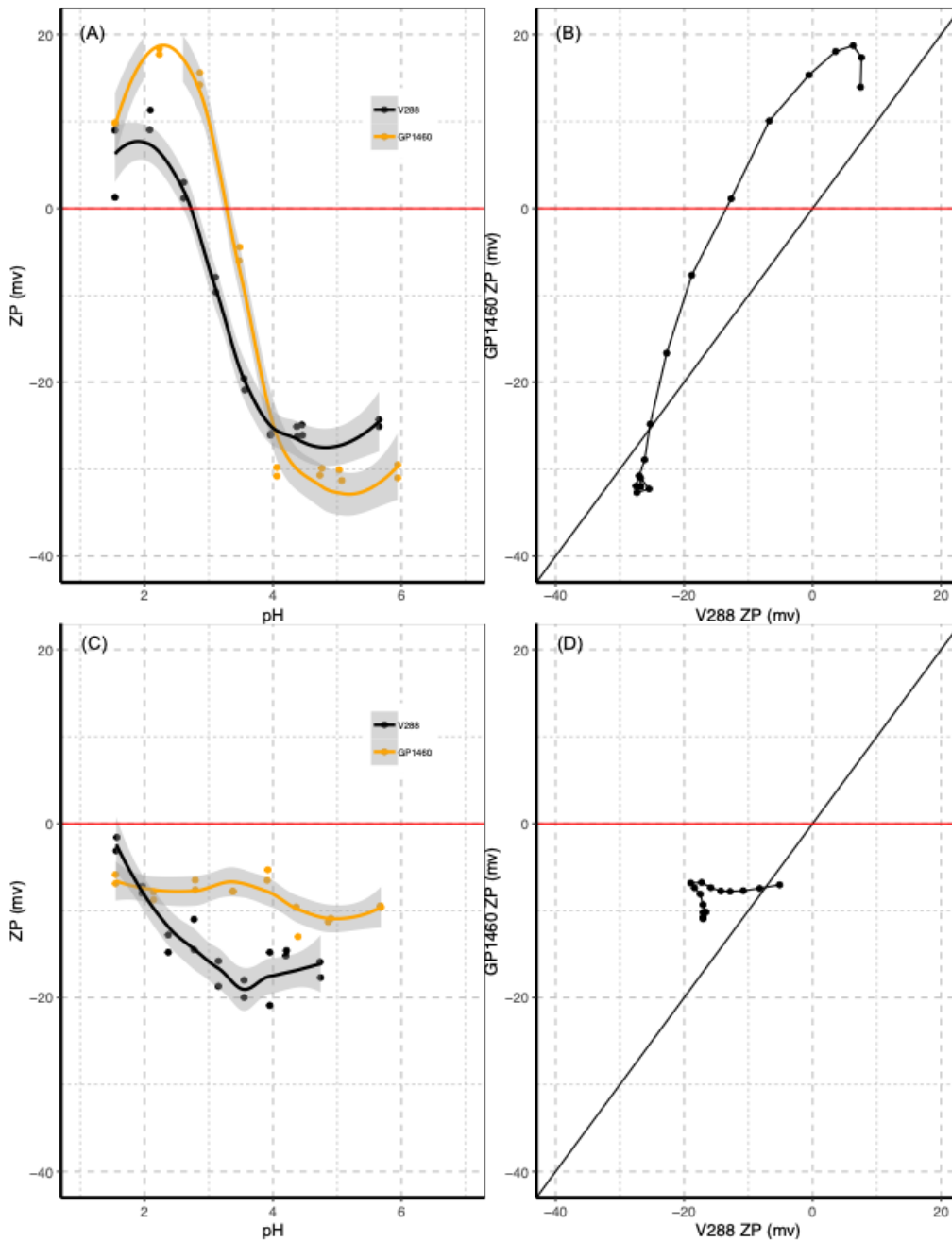


Figure 11 Comparison of Zeta potential titration and similarity models in *S.gordonii* with GtfG expressing H1 (orange line) with wild type (black line). The zeta potential titration curve is shown in 0 mM and 150 mM salt concentration in panel (A) and (C) respectively. The data shows more negative surface charge distribution in higher pH, more than 4 compared to V288. However, it reveals more positive surface charge than V288 in lower pH. The positive surface charge distribution is notable in 150 mM NaCl concentration in panel (C). The similarity analysis showed, although GP1460 has different behavior in zeta potential titration curves compared to wild type, the trends are not far from wild type.

In zeta potential comparison of *S.gordonii* mutants form, GP1458 ( $\Delta$ FbpA) with wild type, revealed the more negative surface charge of mutants form compared with wild type. However, at higher pH (more than 5) the zeta potential titration curve becomes more similar to wild type curve. As shown in Figure 9, the zeta potential titrations in higher concentration becomes more positive than wild type at pH more than 2 and the graph became flat and they lost their isoelectric point, similar to wild type. The similarity model shows the comparisons which are not too far from 45-degree line in Figure 9 right sides.

GP1459 ( $\Delta$ RPS) with expressing H1 shows different behavior compared with wild type and its similarity model proved the high differences in all salt concentrations. The result is shown in Figure 10. GP1459 has more positive surface charge distribution in all pH compared to wild type. GP1459 showed the similar behavior as GP1413 the RPS mutant without expressing heterologous antigen, and their zeta potential titrations curves were similar compared to wildtype. The comparison of GP1441 (with H1 insertion) did not show notable differences with wild type (V288) (data not shown) which was a prove to this.

Analysis of zeta potential titration in *S.gordonii* mutants form, GP1460 ( $\Delta$ GtfG) expressing H1 with wild type, showed slightly more positive surface charge of mutant forms in lower pH (less than 4) and more negative in higher pH (more than 4). The zeta potential titration of GP1460 is similar to wild type based on similarity analysis, however, it has a different trend as shown in Figure 11. With increasing ionic strength, the zeta potential titration curve becomes flat and pH independent.

**IEP of mutant *S.gordonii* indicate the reduction of anionic groups on the surface of bacterium compared to wild type.**

The isoelectric point was calculated through zeta potential pH titration on predicted data. The calculated data were obtained through local polynomial regression fitting. The isoelectric point of *S.gordonii* was 2.72 for wild type (V288), however, a significant variation in the isoelectric point, range from 1.94 to 3.97 was detected in different mutant strains.



Table 7 Isoelectric point (IEP) of *S.gordonii* mutants.

	V288	GP1413	GP1441	GP1458	GP1459	GP1460
0mM	2.72	3.89	3.39	1.94	3.56	3.28
10mM	2.40	3.97	2.70	0.00	3.44	2.90
50mM	0.00	3.71	0.00	0.00	3.35	0.00
150mM	0.00	3.62	0.00	0.00	3.63	0.00

The isoelectric points of mutants *S.gordonii* expressing H1 are shown in Table 7 compared with GP1441 (with expressed H1 and no mutation), GP1413 (with RPS mutation). Between mutants *S.gordonii* expressing H1, GP1458 ( $\Delta$ FbpA) showed the lowest IEP, the pH value of 1.94 and GP1459 ( $\Delta$ RPS) showed the highest IEP at pH value of 3.56.

The isoelectric points less than 2.8 indicate the presence of anionic residues with negative charged phosphate and carboxylic groups on the bacterial surface (Rijnaarts et al., 1995) which was seen in *S.gordonii* wild type with 2.72 (Table 7). With increasing ionic strength most of strains lost their isoelectric point as a result of changes in electromobility and zeta potential with the alteration in conductivity. However, strains with RPS deletion GP1413 and GP1459 did not lose their IEP even in high salt concentration.

## Discussion

In this study we assessed the zeta potential measurement to evaluate bacterial surface charge distribution and isoelectric point (IEP) as well as antigenicity and immunogenicity of modified *S.gordonii* strains. The zeta potential experiment was set with automatic *pH* titration through MPT-2 titrator connected to DLS ZetaSizer Nano ZS90, which start from the *pH* of bacterial sample to final *pH* of 1.5. Four different salt concentrations of 0, 10, 50, 150 mM NaCl were used to analyze the influence of different ionic strength on zeta potential and surface charge distribution. The experiments were done three times for each strain and the average was calculated. All bacteria were cultured in the same condition and selected in mid-exponential growth phase based on their growth curve. A similarity model through graphical tools was described to have better understanding of the zeta potential titration curves. In short, the differences between zeta potential curves of two bacteria were calculated at the same *pH*. The predicted data used by similarity model are calculated by local polynomial regression fitting.

In vitro and in vivo studies, mutant strains of the *fbpA*, *RPS*, *gtfG* genes and the unmutated control strain were used to study antigenicity and immunogenicity. Flow cytometric analysis of the different mutant bacterial strains, carried out by using H1-specific antibodies, it has shown that the absence of the *RPS* molecule allows a higher heterologous antigen recognition, while the removal of other components do not alter the exposure of H1. The immunogenicity of mutant strains expressing H1 has been studied in subcutaneously immunized Balb/c mice. The analysis of the H1-specific antibody response in the serum of immunized mice showed that the response induced by the mutant strains for *FbpA* and *GtfG* is similar to the non-mutant strain responses. In contrast, *RPS* mutant strains (surface polysaccharide) induced a significantly reduction of specific IgG H1 response compared to the non-mutated control. The study of cellular response, analysis of the production of IFN-gamma by ELISPOT assay, showed a significant reduction in production of IFN-gamma in mice immunized with *RPS* mutant strains. A reduced IFN-gamma response was also observed in mice immunized with the *GtfG* mutated strain whose removal had not influenced the humoral response. The interaction of the mutant bacteria in vitro assay with human monocytic cell line THP-1 has been shown that the expression of the adhesion molecule CD54 on THP-1 cells is not affected by the removal of bacterial surface components studied.

Different modification on *S.gordonii* surface alter the zeta potential measurements, beside changing the isoelectric points in different ionic strength. The mutants *S.gordonii* expressing H1 showed different isoelectric points. The isoelectric points less than 2.8 indicate the presence of anionic residues with negative charged phosphate and carboxylic groups on the bacterial surface (Rijnaarts et al., 1995) which was seen in *S.gordonii* wild type with 2.72. The IEP of *S.gordonii* mutants were higher than 3.2 indicating that there is a remarkable reduction of anionic groups on the surface of GP1459. Therefore, we can conclude that the mutant strains would not have limitation in attachment because of steric interaction of anionic groups. However, more studies should be done to confirm this hypothesis.

In zeta potential analysis, with increasing salt concentration, all bacteria revealed less electronegativity as a result of raising the solution conductivity. Also, they lost their isoelectric points in higher ionic strength and the zeta potential titration curves become flat and *pH* independent.

Mutants *S.gordonii* expressing H1 showed different zeta potential compared to the wild type in *pH* gradient. GP1459 (with  $\Delta$ RPS and expressing H1) showed more positive surface charge distribution (Figure 10), also it has the less adhesion to collagen proteins (Giomarelli et al., 2006) and less immunogenicity (data not shown) in comparison with GP1458 and GP1460, other mutants *S.gordonii* expressing H1. Other mutants showed different zeta potential titration behavior, more positive in some part of zeta potential titration curve and more negative in other parts compared to wild type, however their trends were not too far from wild type trend in general as shown by similarity model. Between mutant strains we studied GP1458 (with  $\Delta$ fbpA expressing H1) showed more similar zeta potential trend and IEP to wild type than other mutants, also had similar antigenicity and immunogenicity to non-mutant strain. This result highlights the correlation of surface charge distribution and adhesion and/or immunogenicity profile of *S.gordonii* mutants.

Our data showed the differences of zeta potential measures in different bacteria which can be influenced by *pH*, ionic strength and more important, the surface modifications both with deletion and insertion of a chemical groups. Based on previous studies, mutant *S.gordonii* has different binding profile to extracellular matrix proteins (Giomarelli et al., 2006) and different mutants of *S.gordonii* expressing H1 showed different immunogenicity profile (data not published). The mutants with more positive surface charge showed less immunogenicity (GP1459), however, more studies should be conducted to have a precise conclusion.

Evaluating zeta potential titration provide a comparison of bacterial surface charge distribution in different pH and ionic strength. The knowledge of physicochemical properties of bacteria and mutant strains expressing heterologous antigens can help to understand many complexities of their adhesions, pathogenesis and immunogenicity. Moreover, the zeta potential titration analysis can be used as a helpful analysis besides other analysis in bacterial research to study physicochemical profiles.

## References

- Al-Numani, D., Segura, M., Doré, M., & Gottschalk, M. (2003). Up-regulation of ICAM-1, CD11a/CD18 and CD11c/CD18 on human THP-1 monocytes stimulated by Streptococcus suis serotype 2. *Clinical and Experimental Immunology*, *133*(1). <https://doi.org/10.1046/j.1365-2249.2003.02189.x>
- Beg, A. M., Jones, M. N., Miller-Torbert, T., & Holt, R. G. (2002). Binding of Streptococcus mutans to extracellular matrix molecules and fibrinogen. *Biochemical and Biophysical Research Communications*, *298*(1), 75–79. [https://doi.org/Pii S0006-291x\(02\)02390-2](https://doi.org/Pii%20S0006-291x(02)02390-2) Doi 10.1016/S0006-291x(02)02390-2
- Busscher, H. J., Bellonfontaine, M. N., Mozes, N., Vandermei, H. C., Sjollem, J., Leonard, A. J., Rouxhet, P. G., & Cerf, O. (1990). An Interlaboratory Comparison of Physicochemical Methods for Studying the Surface-Properties of Microorganisms - Application to Streptococcus-Thermophilus and Leuconostoc-Mesenteroides. *Journal of Microbiological Methods*, *12*(2), 101–115. [https://doi.org/Doi 10.1016/0167-7012\(90\)90020-7](https://doi.org/Doi%2010.1016/0167-7012(90)90020-7)
- Busscher, H. J., & Elwing, H. (1999). Special issue: Self assembled monolayers and gradient surfaces. *Colloids and Surfaces B-Biointerfaces*, *15*(1), 1. %3CGo
- Christie, J., McNab, R., & Jenkinson, H. F. (2002). Expression of fibronectin-binding protein FbpA modulates adhesion in Streptococcus gordonii. *Microbiology-Sgm*, *148*, 1615–1625. [https://doi.org/Doi 10.1099/00221287-148-6-1615](https://doi.org/Doi%2010.1099/00221287-148-6-1615)
- Cisar, J. O., Sandberg, A. L., Abeygunawardana, C., Reddy, G. P., & Bush, C. A. (1995). Lectin Recognition of Host-Like Saccharide Motifs in Streptococcal Cell-Wall Polysaccharides. *Glycobiology*, *5*(7), 655–662. [https://doi.org/DOI 10.1093/glycob/5.7.655](https://doi.org/DOI%2010.1093/glycob/5.7.655)
- Cisar, J. O., Sandberg, A. L., Reddy, G. P., Abeygunawardana, C., & Bush, C. A. (1997). Structural and antigenic types of cell wall polysaccharides from viridans group streptococci with receptors for oral actinomyces and streptococcal lectins. *Infection and Immunity*, *65*(12), 5035–5041. %3CGo
- Corinti, S., Medaglini, D., Cavani, A., Rescigno, M., Pozzi, G., Ricciardi-Castagnoli, P., & Girolomoni, G. (1999). Human dendritic cells very efficiently present a heterologous antigen expressed on the surface of recombinant gram-positive bacteria to CD4+ T lymphocytes. *Journal of Immunology (Baltimore, Md. : 1950)*, *163*(6).
- Corinti, S., Medaglini, D., Prezzi, C., Cavani, A., Pozzi, G., & Girolomoni, G. (2000). Human dendritic cells are superior to B cells at presenting a major histocompatibility complex class II-

- restricted heterologous antigen expressed on recombinant *Streptococcus gordonii*. *Infection and Immunity*, 68(4), 1879–1883. [https://doi.org/Doi 10.1128/Iai.68.4.1879-1883.2000](https://doi.org/Doi%2010.1128/Iai.68.4.1879-1883.2000)
- Douglas, C. W., Heath, J., Hampton, K. K., & Preston, F. E. (1993). Identity of viridans streptococci isolated from cases of infective endocarditis. *J Med Microbiol*, 39(3), 179–182. <https://doi.org/10.1099/00222615-39-3-179>
- Giomarelli, B., Visai, L., Hijazi, K., Rindi, S., Ponzio, M., Iannelli, F., Speziale, P., & Pozzi, G. (2006). Binding of *Streptococcus gordonii* to extracellular matrix proteins. *Fems Microbiology Letters*, 265(2), 172–177. <https://doi.org/10.1111/j.1574-6968.2006.00479.x>
- Harkes, G., Feijen, J., & Dankert, J. (1991). Adhesion of *Escherichia-Coli* on to a Series of Poly(Methacrylates) Differing in Charge and Hydrophobicity. *Biomaterials*, 12(9), 853–860. [https://doi.org/Doi 10.1016/0142-9612\(91\)90074-K](https://doi.org/Doi%2010.1016/0142-9612(91)90074-K)
- Hermansson, M. (1999). The DLVO theory in microbial adhesion. *Colloids and Surfaces B-Biointerfases*, 14(1–4), 105–119. [https://doi.org/Doi 10.1016/S0927-7765\(99\)00029-6](https://doi.org/Doi%2010.1016/S0927-7765(99)00029-6)
- Iannelli, F., & Pozzi, G. (2004). Method for introducing specific and unmarked mutations into the chromosome of *Streptococcus pneumoniae*. *Mol Biotechnol*, 26(1), 81–86. <https://doi.org/10.1385/MB:26:1:81>
- Jenkinson, H. F., & Lamont, R. J. (1997). Streptococcal adhesion and colonization. *Critical Reviews in Oral Biology & Medicine*, 8(2), 175–200. [https://doi.org/Doi 10.1177/10454411970080020601](https://doi.org/Doi%2010.1177/10454411970080020601)
- Jucker, B. A., Harms, H., & Zehnder, A. J. B. (1996). Adhesion of the positively charged bacterium *Stenotrophomonas (Xanthomonas) maltophilia* 70401 to glass and teflon. *Journal of Bacteriology*, 178(18), 5472–5479. [https://doi.org/DOI 10.1128/jb.178.18.5472-5479.1996](https://doi.org/DOI%2010.1128/jb.178.18.5472-5479.1996)
- KINASHI, T. (2019). Leukocyte integrins and their regulation. *Japanese Journal of Thrombosis and Hemostasis*, 30(4). <https://doi.org/10.2491/jjsth.30.586>
- Kishimoto, T. K., Larson, R. S., Corbi, A. L., Dustin, M. L., Staunton, D. E., & Springer, T. A. (1989). The Leukocyte Integrins. *Advances in Immunology*, 46(C). [https://doi.org/10.1016/S0065-2776\(08\)60653-7](https://doi.org/10.1016/S0065-2776(08)60653-7)
- Kolenbrander, P. E., & London, J. (1993). Adhere Today, Here Tomorrow - Oral Bacterial Adherence. *Journal of Bacteriology*, 175(11), 3247–3252. [https://doi.org/DOI 10.1128/jb.175.11.3247-3252.1993](https://doi.org/DOI%2010.1128/jb.175.11.3247-3252.1993)
- Lowrance, J. H., Baddour, L. M., & Simpson, W. A. (1990). The Role of Fibronectin Binding in the Rat Model of Experimental Endocarditis Caused by *Streptococcus-Sanguis*. *Journal of Clinical Investigation*, 86(1), 7–13. [https://doi.org/Doi 10.1172/Jci114717](https://doi.org/Doi%2010.1172/Jci114717)

- Lyklema, J. (1994). On the Slip Process in Electrokinetics. *Colloids and Surfaces A-Physicochemical and Engineering Aspects*, 92(1–2), 41–49. [https://doi.org/Doi 10.1016/0927-7757\(94\)02727-7](https://doi.org/Doi 10.1016/0927-7757(94)02727-7)
- Mcintire, F. C., Crosby, L. K., Vatter, A. E., Cisar, J. O., Mcneil, M. R., Bush, C. A., Tjoa, S. S., & Fennessey, P. V. (1988). A Polysaccharide from Streptococcus-Sanguis 34 That Inhibits Coaggregation of S-Sanguis 34 with Actinomyces-Viscosus T14v. *Journal of Bacteriology*, 170(5), 2229–2235. <https://doi.org/DOI 10.1128/jb.170.5.2229-2235.1988>
- Mozes, N., & Rouxhet, P. G. (1987). Methods for Measuring Hydrophobicity of Microorganisms. *Journal of Microbiological Methods*, 6(2), 99–112. [https://doi.org/Doi 10.1016/0167-7012\(87\)90058-3](https://doi.org/Doi 10.1016/0167-7012(87)90058-3)
- Oh, J. K., Yegin, Y., Yang, F., Zhang, M., Li, J., Huang, S., Verkhoturov, S. V., Schweikert, E. A., Perez-Lewis, K., Scholar, E. A., Taylor, T. M., Castillo, A., Cisneros-Zevallos, L., Min, Y., & Akbulut, M. (2018). The influence of surface chemistry on the kinetics and thermodynamics of bacterial adhesion. *Scientific Reports*, 8(1). <https://doi.org/10.1038/s41598-018-35343-1>
- Poortinga, A. T., Bos, R., Norde, W., & Busscher, H. J. (2002). Electric double layer interactions in bacterial adhesion to surfaces. In *Surface Science Reports* (Vol. 47, Issue 1, pp. 1–32). Elsevier. [https://doi.org/10.1016/S0167-5729\(02\)00032-8](https://doi.org/10.1016/S0167-5729(02)00032-8)
- Pozzi, G., Oggioni, M. R., Manganelli, R., & Fischetti, V. A. (1992). Expression of M6 Protein Gene of Streptococcus-Pyogenes in Streptococcus-Gordonii after Chromosomal Integration and Transcriptional Fusion. *Research in Microbiology*, 143(5), 449–457. [https://doi.org/Doi 10.1016/0923-2508\(92\)90090-B](https://doi.org/Doi 10.1016/0923-2508(92)90090-B)
- Reddy, G. P., Abeygunawardana, C., Bush, C. A., & Cisar, J. O. (1994). The Cell-Wall Polysaccharide of Streptococcus-Gordonii-38 - Structure and Immunochemical Comparison with the Receptor Polysaccharides of Streptococcus-Oralis-34 and Streptococcus-Mitis J22. *Glycobiology*, 4(2), 183–192. <https://doi.org/DOI 10.1093/glycob/4.2.183>
- Rijnaarts, H. H. M., Norde, W., Lyklema, J., & Zehnder, A. J. B. (1995). The Isoelectric Point of Bacteria as an Indicator for the Presence of Cell-Surface Polymers That Inhibit Adhesion. *Colloids and Surfaces B-Biointerfaces*, 4(4), 191–197. [https://doi.org/Doi 10.1016/0927-7765\(94\)01164-Z](https://doi.org/Doi 10.1016/0927-7765(94)01164-Z)
- Rosan, B. (1981). Microbial adhesion to surfaces. *Science*, 214(4523), 902–903. <https://doi.org/10.1126/science.214.4523.902-a>
- Saito, T., Takatsuka, T., Kato, T., Ishihara, K., & Okuda, K. (1997). Adherence of oral streptococci to an immobilized antimicrobial agent. *Archives of Oral Biology*, 42(8), 539–545.

[https://doi.org/Doi.10.1016/S0003-9969\(97\)00054-X](https://doi.org/Doi.10.1016/S0003-9969(97)00054-X)

- Satou, N., Fukunaga, A., & Shintani, H. (1988). Studies on the Adherence of Oral Streptococci on Solid-Surface. *Journal of Dental Research*, *67*(4), 736. %3CGo
- Shirkhorshidi, A. S., Aghabozorgi, S., & Wah, T. Y. (2015). A Comparison Study on Similarity and Dissimilarity Measures in Clustering Continuous Data. *Plos One*, *10*(12). <https://doi.org/ARTN.e0144059> 10.1371/journal.pone.0144059
- Skvarla, J. (1993). A Physicochemical Model of Microbial Adhesion. *Journal of the Chemical Society-Faraday Transactions*, *89*(15), 2913–2921. <https://doi.org/DOI.10.1039/ft9938902913>
- Sommer, P., Gleyzal, C., Guerret, S., Etienne, J., & Grimaud, J. A. (1992). Induction of a putative laminin-binding protein of *Streptococcus gordonii* in human infective endocarditis. *Infect Immun*, *60*(2), 360–365. <https://www.ncbi.nlm.nih.gov/pubmed/1530927>
- Switalski, L. M., Murchison, H., Timpl, R., Curtiss, R., & Hook, M. (1987). Binding of Laminin to Oral and Endocarditis Strains of Viridans Streptococci. *Journal of Bacteriology*, *169*(3), 1095–1101. <https://doi.org/DOI.10.1128/jb.169.3.1095-1101.1987>
- Takahashi, Y., Yajima, A., Cisar, J. O., & Konishi, K. (2004). Functional analysis of the *Streptococcus gordonii* DL1 sialic acid-binding adhesin and its essential role in bacterial binding to platelets. *Infection and Immunity*, *72*(7), 3876–3882. <https://doi.org/10.1128/Iai.72.7.3876-3882.2004>
- Tanzer, J. M., Grant, L., Thompson, A., Li, L., Rogers, J. D., Haase, E. M., & Scannapieco, F. A. (2003). Amylase-binding proteins A (AbpA) and B (AbpB) differentially affect colonization of rats' teeth by *Streptococcus gordonii*. *Microbiology*, *149*(Pt 9), 2653–2660. <https://doi.org/10.1099/mic.0.26022-0>
- Thornton, J., & McDaniel, L. S. (2005). THP-1 monocytes up-regulate intercellular adhesion molecule 1 in response to pneumolysin from *Streptococcus pneumoniae*. *Infection and Immunity*, *73*(10). <https://doi.org/10.1128/IAI.73.10.6493-6498.2005>
- Tuson, H. H., & Weibel, D. B. (2013). Bacteria-surface interactions. In *Soft Matter* (Vol. 9, Issue 17). <https://doi.org/10.1039/c3sm27705d>
- Vaccasmith, A. M., Jones, C. A., Levine, M. J., & Stinson, M. W. (1994). Glucosyltransferase Mediates Adhesion of *Streptococcus-Gordonii* to Human Endothelial-Cells in-Vitro. *Infection and Immunity*, *62*(6), 2187–2194. %3CGo
- Vasudevan, R., Kennedy, A. J., Merritt, M., Crocker, F. H., & Baney, R. H. (2014). Microscale patterned surfaces reduce bacterial fouling-microscopic and theoretical analysis. *Colloids and Surfaces B: Biointerfaces*, *117*. <https://doi.org/10.1016/j.colsurfb.2014.02.037>



- Vercellotti, G. M., McCarthy, J. B., Lindholm, P., Peterson, P. K., Jacob, H. S., & Furcht, L. T. (1985). Extracellular-Matrix Proteins (Fibronectin, Laminin, and Type-Iv Collagen) Bind and Aggregate Bacteria. *American Journal of Pathology*, *120*(1), 13–21. %3CGo
- Vickerman, M. M., & Clewell, D. B. (1997). Regulation of *Streptococcus gordonii* glucosyltransferase. *Streptococci and the Host*, *418*, 661–664. %3CGo
- Vickerman, M. M., Sulavik, M. C., & Clewell, D. B. (1995). Molecular analysis of *Streptococcus gordonii* glucosyltransferase phase variants. *Genetics of Streptococci, Enterococci and Lactococci*, *85*, 309–314. %3CGo
- Vickerman, M. M., Sulavik, M. C., Minick, P. E., & Clewell, D. B. (1996). Changes in the carboxyl-terminal repeat region affect extracellular activity and glucan products of *Streptococcus gordonii* glucosyltransferase. *Infection and Immunity*, *64*(12), 5117–5128. %3CGo
- Watanakunakorn, C., & Pantelakis, J. (1993). Alpha-hemolytic streptococcal bacteremia: a review of 203 episodes during 1980-1991. *Scand J Infect Dis*, *25*(4), 403–408.  
<https://www.ncbi.nlm.nih.gov/pubmed/8248738>
- Wilson, W. W., Wade, M. M., Holman, S. C., & Champlin, F. R. (2001). Status of methods for assessing bacterial cell surface charge properties based on zeta potential measurements. *Journal of Microbiological Methods*, *43*(3), 153–164. [https://doi.org/Doi.10.1016/S0167-7012\(00\)00224-4](https://doi.org/Doi.10.1016/S0167-7012(00)00224-4)
- Zhang, Y., Lei, Y., Nobbs, A., Khammanivong, A., & Herzberg, M. C. (2005). Inactivation of *Streptococcus gordonii* SspAB alters expression of multiple adhesin genes. *Infection and Immunity*, *73*(6), 3351–3357. <https://doi.org/10.1128/IAI.73.6.3351-3357.2005>

## CHAPTER 3

The human pathogen *Streptococcus pneumoniae*

## Introduction

*Streptococcus pneumoniae* or pneumococcus was first isolated in 1881, and the long history of research on this Gram-positive bacterium has yielded numerous scientific discoveries of landmark importance, including Gram staining, bacterial transformation, and the acute phase response (Ablij & Meinders, 2002; Watson et al., 1993).

*Streptococcus pneumoniae* is an extracellular encapsulated Gram-positive facultative anaerobe. Morphologically they are lancet-shaped cocci (elongated spheres) with diameter from 0.5 to 2 micrometers. This pathogen is non-motile, catalase negative, optochin-sensitive, and does not form spores (Avery et al., 1944; Lanie et al., 2007).

Currently, over 95 different serotype structures have been identified based on its polysaccharide capsule, which covers is made of peptidoglycans and unique teichoic acid structures (Weiser et al., 2018). All these serotypes differ in virulence capabilities, prevalence, and drug resistance (Geno et al., 2015). Between them serotypes 1, 4 and 7F are typically found associated with invasive diseases, and 6B, 14, 19F, and 23F are commonly found in the nasopharynx of carriers, which play a role in transmission (Sandgren et al., 2005). Serotypes 6B, 14, 19F, and 23F still have the ability to cause invasive disease as well.

Pneumococcus lacks environmental reservoirs and commonly establishes asymptomatic residence in healthy individuals nasopharynxes (Weiser, 2010). The natural reservoir of *S. pneumoniae* is the human nasopharynx, and colonization of children is especially common, with essentially all children being colonized multiple times by the age of two (Gray et al., 1980). The disease is transmitted from person to person through direct contact of respiratory secretions by droplets or aerosols (sneezing and coughing). Depending on the entry route, pneumococcus can lead to otitis media, meningitis, pneumonia, and other manifestations (Weiser et al., 2018).

Pneumococcus colonizes the nasopharynx (Bogaert et al., 2004; van der Poll & Opal, 2009) and attach to epithelial cells of the nasopharyngeal cavity and reside for short periods of time (Siegel & Weiser, 2015). Colonization occurs through pneumococcal binding to cell-surface carbohydrates such as N-acetyl glucosamine on the non- inflamed epithelium (Bogaert et al., 2004; Henriques-Normark & Tuomanen, 2013). Pneumococcus prevalence and asymptomatic colonization of upper

respiratory tracts and its ability to translocate into the distal lung, blood, and other organs and cause severe invasive disease, as well as the rise of antibiotic resistance and its ability to escape the immune response, affords it to be considered as one of the most important causes of morbidity and mortality world-wide and highlights the need for a better understanding of our immune responses (Kadioglu et al., 2008; Örtqvist et al., 2005; van der Poll & Opal, 2009).

Between these diseases caused by pneumococcus, pneumonia still remains as one of the leading causes of morbidity and mortality in the United States. According to the World Health Organization (WHO), pneumonia is the largest cause of death in children worldwide with the highest prevalence in regions such as South Asia and sub-Saharan Africa (O'Brien et al., 2009). Pneumonia is responsible for 16 percent of all deaths of children under 5 years old. With the advent of pneumococcal vaccines, early diagnosis, and novel therapeutics, the incidence has declined. Between 1996 and 2011, inpatient deaths in the United States had decreased by 4.4 people per 100,000, however, the incidence rate still remains high (Chang et al., 2016). Changes in morbidity and mortality of pneumococcal pneumonia is dependent on patient age, virulence capacity of the pneumococcal strain, seasonality, and the state of the host immune system.

## **Pneumococcal virulence factors**

In order for the bacteria to multiply and establish themselves within the host, many bacteria release microbial components involved in tissue adherence and colonization, invasion into a cell, protection of self through capsulation, and release of both endotoxins and exotoxins. These components are often considered virulence factors for the host and many other numerous virulence factors are also involved (Brooks & Mias, 2018; R. A. Hirst et al., 2004; Jedrzejewski, 2001). This section will briefly summarize a few selected virulence factors that play an important role in the innate immune response within the host.

### **Polysaccharide capsule**

*S. pneumoniae* also has a wide array of virulence factors that enable it to avoid these immune defenses. The most notable means of evading the immune system by *S. pneumoniae* is definitively the polysaccharide capsule. The negative charge of most pneumococcal capsules electrostatically prevents entrapment of the bacteria by mucus, which is also negatively charged (Nelson et al., 2007). The steric hindrance of the capsule prevents efficient binding of complement, acute phase

proteins, and antibody specific to internal bacterial structures (Hyams et al., 2010). Even when such immune effectors manage to bind the bacteria, the capsule allows evasion of efficient opsonophagocytic mechanisms by sterically hindering their interactions with corresponding receptors on phagocytes (Hyams et al., 2010).

### **Autolysin**

The pneumococcal cell wall contains many virulence proteins that are toxic to host cells. One protein, autolysin is an intracellular protein that is produced only by Gram-positive bacteria. The protein cleaves the lactyl-amide bond that links the stem peptides and the glycan strands of the peptidoglycan, resulting in hydrolysis of the bacterial cell wall (Howard & Gooder, 1974). It has suggested that hydrolysis of the bacterial cell wall allows for cell wall virulence factors and cytosolic factors such as pneumolysin to be released (Martner et al., 2008).

### **Pneumolysin**

Pneumolysin is a hemolytic, thiol-activated, cytotoxic protein produced by pneumococcus (Kreger & Bernheimer, 1969) and released during bacterial growth and autolysis. This potent molecule has the ability to activate the host's classic complement pathway, modulate cytokine and chemokine release, and increase apoptosis of immune cells.

### **Bacterial enzymes**

In addition to these virulence factors, bacterial enzymes are another main class of pneumococcal virulence factors enabling innate immune invasion. The enzymes PdgA and Adr, for example, modify the cell wall to confer resistance to degradation by mucosal antimicrobial peptides (Davis et al., 2008). The bacterial enzymatic toxins cause epithelial cell damage and prevents effective mucociliary clearance (Robert A. Hirst et al., 2000).

## **Immunity**

The lung immune system includes complex and coordinated responses which protect the lungs and maintain their physiological respiration functions (Quinton et al., 2018). These immune responses need well-established, balanced reactions to resist the microbial pathology and clear the microbe on one side and limit the damages that it itself creates and be able to restore the lung tissue's

homeostasis on the other side. An imbalance on either side of the balance can disturb homeostasis and lead to uncontrolled pneumonia (Quinton & Mizgerd, 2015).

Upon entering a new naive host, the pneumococcus faces some barriers to initial colonization, including the mucus layer and anti-microbial peptides such as lysozyme secreted by nasal epithelial cells (Weiser et al., 2018). Microbes in the distal lungs rapidly face several defenses of the innate immune response, beginning with the physical barriers like the mucociliary response, which acts to restrain and remove the microbe out of the lung, or the epithelial barrier itself, which prevents the microbe from entering the internal lung microenvironment (Sichien et al., 2017). Epithelial cells secrete along with other immune cells several antimicrobial chemicals like lysozymes, lactoferrins, defensins, immunoglobulins, opsonin, and others (Whitsett & Alenghat, 2015). These antimicrobial chemicals act via several different mechanisms to control and remove the invading microbe, including creating holes in the microbe's membranes, sequestering nutrients from the microbes, and engulfing the microbe, enhancing their recognition and engulfment by resident phagocytic cells (Whitsett & Alenghat, 2015).

If pneumococci bypass these barriers, they would counter with highly phagocytic alveolar macrophages of the lung, which are activated after detection of the bacteria via pattern recognition receptors (PRR). Clearance by alveolar macrophage-mediated phagocytosis is sufficient to prevent severe infection by bacteria that reach the alveoli in most cases of pneumococcal aspiration (Shenoy & Orihuela, 2016). However, when bacteria persist, macrophages and epithelial cells in the lung can secrete chemokines such as interleukin (IL)-8, chemokine (C-X-C motif) ligand 5 (CXCL5), and granulocyte-macrophage colony-stimulating factor (GM-CSF), which call in neutrophils from the circulation to aid in bacterial killing (Shenoy & Orihuela, 2016; Yamamoto et al., 2014).

Phagocytic cells can help recruit other cells including lymphocytes. Lymphocytes require additional help from innate cells called antigen-presenting cells (APC) like macrophages and dendritic cells to get activated (O'Garra et al., 1998; Sallusto & Lanzavecchia, 2000; Sinigaglia et al., 1999). APCs present the microbial processed peptides (antigens) to lymphocytes through molecules present on their surfaces called major histocompatibility complex proteins (MHC-I and MHC-II)(Neefjes et al., 2011). Once activated, lymphocytes undergo rapid proliferation and build a massive army that, unlike phagocytic cells, specifically target the presented antigens with a specific arsenal. Lymphocytes produce such a robust, specific response that it needs additional restraints to prevent unnecessary activation of lymphocytes by harmless non- immunogenic peptides and self-antigens;

these restraints come in the form of secondary signals from APC that are critical to lymphocyte activation (Bonilla & Oettgen, 2010).

## **Prevention and vaccination**

Current vaccinations against pneumococcal infections are serotype specific with two approved pneumococcal vaccines available. The first attempt at vaccination used whole-cell pneumococcus among South African gold miners in 1911 and reduced pneumonia cases by 25-50% in the population. However, scientists found that serotype specific targeting would be more powerful than using whole-cell pneumococcus (Geno et al., 2015). In 1983, the first serotype specific polysaccharide vaccine, Pneumo-23 was approved. Throughout the years, the pneumococcal vaccines have been modified.

Pneumovax (PPSV23) and Prevnar (PCV13) are the two currently approved vaccines. PPSV23 contains polysaccharide antigens against 23 capsular serotypes (1, 2, 3, 4, 5, 6B, 7F, 8, 9N, 9V, 10A, 11A, 12F, 14, 15B, 17F, 18C, 19F, 19A, 20, 22F, 23F, and 33F). PCV13 is a conjugated vaccine in which bacterial polysaccharides are covalently conjugated to an immunologic carrier protein (Bonten et al., 2015; Isturiz & Webber, 2015). PCV13 protects against 13 capsular serotypes (1, 3, 4, 5, 6A, 6B, 7F, 9V, 14, 18C, 19A, 19F and 23F). PPSV23 elicits a T-cell independent response which results in poor immunogenicity in infants and older adults (Westerink et al., 2012). Additionally, B cell responses are not fully developed in infants and are required for efficacy with the polysaccharide vaccine (Timens et al., 1989). The creation of the conjugate vaccine, PCV13, allowed for antibody responses, T cell recruitment, and formation of immunological memory in infants under 2 years of age to occur (Stein, 1992). Pneumococcal infections have seen dramatic reductions since the introduction of serotype specific pneumococcal vaccines, however, the incidence of invasive pneumococcus displaying serotypes not included in the PPS23 and PCV13 vaccinations have increased in asymptomatic carriers (Pilishvili et al., 2010). Additionally, occurrence of invasive disease from bacteria with serotypes not covered by the vaccine have increased (Weinberger et al., 2011).

## **Research objective**

Pneumonia is a leading cause of invasive diseases worldwide and is responsible for the deaths of 1 in 4 children. The most frequent bacterial cause of pneumonia stems from *Streptococcus*

*pneumoniae*. Early invasion of the bacterium into the lungs is often subclinical and is rapidly controlled. During the bacterial invasion, macrophages are among the first host responders in driving an appropriate immune response in the airspace of the lungs. The host-pathogen interactions determine the intensity of disease and pathogenic proteins can cause differential rewiring of the host environment. Different pneumococcal proteins can drive unique host responses and enhanced understanding of how pneumococcus regulates this process may provide insight into new potential antimicrobial targets. Currently, the majority of therapeutic targets focus on the polysaccharide wall and proteins in the cell wall. An understanding disease mechanism as well as host responses will be valuable in different fields of treatments and preventions such as new antibiotics discovery and vaccines efficacy. To achieve this, development of an animal model which can mimic human interactions with bacteria should be crucial. In the second part of my project, we studied mice models of pneumonia disease caused by *Streptococcus pneumoniae* with different administration routes of infection.



## Bibliography

- Ablij, H. C., & Meinders, A. E. (2002). C-reactive protein: history and revival. *European Journal of Internal Medicine*, 13(7), 412–422. [https://doi.org/10.1016/S0953-6205\(02\)00132-2](https://doi.org/10.1016/S0953-6205(02)00132-2)
- Avery, O. T., Macleod, C. M., & McCarty, M. (n.d.). *STUDIES ON THE CHEMICAL NATURE OF THE SUBSTANCE INDUCING TRANSFORMATION OF PNEUMOCOCCAL TYPES INDUCTION OF TRANSFORMATION BY A DESOXYRIBONUCLEIC ACID FRACTION ISOLATED FROM PNEUMOCOCCUS TYPE III.*
- Bogaert, D., De Groot, R., & Hermans, P. W. M. (2004). Streptococcus pneumoniae colonisation: The key to pneumococcal disease. *Lancet Infectious Diseases*, 4(3), 144–154. [https://doi.org/10.1016/S1473-3099\(04\)00938-7](https://doi.org/10.1016/S1473-3099(04)00938-7)
- Bonilla, F. A., & Oettgen, H. C. (2010). Adaptive immunity. *The Journal of Allergy and Clinical Immunology*, 125(2 Suppl 2). <https://doi.org/10.1016/J.JACI.2009.09.017>
- Bonten, M. J. M., Huijts, S. M., Bolkenbaas, M., Webber, C., Patterson, S., Gault, S., van Werkhoven, C. H., van Deursen, A. M. M., Sanders, E. A. M., Verheij, T. J. M., Patton, M., McDonough, A., Moradoghli-Haftvani, A., Smith, H., Mellelieu, T., Pride, M. W., Crowther, G., Schmoele-Thoma, B., Scott, D. A., ... Grobbee, D. E. (2015). Polysaccharide conjugate vaccine against pneumococcal pneumonia in adults. *The New England Journal of Medicine*, 372(12), 1114–1125. <https://doi.org/10.1056/NEJMOA1408544>
- Brooks, L. R. K., & Mias, G. I. (2018). Streptococcus pneumoniae's Virulence and Host Immunity: Aging, Diagnostics, and Prevention. *Frontiers in Immunology*, 9(JUN). <https://doi.org/10.3389/FIMMU.2018.01366>
- Chang, D. H., Bednarczyk, R. A., Becker, E. R., Hockenberry, J. M., Weiss, P. S., Orenstein, W. A., & Omer, S. B. (2016). Trends in U.S. hospitalizations and inpatient deaths from pneumonia and influenza, 1996-2011. *Vaccine*, 34(4), 486–494. <https://doi.org/10.1016/J.VACCINE.2015.12.003>
- Davis, K. M., Akinbi, H. T., Standish, A. J., & Weiser, J. N. (2008). Resistance to Mucosal Lysozyme Compensates for the Fitness Deficit of Peptidoglycan Modifications by Streptococcus pneumoniae. *PLoS Pathogens*, 4(12). <https://doi.org/10.1371/JOURNAL.PPAT.1000241>
- Geno, K. A., Gilbert, G. L., Song, J. Y., Skovsted, I. C., Klugman, K. P., Jones, C., Konradsen, H.

- B., & Nahm, M. H. (2015). Pneumococcal capsules and their types: Past, present, and future. *Clinical Microbiology Reviews*, 28(3), 871–899. <https://doi.org/10.1128/CMR.00024-15/FORMAT/EPUB>
- Gray, B. M., Converse, G. M., & Dillon, H. C. (1980). Epidemiologic studies of *Streptococcus pneumoniae* in infants: acquisition, carriage, and infection during the first 24 months of life. *The Journal of Infectious Diseases*, 142(6), 923–933. <https://doi.org/10.1093/INFDIS/142.6.923>
- Henriques-Normark, B., & Tuomanen, E. I. (n.d.). *The Pneumococcus: Epidemiology, Microbiology, and Pathogenesis*. <https://doi.org/10.1101/cshperspect.a010215>
- Hirst, R. A., Kadioglu, A., O’Callaghan, C., & Andrew, P. W. (2004). The role of pneumolysin in pneumococcal pneumonia and meningitis. *Clinical and Experimental Immunology*, 138(2), 195–201. <https://doi.org/10.1111/J.1365-2249.2004.02611.X>
- Hirst, Robert A., Sikand, K. S., Rutman, A., Mitchell, T. J., Andrew, P. W., & O’Callaghan, C. (2000). Relative roles of pneumolysin and hydrogen peroxide from *Streptococcus pneumoniae* in inhibition of ependymal ciliary beat frequency. *Infection and Immunity*, 68(3), 1557–1562. <https://doi.org/10.1128/IAI.68.3.1557-1562.2000>
- Howard, L. V., & Gooder, H. (1974). Specificity of the autolysin of *Streptococcus* (*Diplococcus*) *pneumoniae*. *Journal of Bacteriology*, 117(2), 796–804. <https://doi.org/10.1128/JB.117.2.796-804.1974>
- Hyams, C., Camberlein, E., Cohen, J. M., Bax, K., & Brown, J. S. (2010). The *Streptococcus pneumoniae* capsule inhibits complement activity and neutrophil phagocytosis by multiple mechanisms. *Infection and Immunity*, 78(2), 704–715. <https://doi.org/10.1128/IAI.00881-09>
- Isturiz, R., & Webber, C. (2015). Prevention of adult pneumococcal pneumonia with the 13-valent pneumococcal conjugate vaccine: CAPiTA, the community-acquired pneumonia immunization trial in adults. *Human Vaccines and Immunotherapeutics*, 11(7), 1825–1827. <https://doi.org/10.1080/21645515.2015.1043502>
- Jedrzejewski, M. J. (2001). Pneumococcal virulence factors: structure and function. *Microbiology and Molecular Biology Reviews : MMBR*, 65(2), 187–207. <https://doi.org/10.1128/MMBR.65.2.187-207.2001>
- Kadioglu, A., Weiser, J. N., Paton, J. C., & Andrew, P. W. (2008). The role of *Streptococcus*

- pneumoniae virulence factors in host respiratory colonization and disease. *Nature Reviews. Microbiology*, 6(4), 288–301. <https://doi.org/10.1038/NRMICRO1871>
- Kreger, A. S., & Bernheimer, A. W. (1969). Physical behavior of pneumolysin. *Journal of Bacteriology*, 98(1), 306–307. <https://doi.org/10.1128/JB.98.1.306-307.1969>
- Lanie, J. A., Ng, W. L., Kazmierczak, K. M., Andrzejewski, T. M., Davidsen, T. M., Wayne, K. J., Tettelin, H., Glass, J. I., & Winkler, M. E. (2007). Genome Sequence of Avery's Virulent Serotype 2 Strain D39 of *Streptococcus pneumoniae* and Comparison with That of Unencapsulated Laboratory Strain R6. *Journal of Bacteriology*, 189(1), 38. <https://doi.org/10.1128/JB.01148-06>
- Martner, A., Dahlgren, C., Paton, J. C., & Wold, A. E. (2008). Pneumolysin Released during *Streptococcus pneumoniae* Autolysis Is a Potent Activator of Intracellular Oxygen Radical Production in Neutrophils. *Infection and Immunity*, 76(9), 4079. <https://doi.org/10.1128/IAI.01747-07>
- Neefjes, J., Jongstra, M. L. M., Paul, P., & Bakke, O. (2011). Towards a systems understanding of MHC class I and MHC class II antigen presentation. *Nature Reviews. Immunology*, 11(12), 823–836. <https://doi.org/10.1038/NRI3084>
- Nelson, A. L., Roche, A. M., Gould, J. M., Chim, K., Ratner, A. J., & Weiser, J. N. (2007). Capsule enhances pneumococcal colonization by limiting mucus-mediated clearance. *Infection and Immunity*, 75(1), 83–90. <https://doi.org/10.1128/IAI.01475-06>
- O'Brien, K. L., Wolfson, L. J., Watt, J. P., Henkle, E., Deloria-Knoll, M., McCall, N., Lee, E., Mulholland, K., Levine, O. S., & Cherian, T. (2009). Burden of disease caused by *Streptococcus pneumoniae* in children younger than 5 years: global estimates. *The Lancet*, 374(9693), 893–902. [https://doi.org/10.1016/S0140-6736\(09\)61204-6](https://doi.org/10.1016/S0140-6736(09)61204-6)
- O'Garra, A., McEvoy, L. M., & Zlotnik, A. (1998). T-cell subsets: chemokine receptors guide the way. *Current Biology : CB*, 8(18). [https://doi.org/10.1016/S0960-9822\(07\)00413-7](https://doi.org/10.1016/S0960-9822(07)00413-7)
- Örtqvist, Å., Hedlund, J., & Kalin, M. (2005). *Streptococcus pneumoniae*: epidemiology, risk factors, and clinical features. *Seminars in Respiratory and Critical Care Medicine*, 26(6), 563–574. <https://doi.org/10.1055/S-2005-925523>
- Pilishvili, T., Lexau, C., Farley, M. M., Hadler, J., Harrison, L. H., Bennett, N. M., Reingold, A., Thomas, A., Schaffner, W., Craig, A. S., Smith, P. J., Beall, B. W., Whitney, C. G., & Moore,

- M. R. (2010). Sustained reductions in invasive pneumococcal disease in the era of conjugate vaccine. *The Journal of Infectious Diseases*, 201(1), 32–41. <https://doi.org/10.1086/648593>
- Quinton, L. J., & Mizgerd, J. P. (2015). Dynamics of lung defense in pneumonia: resistance, resilience, and remodeling. *Annual Review of Physiology*, 77, 407–430. <https://doi.org/10.1146/ANNUREV-PHYSIOL-021014-071937>
- Quinton, L. J., Walkey, A. J., & Mizgerd, J. P. (2018). Integrative Physiology of Pneumonia. *Physiological Reviews*, 98(3), 1417–1464. <https://doi.org/10.1152/PHYSREV.00032.2017>
- Sallusto, F., & Lanzavecchia, A. (2000). Understanding dendritic cell and T-lymphocyte traffic through the analysis of chemokine receptor expression. *Immunological Reviews*, 177, 134–140. <https://doi.org/10.1034/J.1600-065X.2000.17717.X>
- Sandgren, A., Albiger, B., Orihuela, C. J., Tuomanen, E., Normark, S., & Henriques-Normark, B. (2005). Virulence in mice of pneumococcal clonal types with known invasive disease potential in humans. *The Journal of Infectious Diseases*, 192(5), 791–800. <https://doi.org/10.1086/432513>
- Shenoy, A. T., & Orihuela, C. J. (2016). Anatomical site-specific contributions of pneumococcal virulence determinants. *Pneumonia (Nathan Qld.)*, 8(1). <https://doi.org/10.1186/S41479-016-0007-9>
- Sichien, D., Lambrecht, B. N., Guilliams, M., & Scott, C. L. (2017). Development of conventional dendritic cells: from common bone marrow progenitors to multiple subsets in peripheral tissues. *Mucosal Immunology*, 10(4), 831–844. <https://doi.org/10.1038/MI.2017.8>
- Siegel, S. J., & Weiser, J. N. (2015). Mechanisms of Bacterial Colonization of the Respiratory Tract. *Annual Review of Microbiology*, 69(1), 425–444. <https://doi.org/10.1146/ANNUREV-MICRO-091014-104209>
- Sinigaglia, F., D’Ambrosio, D., & Rogge, L. (1999). Type I interferons and the Th1/Th2 paradigm. *Developmental and Comparative Immunology*, 23(7–8), 657–663. [https://doi.org/10.1016/S0145-305X\(99\)00039-7](https://doi.org/10.1016/S0145-305X(99)00039-7)
- Stein, K. E. (1992). Thymus-independent and thymus-dependent responses to polysaccharide antigens. *The Journal of Infectious Diseases*, 165 Suppl 1, S49–S52. [https://doi.org/10.1093/INFDIS/165-SUPPLEMENT\\_1-S49](https://doi.org/10.1093/INFDIS/165-SUPPLEMENT_1-S49)
- Timens, W., Boes, A., Rozeboom-Uiterwijk, T., & Poppema, S. (1989). Immaturity of the human

- splenic marginal zone in infancy. Possible contribution to the deficient infant immune response. *The Journal of Immunology*, 143(10).
- van der Poll, T., & Opal, S. M. (2009). Pathogenesis, treatment, and prevention of pneumococcal pneumonia. *The Lancet*, 374(9700), 1543–1556. [https://doi.org/10.1016/S0140-6736\(09\)61114-4](https://doi.org/10.1016/S0140-6736(09)61114-4)
- Watson, D. A., Musher, D. M., Jacobson, J. W., & Verhoef, J. (1993). A Brief History of the Pneumococcus in Biomedical Research: A Panoply of Scientific Discovery. *Clinical Infectious Diseases*, 17(5), 913–924. <https://doi.org/10.1093/CLINIDS/17.5.913>
- Weinberger, D. M., Malley, R., & Lipsitch, M. (2011). Serotype replacement in disease after pneumococcal vaccination. *Lancet (London, England)*, 378(9807), 1962–1973. [https://doi.org/10.1016/S0140-6736\(10\)62225-8](https://doi.org/10.1016/S0140-6736(10)62225-8)
- Weiser, J. N. (n.d.). *The pneumococcus: why a commensal misbehaves*. <https://doi.org/10.1007/s00109-009-0557-x>
- Weiser, J. N., Ferreira, D. M., & Paton, J. C. (2018). Streptococcus pneumoniae: transmission, colonization and invasion. *Nature Reviews Microbiology* 2018 16:6, 16(6), 355–367. <https://doi.org/10.1038/s41579-018-0001-8>
- Westerink, M. A. J., Schroeder, H. W., & Nahm, M. H. (2012). Immune Responses to pneumococcal vaccines in children and adults: Rationale for age-specific vaccination. *Aging and Disease*, 3(1), 51. /pmc/articles/PMC3320805/
- Whitsett, J. A., & Alenghat, T. (2015). Respiratory epithelial cells orchestrate pulmonary innate immunity. *Nature Immunology*, 16(1), 27–35. <https://doi.org/10.1038/NI.3045>
- Yamamoto, K., Ahyi, A. N. N., Pepper-Cunningham, Z. A., Ferrari, J. D., Wilson, A. A., Jones, M. R., Quinton, L. J., & Mizgerd, J. P. (2014). Roles of lung epithelium in neutrophil recruitment during pneumococcal pneumonia. *American Journal of Respiratory Cell and Molecular Biology*, 50(2), 253–262. <https://doi.org/10.1165/RCMB.2013-0114OC>

# CHAPTER 4

## **Immune Memory After Respiratory Infection With *Streptococcus pneumoniae* Is Revealed by in vitro Stimulation of Murine Splenocytes With Inactivated Pneumococcal Whole Cells: Evidence of Early Recall Responses by Transcriptomic Analysis**

Isabelle Franco Moscardini<sup>1,2</sup>, Francesco Santoro<sup>1,\*</sup>, Monica Carraro<sup>1</sup>, Alice Gerlini<sup>2</sup>, Fabio Fiorino<sup>1</sup>, Chiara Germoni<sup>1</sup>, Samaneh Gholami<sup>1</sup>, Elena Pettini<sup>1</sup>, Donata Medaglini<sup>1</sup>, Francesco Iannelli<sup>1</sup>, Gianni Pozzi<sup>1</sup>

<sup>1</sup>Laboratory of Molecular Microbiology and Biotechnology (LAMMB), Department of Medical Biotechnologies, University of Siena, Siena, Italy

<sup>2</sup>Microbiotec srl, Siena, Italy



# Immune Memory After Respiratory Infection With *Streptococcus pneumoniae* Is Revealed by *in vitro* Stimulation of Murine Splenocytes With Inactivated Pneumococcal Whole Cells: Evidence of Early Recall Responses by Transcriptomic Analysis

## OPEN ACCESS

### Edited by:

Eisa Bou Ghanem,  
University at Buffalo, United States

### Reviewed by:

Sarah Clark,  
University of Colorado, United States  
Olanrewaju B. Morenikeji,  
University of Pittsburgh at Bradford,  
United States

### \*Correspondence:

Francesco Santoro  
santoro@unisi.it

### Specialty section:

This article was submitted to  
Molecular Bacterial Pathogenesis,  
a section of the journal  
Frontiers in Cellular and  
Infection Microbiology

Received: 05 February 2022

Accepted: 21 April 2022

Published: 20 June 2022

### Citation:

Moscardini IF, Santoro F, Carraro M,  
Gerlini A, Fiorino F, Germoni C,  
Gholami S, Pettini E, Medaglini D,  
Iannelli F and Pozzi G (2022) Immune  
Memory After Respiratory Infection  
With *Streptococcus pneumoniae* Is  
Revealed by *in vitro* Stimulation of  
Murine Splenocytes With Inactivated  
Pneumococcal Whole Cells: Evidence  
of Early Recall Responses by  
Transcriptomic Analysis.  
*Front. Cell. Infect. Microbiol.* 12:869763.  
doi: 10.3389/fcimb.2022.869763

Isabelle Franco Moscardini<sup>1</sup>, Francesco Santoro<sup>2\*</sup>, Monica Carraro<sup>2</sup>, Alice Gerlini<sup>1</sup>,  
Fabio Fiorino<sup>2</sup>, Chiara Germoni<sup>2</sup>, Samaneh Gholami<sup>2</sup>, Elena Pettini<sup>2</sup>, Donata Medaglini<sup>2</sup>,  
Francesco Iannelli<sup>2</sup> and Gianni Pozzi<sup>2</sup>

<sup>1</sup> Microbiotec srl, Siena, Italy, <sup>2</sup> Laboratory of Molecular Microbiology and Biotechnology (LAMMB), Department of Medical Biotechnologies, University of Siena, Siena, Italy

The *in vitro* stimulation of immune system cells with live or killed bacteria is essential for understanding the host response to pathogens. In the present study, we propose a model combining transcriptomic and cytokine assays on murine splenocytes to describe the immune recall in the days following pneumococcal lung infection. Mice were sacrificed at days 1, 2, 4, and 7 after *Streptococcus pneumoniae* (TIGR4 serotype 4) intranasal infection and splenocytes were cultured in the presence or absence of the same inactivated bacterial strain to access the transcriptomic and cytokine profiles. The stimulation of splenocytes from infected mice led to a higher number of differentially expressed genes than the infection or stimulation alone, resulting in the enrichment of 40 unique blood transcription modules, including many pathways related to adaptive immunity and cytokines. Together with transcriptomic data, cytokines levels suggested the presence of a recall immune response promoting both innate and adaptive immunity, stronger from the fourth day after infection. Dimensionality reduction and feature selection identified key variables of this recall response and the genes associated with the increase in cytokine concentrations. This model could study the immune responses involved in pneumococcal infection and possibly monitor vaccine immune response and experimental therapies efficacy in future studies.

**Keywords:** *Streptococcus pneumoniae*, *in vitro* stimulation, Transcriptomic Analysis, Recall immune responses, lung infection, cytokines/chemokines

## 1 INTRODUCTION

*Streptococcus pneumoniae* is a major human pathogen responsible for various diseases, including life-threatening conditions such as pneumonia, sepsis, and meningitis (Weiser et al., 2018). Current vaccines have been very efficient in reducing the death toll caused by this pathogen. However, strains not covered by the available vaccines represent a growing concern, demanding new serotype-independent strategies (Kaplan et al., 2013; Pichichero, 2017; Briles et al., 2019). Models to assess the response to new vaccine candidates would be of great use.

*In vitro* stimulation with live or killed bacteria has been used for decades for understanding the host's response to different pathogens, including *S. pneumoniae* (Zhan and Cheers, 1995; Schultz et al., 1998; Wu et al., 2011; de Stoppelaar et al., 2016). This technique has also been applied in vaccine studies, characterizing the immune response after a second stimulus (Paranavitana et al., 2010; Moffitt et al., 2011; Shao et al., 2015). Changes in gene expression and in cytokine concentration were metrics assessed by some of these works to study the immune profile of pneumococcal infection. In the present work, we propose the combination of transcriptomic and cytokine assays from murine splenocytes to assess the immune memory built in the days following pneumococcal infection.

The spleen plays a vital role in host defenses against encapsulated blood-borne pathogens due to its elevated perfusion and efficient immune surveillance of the circulatory system (Cerutti et al., 2013). In a pneumococcal bacteremia model, bacteria present a tropism to the spleen, and macrophages present in the splenic Red Pulp (RP) are responsible for an initial binding and subsequent clearance of *S. pneumoniae* mediated by mature neutrophils present on the RP (Deniset et al., 2017; Ercoli et al., 2018). Moreover, the splenic Marginal Zone (MZ) is a crucial area of antigen presentation to MZ B cells that are capable of rapidly differentiating into plasmablasts, secreting low-affinity IgM and IgG (Cerutti et al., 2013).

RNA sequencing technologies permit us to gain insights into the host's response due to the possibility of analyzing the changes in gene expression in different conditions. The transcriptomic information can be integrated with other biological layers or clinical data, permitting a more comprehensive understanding of biological processes in response to perturbations such as infection and vaccination.

In the current work, we propose the study of the host systemic responses to a pneumococcal lung infection by assessing gene expression and cytokine profiles of splenocytes, identifying biological pathways and the key features involved in this process.

## 2 METHODS

### 2.1 Animals and Animal Infection

Seven-week female C57BL/6 mice (Charles River Italia, Italy) were treated according to national guidelines (Decreto Legislativo 26/2014) utilizing the three R's principles. Animals

were maintained under specific pathogen-free conditions in the animal facility of the Laboratory of Molecular Microbiology and Biotechnology (L.A.M.M.B.), Department of Medical Biotechnologies at University of Siena, at 20–24°C, with 55 ± 10% of humidity, with food and water *ad libitum*. The study was approved by the Italian Ministry of Health with authorization n° 304/2018-PR. As previously described (Kadioglu et al., 2011) male and female mice respond differently to pneumococcal infection and, therefore the use of only female mice can be considered a limitation of this study.

Mouse-passaged TIGR4 strain of *S. pneumoniae* (Gerlini et al., 2014) was inoculated 1:50 in TSB (Tryptic-Soy Broth, Becton Dickinson, USA) supplemented with 0.1% of glucose (PanReac, Applichem, Italy), 1% of yeast extract (Oxoid, UK) and 0.016 M K<sub>2</sub>HPO<sub>4</sub> (Sigma-Aldrich, USA) (TSB-GYP). The bacterial culture in mid-exponential phase ( $\approx$ OD<sub>590</sub> = 0.6), was centrifuged at 2,000 x g for 10 minutes and resuspended in an appropriate volume of saline. Before the centrifugation, the culture was Gram-stained and bacterial vital counts were performed using the multilayer plating method (Iannelli et al., 2021). Each mouse was anesthetized by intraperitoneal administration of 15 mg/kg tiletamine hydrochloride/zolazepam and 4 mg/kg xylazine and intranasally infected by instillation of 10<sup>7</sup> CFU of TIGR4, prepared as described above, in the volume of 25 µl/nostril in TSB. Mice were euthanized at different time points with overdose of anesthesia and cervical dislocation, as shown in **Figure 1**. Non-infected mice composed the baseline group. Each group included 6 animals.

### 2.2 Sample Collection

After aseptic removal at different time points (days 0, 1, 2, 4, and 7 after infection), spleens were meshed onto 70 µm nylon screens (Sefar Italia, Italy) using a scalpel and scraper. Cells were washed two times in RPMI (Sigma-Aldrich) supplemented with 10% of fetal bovine serum (FBS, Gibco, USA) and 1% of penicillin-streptomycin (Sigma-Aldrich)(cRPMI), treated with red blood cells lysis buffer according to manufacturer instruction (eBioscience, USA), and resuspended in cRPMI for cell counting by an automatic cell counter (Bio-Rad, USA). Lungs were aseptically removed, meshed onto 40 µm nylon screens (Sefar Italia, Italy), suspended in 1 ml of TSB containing glycerol at a final concentration of 10% and frozen at -70°C.

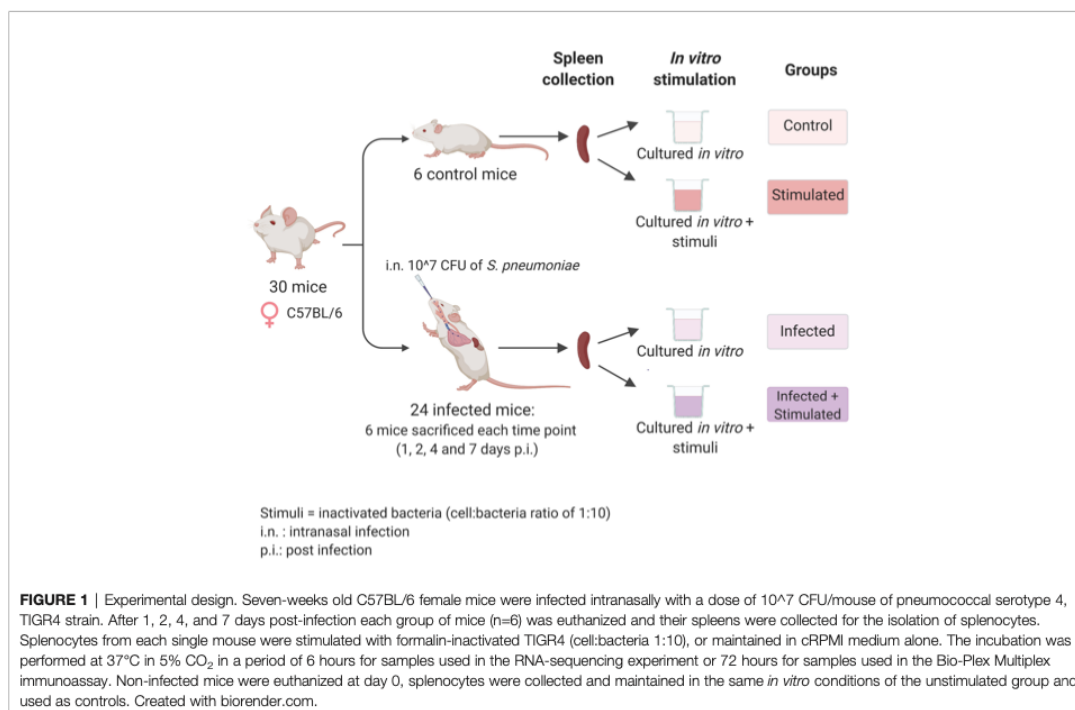
### 2.3 Bacterial Cells Counts in Lungs

Bacterial colony forming units (CFUs) were determined by plating appropriate dilutions of frozen lungs using a multilayer plating procedure (Iannelli et al., 2021). The lower limit of detection was 10 CFU/ml. CFUs were counted at 1, 2, 4, and 7 days after intranasal infection and in the mock infected control group.

### 2.4 Preparation of Inactivated Whole Cells of *S. pneumoniae*

TIGR4 was inoculated 1:1000 (v:v) in 1 L of pre-heated (37°C) TSB-GYP in a GLS80 1 liter bottle (Duran, USA). Temperature was maintained constant at 37°C, the pH was continuously measured with a probe (InPro3030, Mettler Toledo) and kept





at 6.9 by peristaltic pump controlled addition of 3M NaOH. Agitation was set at 100 rpm. Growth was monitored by aseptically drawing aliquots and measuring their  $\text{OD}_{590}$  in a Spectronic 200 spectrophotometer (ThermoFisher). At the peak  $\text{OD}_{590}$  (about 2.5, corresponding to  $10^9$  CFU/ml) bacteria were harvested by centrifugation, resuspended in PBS/10% glycerol and frozen at  $-70^\circ\text{C}$ . TIGR4 bacteria were then thawed and inactivated by treatment with 1.5% formalin for 2 hours on a roller mixer at room temperature, then washed twice and resuspended in water.

## 2.5 Splenocyte Stimulation and Cytokine Secretion Assay

Splenocytes were cultured in a U-bottom 96-well plate in triplicate for 72 hours at  $37^\circ\text{C}$  with  $5\%$   $\text{CO}_2$  in cRPMI.

Splenocyte cultures were incubated in the presence or not of inactivated TIGR4, at a cell:bacteria ratio of 1:10. Unstimulated control splenocytes were cultured in cRPMI alone, and positive control splenocytes were stimulated with 50 ng/ml of phorbol 12-myristate 13-acetate (PMA) and 1  $\mu\text{M}$  of Ionomycin (both from Sigma-Aldrich). After stimulation, cells were harvested and centrifuged at  $500 \times g$  for 15 minutes at  $4^\circ\text{C}$ . The supernatant was recovered and frozen at  $-70^\circ\text{C}$  for subsequent Luminex immunoassay.

A broad screening panel consisting of a biologically-relevant collection of adaptive immunity cytokines, pro-inflammatory cytokines, and anti-inflammatory cytokines was used. In

particular, IL-1 $\alpha$ , IL-1 $\beta$ , IL-2, IL-3, IL-4, IL-5, IL-6, IL-9, IL-10, IL-12p40, IL-12p70, IL-13, IL-17, G-CSF, GM-CSF, IFN $\gamma$ , and TNF- $\alpha$ , and of the chemokines Eotaxin, KC, MCP-1 (MCAF), MIP-1 $\alpha$ , MIP-1 $\beta$ , and RANTES production by *in vitro* stimulated splenocytes was assessed with the BioPlex pro mouse cytokine group 1 - panel 23-plex immunoassay (Bio-Rad, USA) according to manufacturer guidelines, and analyzed by Bio-Plex Magpix Multiplex reader (Bio-Rad). Cytokine and chemokine concentration was expressed as picograms per milliliter (pg/ml) and were calculated using Bio-Plex Manager 6.1.

## 2.6 Splenocyte Stimulation for RNA-Sequencing

In a U-bottom plate,  $1 \times 10^6$  splenocytes/well were seeded in quintuplicate and cultured for 6 hours at  $37^\circ\text{C}$  with  $5\%$   $\text{CO}_2$  in cRPMI in the presence of inactivated TIGR4 at a cell:bacteria ratio of 1:10. Unstimulated control splenocytes were cultured in cRPMI alone. Upon stimulation, cell replicates were centrifuged at  $500 \times g$  for 10 minutes at  $4^\circ\text{C}$ . The supernatant was discarded, the pellet resuspended in 50  $\mu\text{l}$  of lysis buffer RA1 (Macherey-Nagel, Germany), flash-frozen in liquid nitrogen, and stored at  $-70^\circ\text{C}$  for subsequent RNA extraction.

## 2.7 RNA Extraction, Library Preparation, and Sequencing

The RNA purification was performed with the NucleoSpin<sup>®</sup> RNA kit (Macherey-Nagel) following manufacturer's

instructions, and, before DNase treatment, the extracted RNA was quantified by the Qubit<sup>®</sup> 2.0 Fluorometer (Invitrogen by Thermo Fisher Scientific, USA), using the Qubit RNA BR (Broad-Range) Assay Kit.

Contaminating DNA was removed from the extracted RNA by adding 10X TURBO DNase Buffer (TURBO DNase, Ambion by Thermo Fisher Scientific) and 1  $\mu$ l of TURBO DNase (Ambion), and samples were incubated at 37°C for 30 minutes. After purification by the RNA Clean & Concentrator Kit (Zymo Research, USA), the obtained RNA was quantified using the Qubit<sup>®</sup> RNA BR Assay Kit.

Library preparation was performed as described in a previous publication (Santoro et al., 2021), using the Ion AmpliSeq<sup>™</sup> Transcriptome Mouse Gene Expression Kit from AmpliSeq (Thermo Fisher Scientific), allowing the amplification of 23,930 target genes. Libraries were diluted to 50 pM and pooled in equal volumes (7  $\mu$ l), with eight individual samples per pool and loaded onto Ion PI<sup>™</sup> Chip v3 using the Ion Chef<sup>™</sup> Instrument. Sequencing was performed using Ion Proton<sup>™</sup> Sequencer.

All described steps were performed according to the manufacturer's instructions.

## 2.8 RNA-Sequencing Data Analysis

R software in version 3.6.3 was used for transcriptomic data analysis. The DESeq2 package (Love et al., 2014), performs differential expression analysis and multiple test correction, returning values of LogFC, and adjusted p values. Genes with an adjusted p-value smaller than 0.05 and an absolute value of log2 Fold Change greater than 0.5 were classified as differentially expressed and then used in the enrichment analysis performed by the hypergeometric test from the *tmod* package (Weiner 3rd and Domaszewska, 2016) using the Blood Transcription Modules (BTM) database (Li et al., 2014).

## 2.9 Cytokine Data Analysis

R software in version 3.6.3 and the software GraphPad Prism 8.0 were used to perform the statistical analysis. The cytokine concentrations between stimulated and unstimulated samples were compared using the Wilcoxon signed-rank test, a non-parametric test used to compare two related samples. Samples from different time points were analyzed using the Mann-Whitney test, a non-parametric test for non-matched samples. A p-value  $\leq 0.05$  was considered statistically significant.

## 2.10 Biomarker Analysis

The DaMiRseq (Chiesa et al., 2018) package was used to find possible biomarkers of the host response to the second stimulus, the inactivated bacteria. Stimulated samples were selected and divided into three groups: baseline, infected samples at days 1 and 2 (early time points), and infected samples at days 4 and 7 (late time points). Following a pipeline that permits normalization, data adjustment, and feature selection, the DaMiRseq package ranked the most important features to distinguish the three classes. The number of selected genes was chosen based on the importance established by the package;

genes with a scaled importance score higher than 0.5 were chosen (**Supplementary Image 1**).

## 2.11 Data Integration

To integrate RNA-sequencing results and the Cytokines Bioplex, we selected the concurrent samples from both experiments, and we performed the sparse version of Partial Least Squares (sPLS), provided by the MixOmics package. The PLS is a multivariate method to integrate two high dimensional matrices, maximizing the covariance between components from two data sets, in our case, the transcriptomic and cytokines assay data. The sparse version, sPLS, applies LASSO penalization in each pair of loading vectors from PLS, performing feature selection and providing the correlation values between the main features in each data set (Lê Cao et al., 2008).

According to the  $Q^2$  criterion, two components would be sufficient to run the model ( $Q^2$  of 0.33931900 and 0.08639437). As suggested by the *tune.spls* function, the optimal variable number was chosen in each component resulting in 16 genes for component 1 and 25 from component 2.

## 3 RESULTS

Groups of six C57BL/6 mice were intranasally inoculated with  $10^7$  CFUs of TIGR4 *S. pneumoniae* to generate lung infection. To study the systemic response induced at early time points afterinfection, we sacrificed animals after 1, 2, 4, and 7 days and isolated their splenocytes. We then stimulated splenocytes from each single mouse with formalin-inactivated whole pneumococcal cells and investigated the host responses by transcriptomic analysis and assessment of cytokine production (**Figure 1**).

### 3.1 Evidence of Pneumococcal Lung Infection in Mice

The weight loss of animals after infection is a critical clinical parameter of disease in the mouse model of infection, evaluated in different challenge murine models with different pathogens (Trammell and Toth, 2011; Pettini et al., 2015; Fiorino et al., 2021). Mouse body weight was measured every 24 hours for a period of seven days. Uninfected mice increased their body weight over time, which reflected their health status. Compared to naive mice, infected mice experienced a significant decrease in body weight soon after infection, and the average difference in the weight between the classes increased over time, being 1.07 grams at day 2 after infection and 1.52 grams at day 7 (**Figure 2A**).

The significance of these findings was assessed using the Mann-Whitney test, which showed significant differences in the weight from day 2 to day 7 after infection, indicating a long-lasting effect of the infection.

Pneumococcal cells were counted in the lungs of infected mice. Cell counts had a peak at day 4 after infection (**Figure 2B**). It is worth to note that, for each time point assayed, 2-5 mice had no detectable pneumococcal cells, suggesting that mice are able

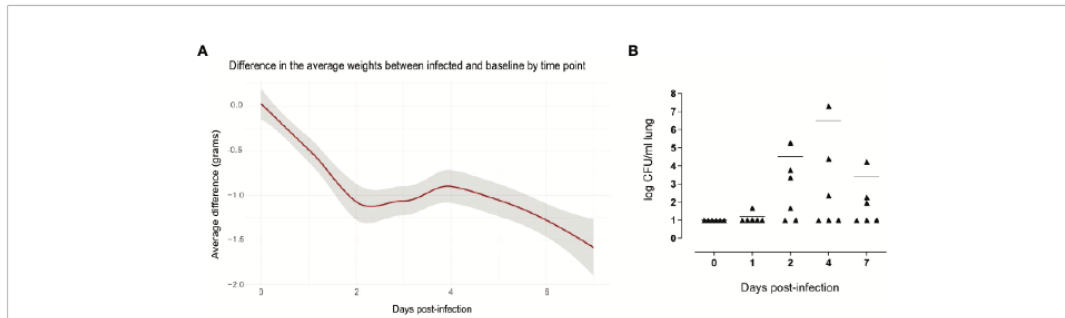


**FIGURE 2** | Evidence of pneumococcal lung infection. Comparison of body weight variation of infected versus baseline (A). Infected (n=36) and uninfected (n=5) mice were weighed every 24 hours for a period of 7 days. Values were obtained subtracting the pre-inoculum body weight from the body weight at each time-point, and then subtracting the mean in the control group from mean of the infected group in each time point. The average differences are expressed in grams and the gray shade represents the 0.95 confidence interval. From days 2 to 7 there were significant differences between the infected and baseline groups ( $p < 0.05$ , calculated using Mann-Whitney test). Pneumococcal cell counts in the lungs (B). The lungs of mice sacrificed at 1, 2, 4 and 7 days after infection (n=6 per group) were collected, homogenized in a final volume of 1 ml and plated using a multilayer plating procedure. Pneumococcal cells were counted after 24 hours and 48 hours of incubation. Lungs of uninfected mice (0 days post-infection) were plated as a negative control. Data are expressed as CFUs/ml lung. The lower limit of detection was 10 CFU/ml lung. Average cell counts had a peak at day 4. For each time point, there were at least 2 mice without detectable pneumococci.

to spontaneously clear pneumococcal lung infection at an infectious dose of  $1 \times 10^7$  CFUs of *S. pneumoniae* TIGR4. When setting up the mouse model, we also counted pneumococcal cells in the blood of six mice at 6 and 12 hours after intranasal infection, and in the blood of 12 mice at 24 and 96 hours after infection. Of those, only one animal had detectable pneumococcal cells in the blood ( $2.4 \times 10^3$  CFU/ml) at 24 hours after infection, suggesting that the infection is essentially limited to the mouse lungs without significant systemic spreading.

### 3.2 *In vitro* Splenocyte Stimulation With Pneumococcal Strain TIGR4 Activates Several Genes Related to Both Branches of the Immune System

Transcriptomic data from spleens of infected and uninfected mice with or without homologous *in vitro* stimulation were analyzed. We performed an Independent Principal Component Analysis (IPCA) and its sparse version, sIPCA, both proposed by MixOmics package (Yao et al., 2012), (i) to observe the distribution of our data, (ii) to understand how stimulation at different time points affects the clustering of samples, (iii) to identify the genes responsible for the main variance among samples, and (iv) to find possible outlier samples.

The IPCA approach (Supplementary Image 2) yielded a better clusterization among experimental groups and time points compared to PCA (data not shown). An outlier control sample was detected and removed. The sparse version of the IPCA (sIPCA, Figure 3) applies soft-thresholding in the independent loading vectors in IPCA, performing feature selection. The graph shows the presence of two well-defined groups in the sIPC1: the stimulated and unstimulated samples.

To better understand the genes that drive the formation of these clusters, the normalized expression values of the 50 genes selected by the first component of the sIPCA were divided into

two heatmaps (Figure 3). Genes positively correlated with the first component (driving the unstimulated cluster) included positive and negative regulators of the immune response, and they presented a decreased expression after stimulation. The genes negatively regulated with the first component (clustering the stimulated samples) were related to cytokines, chemokines, and inflammation, all of them presenting an increased expression compared to unstimulated samples.

### 3.3 Stimulation of Splenocytes From Infected Mice Highlights Biological Pathways of Pneumococcus Infection

We then proceeded with the differential expression analysis using the *DESeq2* package. To understand the biological alterations caused by the infection and the subsequent *in vitro* stimulation with inactivated pneumococcus, enrichment analysis was performed using three different comparisons. (i) Spleens from infected mice, (ii) stimulated spleens from non-infected mice, and (iii) stimulated spleens from infected mice, at different time points after infection, were all compared with control spleens.

The number of differentially expressed genes (DEGs) for each condition at each time point is presented in Figure 4. As expected, the stimulation of infected samples led to a higher number of DEGs compared to only infected samples, including specific genes that were not differentially expressed in the infection or stimulation alone. Days 4 and 7 presented the highest values of specific DEGs, in particular, new immune related genes and microRNAs were found, such as *Il2*, *Foxp3*, *Il16a*, *Ccr1* and *Mir155hg*.

The enrichment analysis was performed using the *Blood Transcription Modules (BTM)* database and the *tmod* package, the complete results of the different groups are reported in the Supplementary Data Sheet 1. Figure 5 shows a summary of the

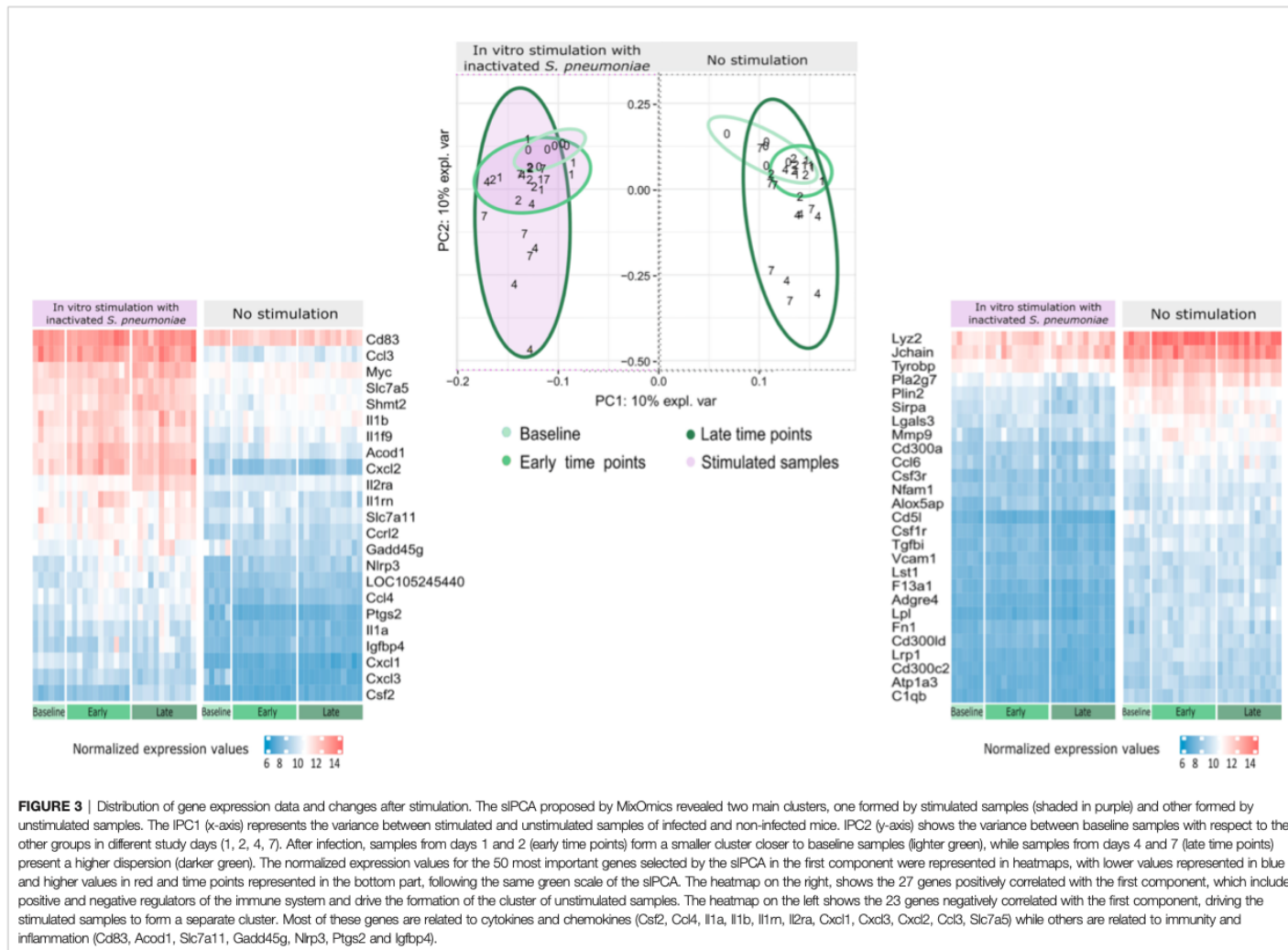
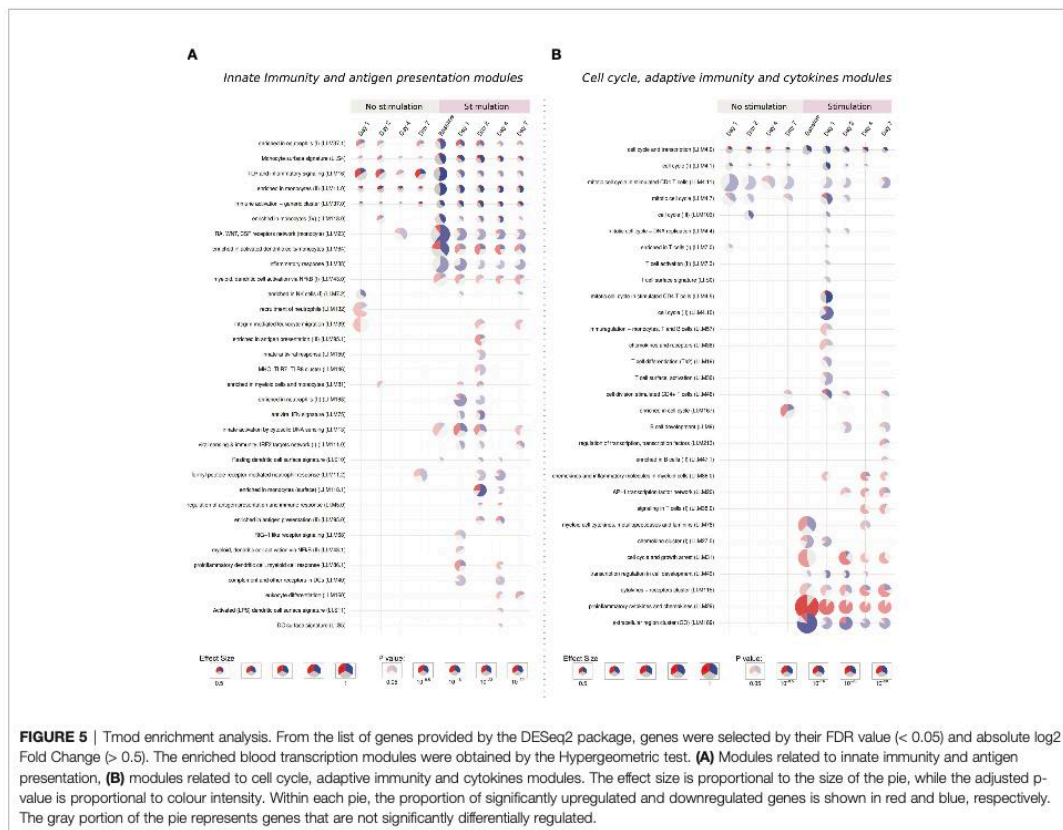
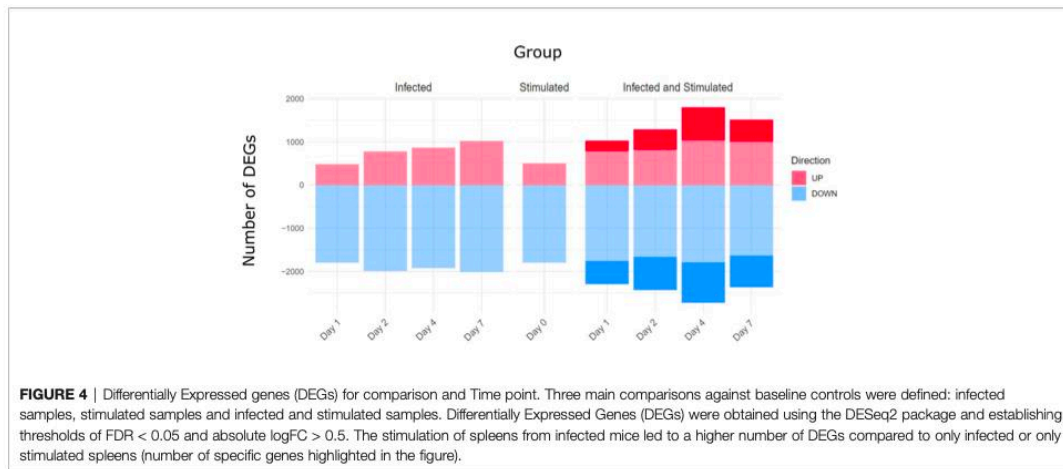


**FIGURE 3** | Distribution of gene expression data and changes after stimulation. The siPCA proposed by MixOmics revealed two main clusters, one formed by stimulated samples (shaded in purple) and other formed by unstimulated samples. The IPC1 (x-axis) represents the variance between stimulated and unstimulated samples of infected and non-infected mice. IPC2 (y-axis) shows the variance between baseline samples with respect to the other groups in different study days (1, 2, 4, 7). After infection, samples from days 1 and 2 (early time points) form a smaller cluster closer to baseline samples (lighter green), while samples from days 4 and 7 (late time points) present a higher dispersion (darker green). The normalized expression values for the 50 most important genes selected by the siPCA in the first component were represented in heatmaps, with lower values represented in blue and higher values in red and time points represented in the bottom part, following the same green scale of the siPCA. The heatmap on the right, shows the 27 genes positively correlated with the first component, which include positive and negative regulators of the immune system and drive the formation of the cluster of unstimulated samples. The heatmap on the left shows the 23 genes negatively correlated with the first component, driving the stimulated samples to form a separate cluster. Most of these genes are related to cytokines and chemokines (Csf2, Ccl4, Il1a, Il1b, Il1rn, Il2ra, Cxcl1, Cxcl2, Ccl3, Slc7a5) while others are related to immunity and inflammation (Cd83, Acod1, Slc7a11, Gadd45g, Nirp3, Ptgs2 and Igfbp4).



main immune system modules activated for each comparison and time point. In total, 87 modules were significantly enriched, only 3 of them being specifically activated in infected samples, while 40 modules were only activated after stimulation of previously infected samples.

### 3.3.1 Activation of Extracellular Matrix, Cell Adhesion, and Innate Immune Response Modules

Five modules were consistently activated at almost all time points in both unstimulated and *in vitro* stimulated groups. Related to monocytes, immune activation, TLR signaling, and cell cycle, these modules showed a different pattern after stimulation, presenting more down-regulated genes. Following the same direction, modules related to the extracellular region, monocytes, and cell cycle are especially enriched in down-regulated genes after stimulation (Figures 5A, B).

The “extracellular region cluster” module shows the downregulation of genes involved in the interaction with extracellular components, growth control, and the vascular endothelium/angiogenesis (HSPG2, GH1, ENG). Moreover, the monocyte chemoattractant CCL2 is also down-regulated, while CCL18, important for the recruitment of T lymphocytes but not monocytes, is up-regulated.

The stimulation down-regulates genes responsible for the proliferation and differentiation of monocytes and macrophages like CSF2RA, CSF1R, and CSF3R, the latter one also important for adhesion. In monocytes modules, other genes linked to the extracellular matrix and cell adhesion followed the same behavior.

The downregulation of extracellular matrix genes could be due to the process of *in vitro* stimulation, decreasing the cell adhesion to the plate surface.

### 3.3.2 Activation of Cell Cycle, Cytokines, and Adaptive Immune Response Modules

The stimulation of infected samples led to the enrichment of many biological pathways not activated in the previous comparisons, including modules related to antiviral response, antigen presentation, T cells, B cells, and chemokines (Figures 5A, B).

On the first day, unstimulated samples presented the enrichment of T cell and cell cycle modules. After stimulation, these same modules are activated, together with many others related to T cells and cell cycle, in both cases enriched mainly by down-regulated genes.

In T cell modules we find down-regulated cell-cycle genes and genes linked to cell adhesion, like VCAM1 and SIR3PG, while ITGA4, another adhesion-related gene, was up-regulated in unstimulated samples but presented no change after stimulation. Negative regulators of the T cell activity (LILRB4, LILRB3, SIT1) were also downregulated, while the few up-regulated genes were mainly related to T cell activation (CD3E, GRAP2, CDCA7, and LAT).

On the other hand, the specific modules in late time points were mostly activated by up-regulated genes. We observe a stronger activation of the “cytokines – receptors cluster”

module and the specific enrichment of pathways like leukocyte differentiation, signaling in T cells, enriched in B cells, among other modules.

Cytokine modules are activated from the stimulation of baseline samples and looking inside these modules, indeed we see many up-regulated genes independently of the time point, especially those from the CCL family, IL1A, IL1RN, and TNF. Other genes such as CSF2, IL2RA, IL6, IL10 and IL1B present a modest increase in stimulation of baseline samples, but a major up-regulation at late time points.

Despite the high number of activated modules, the response to the stimuli after a previous infection does not show general up-regulation of the immune and inflammatory response. This second contact with the pathogen through the *in vitro* stimulation permitted us to appreciate biological processes which could not be detected in the primary infection, especially those related to antigen presentation, adaptive immunity, and cytokines. These processes are possibly related to a recall immune response starting within the first days after infection.

### 3.4 Cytokines Assay Suggests the Promotion of Innate and Adaptive Immune Responses From Day 4 After Infection

Regarding the concentration of cytokines in splenocyte culture supernatants, the infection without subsequent stimulation did not result in significant increases in the concentration of cytokines, with exception of IL-17a at day 7 after infection (data not shown).

The stimulation process induced a significant increase in KC and MIP-1a, compared to baseline samples (median of differences of 42.46 and 184.4 pg/ml, respectively). Despite cytokine changes between stimulated and control samples being noticeable in early stages, they increased considerably upon *in vitro* stimulation, at days 4 and 7 after the infection (Figure 6).

The comparison of stimulated samples from days 4 and 7 after infection with only infected samples showed a significant increase in all cytokine concentrations, with exception of MCP-1 and IL12p40 (Figure 6 and Supplementary Image 3), suggesting the involvement of both innate and adaptive branches of the immune system. This increase was more accentuated on day 7, in which the difference in the median between the stimulated and unstimulated groups was 2597 pg/ml for IL-17A, 769 pg/ml for GM-CSF and 374 pg/ml for IFN-gamma.

### 3.5 Gene Expression and Cytokines Data Integration Indicate Specific Patterns of Recall Immune Response After Stimulation

To identify the genes correlated with the increase in the concentration of cytokines, especially at late time points, data integration was performed using the sparse version of Partial Least Squares (sPLS), from MixOmics package. PLS can integrate two types of data measured on the same sample by maximizing the covariance between the components of each data set. The sparse version applies LASSO  $\ell_1$  penalizations in PLS analysis to perform feature selection.

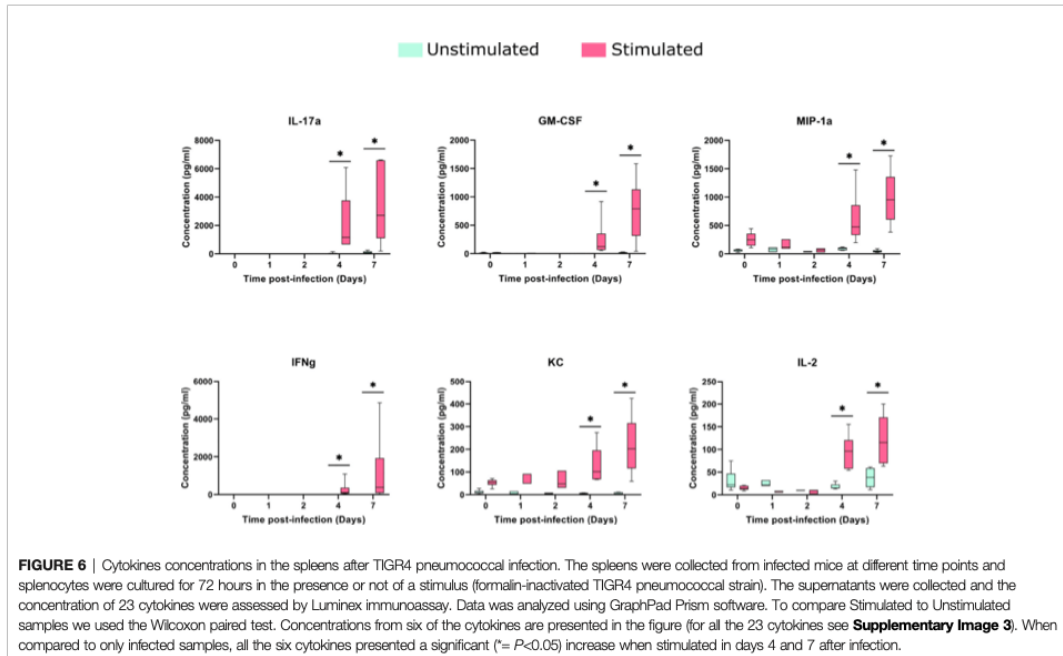


**FIGURE 6** | Cytokines concentrations in the spleens after TIGR4 pneumococcal infection. The spleens were collected from infected mice at different time points and splenocytes were cultured for 72 hours in the presence or not of a stimulus (formalin-inactivated TIGR4 pneumococcal strain). The supernatants were collected and the concentration of 23 cytokines were assessed by Luminex immunoassay. Data was analyzed using GraphPad Prism software. To compare Stimulated to Unstimulated samples we used the Wilcoxon paired test. Concentrations from six of the cytokines are presented in the figure (for all the 23 cytokines see **Supplementary Image 3**). When compared to only infected samples, all the six cytokines presented a significant (\*=  $P < 0.05$ ) increase when stimulated in days 4 and 7 after infection.

As expected, the *in vitro* stimulated samples formed a different cluster compared to the non-stimulated samples, although there is a different behavior regarding time points in each cluster (**Figure 7A**). In the non-stimulated cluster there is a perturbation caused by infection, but some samples from day 7 cluster together with control samples from day 0. On the other hand, *in vitro* stimulated samples presented a different pattern, samples from days 4 and 7 form a new cluster, driven by the increase in cytokine concentration and the expression of certain genes (**Figure 7B**).

By performing data integration and feature selection, sPLS identifies the genes whose expression is strongly associated with the concentrations of cytokines, providing the correlation value for each variable. The genes with the highest values of correlation with the 23 cytokines were Cd69, Csf2, Il2ra, and Il2 (**Figure 7C**). Other genes related to the immune system (Foxp3, Tnfrsf4, Tnfrsf9, Il10, and Il6) were also found positively correlated with the cytokines.

### 3.6 Possible Biomarkers Elicited by *In Vitro* Stimulation

We aimed to understand if feature selection could summarize the impact of a previous infection on stimulated samples, indicating possible biomarkers of this infection. We applied the DaMiR-seq package, which provides data normalization, feature selection, and classification, based on different machine learning techniques. Three groups were established based on the transcriptomics and cytokine data distribution, focusing on the stimulation of uninfected samples, samples from early time

points after infection (days 1 and 2), and samples from late time points (days 4 and 7).

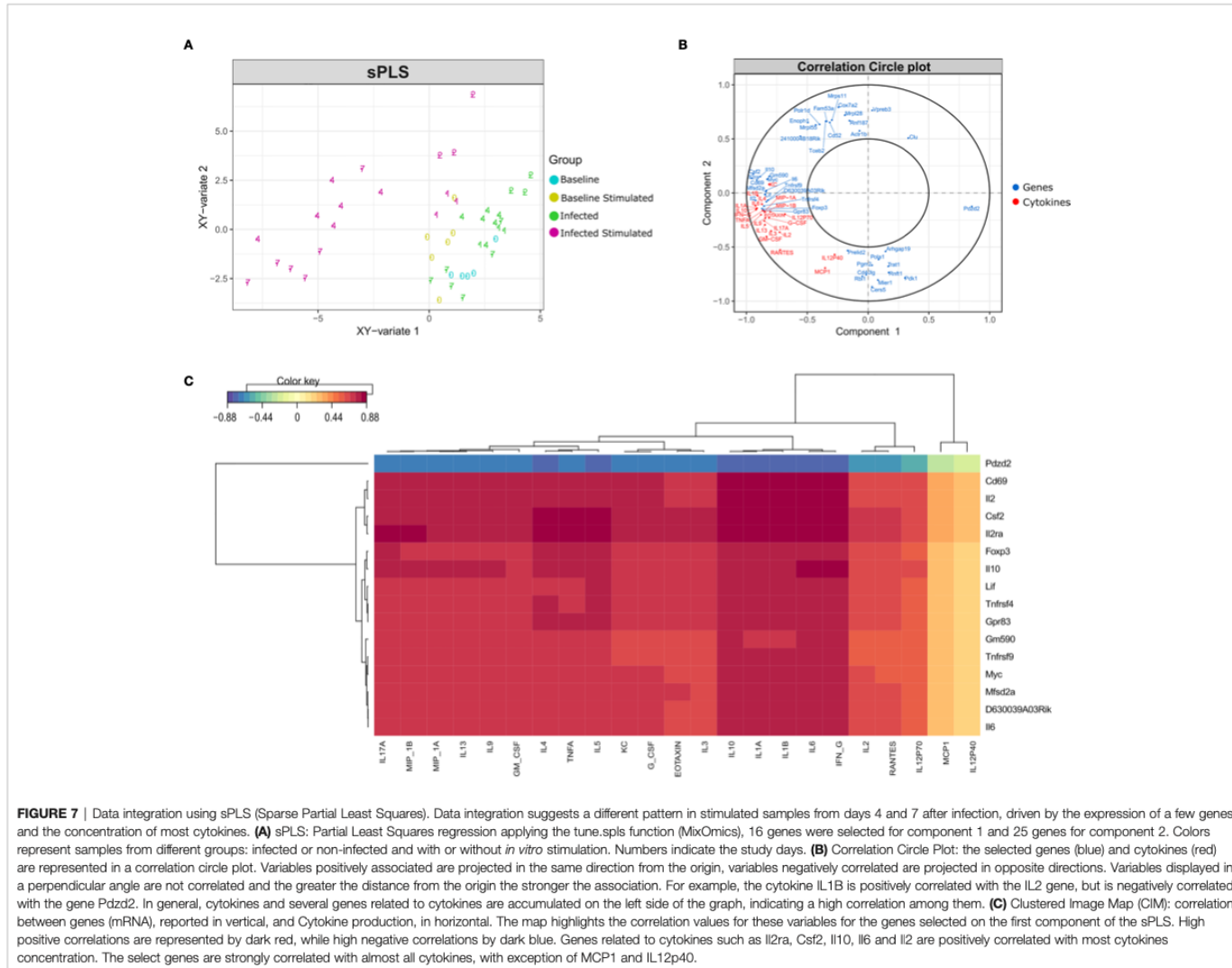
Eleven genes were chosen by applying a threshold of 0.5 to the scaled importance score identified by the DaMiR-seq package (**Supplementary Image 1**). These 11 genes allowed a clear clusterization of the three groups (**Figure 8**).

When compared to baseline stimulated samples, Fpr1, Nlrp3, and Slpi presented an increased expression in infected stimulated samples, independently of the time point. The stimulation of samples from early time points after the infection led to the increase in the expression of other inflammatory genes like Serpinb2 and Ch11 (Chitinase-3-like protein 1), and these values started to decrease in the subsequent days. At late time points, three other important genes, related to cytokine activity, had their expression increased when compared to the other groups: Ccr4, Csf2, and Il2.

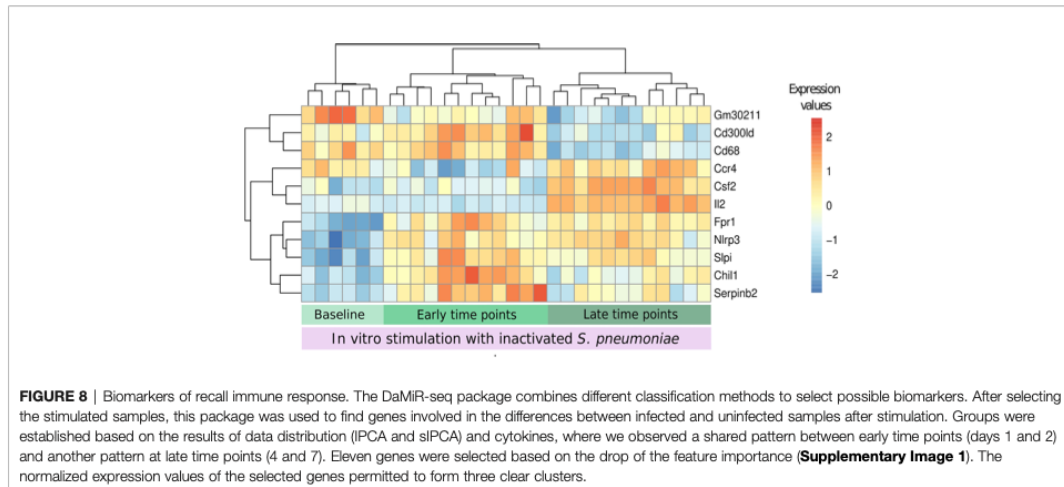
Despite the small number of samples being a limitation for this type of analysis, the feature selection summarizes the new immunological processes that arise after the stimulation of infected samples and suggests the use of the *in vitro* stimulation model to detect the presence of a previous pneumococcal infection by measuring the expression of a few genes.

## 4 DISCUSSION

To characterize the host response to *S. pneumoniae* we proposed a murine model of intranasal infection followed by an *in vitro*







stimulation of splenocytes with inactivated bacterial whole cells, at different time points after infection. Using a transcriptomic-based approach, our study has highlighted genes and biological pathways associated with the stimulation of baseline and previously infected samples, as well as the cytokines involved in the same processes.

In accordance with the genes selected by the sIPCA, the enrichment analysis has shown that the simple presence of inactivated bacteria leads to the activation of cytokines genes and different immune system pathways, mainly related to innate immunity. However, when this stimulation occurs in previously infected samples, there is a higher number of DEGs, revealing 40 new biological modules distributed across time points.

Stimulated samples presented downregulation of monocytes modules, together with the upregulation of antigen presentation and cytokine modules, which were also reported in gene expression data from alveolar macrophages (AM) in a pneumococcal colonization study, when comparing volunteers that developed carriage or not after experimental human pneumococcal challenge (Mitsi et al., 2020). In fact, the study did not suggest an increase in monocytes, but a higher monocyte-AM differentiation in people that developed carriage. On the other hand, monocytes seem to be recruited at the nose after the establishment of carriage (Jochems et al., 2018).

Recent vaccine studies have emphasized that innate immunity modules, including antigen presentation and dendritic cell activation, demonstrate stronger activation after a second contact with the antigen. Using an *in vivo* boost with the antigen alone following the priming with a chimeric vaccine against *Mycobacterium tuberculosis*, Santoro et al. have observed a faster and more robust response of dendritic cells and antigen presentation (Santoro et al., 2018). Similar results were recently observed in a different context, with an mRNA vaccine against SARS-CoV-2, in which the second dose activated new antigen presentation modules (Arunachalam et al., 2021).

Transcriptomics results have shown the presence of a particular response after a second contact with the pathogen and the concentrations of the cytokines suggested that this response is marked by different patterns of activation, with the stimulation allowing a better classification between early time points (1 and 2 days) and late time points (4 and 7) after infection. Moreover, the activated modules and the concentration of the soluble modulators suggested that both innate and adaptive branches of the immune system are promoted by the stimulation, suggesting cooperation between them.

In our model, cytokines secreted by macrophages, like MIP-1a (CCL3), KC (CXCL1), IL-1a, IL-1b, and IL-6 had a small, although significant, increase after stimulation of baseline samples. After stimulation of early time points, a small increase in the concentration of MIP-1b, RANTES, and TNF- $\alpha$  was observed, although not statistically significant. When the *in vitro* stimulus occurs at late time points after infection, the concentration of all these cytokines significantly increases, especially at day 7. In fact, innate immune responses to pneumococcus are known for polarization towards Th1 and Th17 responses through the release of cytokines (Bogaert et al., 2009).

Following this reasoning, it was expected that after the stimulation of baseline samples the cytokines linked to the adaptive immunity activation such as IL-17, IFN $\gamma$ , and IL-2 did not present an increased concentration in comparison to unstimulated samples. G-CSF and GM-CSF presented a small increase, although not significant. Again, at early time points no important changes are seen, but at late time points, a significant increase in the concentration was observed for all these cytokines, suggesting the activation of a Th1 and Th17 response starting around day 4. A strong Th1 response characterized by high levels of IFN $\gamma$  was also demonstrated in a murine model of bacterial meningitis by type 4 *S. pneumoniae*, already 48 hours after infection. (Pettini et al., 2015).

A previous study has highlighted the action of CD8 $^{+}$  T cells in helping AM to develop high MHC II expression after adenovirus

infection, a process that started coincidentally with the entry of T cells in the alveolar tissue, around 5 days after the infection (Yao et al., 2018). The activation of T cells in the spleen could follow a similar behavior in supporting macrophage activity and consequently increasing cytokine release.

Biomarker analysis and sPLS integration were employed to find genes that characterize the recall immune response and correlate with the increase in the concentration of the cytokines. Among the genes found positively correlated by the sPLS method, many were linked to the immune response. The TNF receptors *Tnfrsf9* and *Tnfrsf4*, are important for Th1 promotion and CD4 responses and, together with *Il2*, *Il2ra*, *Foxp3* and *Il10* participate in the “NF-kappaB signaling” biological pathway (Cho et al., 2021). Moreover, these genes are also associated with regulatory T cells, along with *Cd69* and *Il6*, two other features found correlated with cytokines in the same analysis (Maloy and Powrie, 2005; Kimura and Kishimoto, 2010; Chaudhry et al., 2011; Yu et al., 2018; Hinterbrandner et al., 2021).

The eleven genes selected as possible biomarkers are capable of correctly clustering the stimulated samples in the studied groups (baseline, early, and late time points, **Figure 8**). These genes could be cross validated in future studies using the same model of pneumococcal lung infection to study vaccine strategies and antimicrobial therapies. A link with pneumococcal infection, colonization, or vaccination was established in the literature for most of the selected genes. The *Il2* and *Csf2* genes were not only the first and third most important genes for the classification of samples regarding the presence of a previous infection but they were also among the genes with the highest correlation with the concentration of different cytokines, together with the *Il2ra* gene. This highlights the importance of the IL-2 signaling pathway to the described recall response. Indeed, different vaccine studies reported an increase in IL-2 cytokine after restimulation with pneumococcal proteins or peptides from these proteins (Kataoka et al., 2011; Singh et al., 2014; Elhaik Goldman et al., 2016; Converso et al., 2017).

*Csf2* gene encodes for Granulocyte/Macrophage colony-stimulating factor (GM-CSF), a cytokine that presented one of the highest concentrations after stimulation of infected samples from late time points. Previous studies have described the increase in *Csf2* expression and GM-CSF concentration in the lungs from mice infected intranasally with *S. pneumoniae* (Steinwede et al., 2011). *In vitro* stimulation of PBMCs with *S. pneumoniae* has also increased the concentration of this cytokine. Furthermore, a protective role of GM-CSF in pneumococcal infection was described with intra-alveolar administration of this cytokine (Schmeck et al., 2004; Steinwede et al., 2011) and the resistance to lung infection attributed to the microbiota was found to be through GM-CSF signaling (Brown et al., 2017).

The lack of *Fpr1* and *Chil1* led to a higher mortality rate in murine models of pneumococcal meningitis and pneumonia, respectively (Dela Cruz et al., 2012; Oldekamp et al., 2014).

*Slpi* is involved in the innate immune response to bacterial infections, regulating the NF-kappa-B activation and inflammatory responses. This gene was up-regulated in the lungs of mice infected with pneumococcus, but the same was not observed in the spleen, suggesting that its expression is modulated at the site of

inflammation in the presence of inflammatory stimuli (Abe et al., 1997). Our data suggested a similar result, since *Slpi* expression did not change in the spleen of infected samples, but only increased after the *in vitro* stimulation.

*Cd300ld* presents no clear link with pneumococcal infection, but its encoded protein, an activating receptor in myeloid and mast cells, was downregulated in the blood of mice infected with *Streptococcus suis* (Dai et al., 2018).

The link of most of the selected genes with the physiopathology of pneumococcal infection supports the use of feature selection and machine learning techniques to unveil gene signatures, potentially finding new features and/or assigning new roles to genes involved in a process, such as recall responses. The changes in cytokines concentration and gene expression are two important ways to assess immunological information after infection or vaccination. Our findings suggest that *in vitro* stimulation is an important step to understanding the systemic response to pneumococcal lung infection and the immunological memory generated by this bacteria. The analysis of transcriptomic and cytokine data revealed a clustering of the samples based on the stage of infection (early vs late), with more intense signals at late time points. Integrative analysis identified few genes, related to the immune system, which could categorize the samples based on the infection stage and which may be useful in future studies to monitor vaccine immune response and experimental therapies efficacy.

## DATA AVAILABILITY STATEMENT

The datasets generated for this study can be found in the GEO database under accession number: <https://www.ncbi.nlm.nih.gov/geo/query/acc.cgi?acc=GSE199605>. The bioinformatic analysis can be accessed at [https://github.com/IsaMoscardini/Spleen\\_stimulation](https://github.com/IsaMoscardini/Spleen_stimulation).

## ETHICS STATEMENT

The animal study was reviewed and approved by the Italian Ministry of Health with authorization n° 304/2018-PR.

## AUTHOR CONTRIBUTIONS

GP, FI and FS conceived and designed the experiments. FS and MC prepared the bacteria for animal infection and for *in vitro* stimulation. MC, FF, SG and EP performed animal experiments. MC and CG performed transcriptomic analysis. MC and FF analysed cytokines. DM secured funding. IM analysed data and drafted the paper with contributions from FS, AG and GP. All the authors reviewed, edited and approved the final version of the manuscript.

## FUNDING

This study was carried out with financial support from the Commission of the European Communities, Seventh

Framework Programme, Innovative Medicines Initiative Joint Undertaking “Biomarkers for Enhanced Vaccine Safety” project BioVacSafe (IMI JU Grant No. 115308).

IM received a PhD fellowship under the Marie Skłodowska-Curie actions (MSCA) – Innovative Training Networks (ITN), Project VacPath (Novel vaccine vectors to resist pathogen challenge) grant agreement No 812915 funded by the European Union’s Horizon 2020 research and innovation programme.

## SUPPLEMENTARY MATERIAL

The Supplementary Material for this article can be found online at: <https://www.frontiersin.org/articles/10.3389/fcimb.2022.869763/full#supplementary-material>

## REFERENCES

- Abe, T., Tominaga, Y., Kikuchi, T., Watanabe, A., Satoh, K., Watanabe, Y., et al. (1997). Bacterial Pneumonia Causes Augmented Expression of the Secretory Leukoprotease Inhibitor Gene in the Murine Lung. *Am. J. Respir. Crit. Care Med.* 156, 1235–1240. doi: 10.1164/ajrccm.156.4.9701075
- Arunachalam, P. S., Scott, M. K. D., Hagan, T., Li, C., Feng, Y., Wimmers, F., et al. (2021). Systems Vaccinology of the BNT162b2 mRNA Vaccine in Humans. *Nature* 596, 410–416. doi: 10.1038/s41586-021-03791-x
- Bogaert, D., Weinberger, D., Thompson, C., Lipsitch, M., and Malley, R. (2009). Impaired Innate and Adaptive Immunity to Streptococcus Pneumoniae and its Effect on Colonization in an Infant Mouse Model. *Infect. Immun.* 77, 1613–1622. doi: 10.1128/IAI.00871-08
- Briles, D. E., Paton, J. C., Mukerji, R., Swiatlo, E., and Crain, M. J. (2019). Pneumococcal Vaccines. *Microbiol. Spectr.* 7(6). doi: 10.1128/microbiolspec.GPP3-0028-2018
- Brown, R. L., Sequeira, R. P., and Clarke, T. B. (2017). The Microbiota Protects Against Respiratory Infection via GM-CSF Signaling. *Nat. Commun.* 8, 1512. doi: 10.1038/s41467-017-01803-x
- Cerutti, A., Cols, M., and Puga, I. (2013). Marginal Zone B Cells: Virtues of Innate-Like Antibody-Producing Lymphocytes. *Nat. Rev. Immunol.* 13, 118–132. doi: 10.1038/nri3383
- Chaudhry, A., Samstein, R. M., Treuting, P., Liang, Y., Pils, M. C., Heinrich, J.-M., et al. (2011). Interleukin-10 Signaling in Regulatory T Cells is Required for Suppression of Th17 Cell-Mediated Inflammation. *Immunity* 34, 566–578. doi: 10.1016/j.immuni.2011.03.018
- Chiesa, M., Colombo, G. I., and Piacentini, L. (2018). DaMiRseq—an R/Bioconductor Package for Data Mining of RNA-Seq Data: Normalization, Feature Selection and Classification. *Bioinformatics* 34, 1416–1418. doi: 10.1093/bioinformatics/btx95
- Cho, J.-W., Son, J., Ha, S.-J., and Lee, I. (2021). Systems Biology Analysis Identifies TNFRSF9 as a Functional Marker of Tumor-Infiltrating Regulatory T-Cell Enabling Clinical Outcome Prediction in Lung Cancer. *Comput. Struct. Biotechnol. J.* 19, 860–868. doi: 10.1016/j.csbj.2021.01.025
- Converso, T. R., Goulart, C., Rodriguez, D., Darrieux, M., and Leite, L. C. C. (2017). Systemic Immunization With Rpotd Reduces Streptococcus Pneumoniae Nasopharyngeal Colonization in Mice. *Vaccine* 35, 149–155. doi: 10.1016/j.vaccine.2016.11.027
- Dai, J., Lai, L., Tang, H., Wang, W., Wang, S., Lu, C., et al. (2018). Streptococcus Suis Synthesizes Deoxyadenosine and Adenosine by 5'-Nucleotidase to Dampen Host Immune Responses. *Virulence* 9, 1509–1520. doi: 10.1080/21505594.2018.1520544
- Dela Cruz, C. S., Liu, W., He, C. H., Jacoby, A., Gornitzky, A., Ma, B., et al. (2012). Chitinase 3-Like-1 Promotes Streptococcus Pneumoniae Killing and Augments Host Tolerance to Lung Antibacterial Responses. *Cell Host Microbe* 12, 34–46. doi: 10.1016/j.chom.2012.05.017
- Deniset, J. F., Surewaard, B. G., Lee, W.-Y., and Kubers, P. (2017). Splenic Ly6Ghigh Mature and Ly6Gint Immature Neutrophils Contribute to Eradication of *S. Pneumoniae*. *J. Exp. Med.* 214, 1333–1350. doi: 10.1084/jem.20161621
- de Stoppelaar, S. F., Claushuis, T. A. M., Schaap, M. C. L., Hou, B., van der Poll, T., Nieuwland, R., et al. (2016). Toll-Like Receptor Signaling Is Not Involved in Platelet Response to Streptococcus Pneumoniae *In Vitro* or *In Vivo*. *PLoS One* 11, e0156977. doi: 10.1371/journal.pone.0156977
- Elhaik Goldman, S., Dotan, S., Talias, A., Lilo, A., Azriel, S., Malka, I., et al. (2016). Streptococcus Pneumoniae Fructose-1,6-Bisphosphate Aldolase, a Protein Vaccine Candidate, Elicits Th1/Th2/Th17-Type Cytokine Responses in Mice. *Int. J. Mol. Med.* 37, 1127–1138. doi: 10.3892/ijmm.2016.2512
- Ercoli, G., Fernandes, V. E., Chung, W. Y., Wanford, J. J., Thomson, S., Bayliss, C. D., et al. (2018). Intracellular Replication of Streptococcus Pneumoniae Inside Splenic Macrophages Serves as a Reservoir for Septicaemia. *Nat. Microbiol.* 3, 600–610. doi: 10.1038/s41564-018-0147-1
- Fiorino, F., Pettini, E., Koeberling, O., Ciabattini, A., Pozzi, G., Martin, L. B., et al. (2021). Long-Term Anti-Bacterial Immunity Against Systemic Infection by Salmonella Enterica Serovar Typhimurium Elicited by a GMMMA-Based Vaccine. *Vaccines (Basel)* 9, 495. doi: 10.3390/vaccines9050495
- Gerlini, A., Colomba, L., Furi, L., Braccini, T., Manso, A. S., Pammolli, A., et al. (2014). The Role of Host and Microbial Factors in the Pathogenesis of Pneumococcal Bacteraemia Arising From a Single Bacterial Cell Bottleneck. *PLoS Pathog.* 10, e1004026. doi: 10.1371/journal.ppat.1004026
- Hinterbrandner, M., Rubino, V., Stoll, C., Forster, S., Schnüriger, N., Radpour, R., et al. (2021). Tnfrsf4-Expressing Regulatory T Cells Promote Immune Escape of Chronic Myeloid Leukemia Stem Cells. *JCI Insight* 6, e151797. doi: 10.1172/jci.insight.151797
- Iannelli, F., Santoro, F., Fox, V., and Pozzi, G. (2021). A Mating Procedure for Genetic Transfer of Integrative and Conjugative Elements (ICEs) of Streptococci and Enterococci. *Methods Protoc.* 4, 59. doi: 10.3390/mps4030059
- Jochems, S. P., Marcon, F., Carniel, B. F., Holloway, M., Mitsi, E., Smith, E., et al. (2018). Inflammation Induced by Influenza Virus Impairs Human Innate Immune Control of Pneumococcus. *Nat. Immunol.* 19, 1299–1308. doi: 10.1038/s41590-018-0231-y
- Kadioglu, A., Cuppone, A. M., Trappetti, C., List, T., Spreafico, A., Pozzi, G., et al. (2011). Sex-Based Differences in Susceptibility to Respiratory and Systemic Pneumococcal Disease in Mice. *J. Infect. Dis.* 204, 1971–1979. doi: 10.1093/infdis/jir657
- Kaplan, S. L., Barson, W. J., Lin, P. L., Romero, J. R., Bradley, J. S., Tan, T. Q., et al. (2013). Early Trends for Invasive Pneumococcal Infections in Children After the Introduction of the 13-Valent Pneumococcal Conjugate Vaccine. *Pediatr. Infect. Dis. J.* 32, 203–207. doi: 10.1097/INF.0b013e318275614b
- Kataoka, K., Fujihashi, K., Oma, K., Fukuyama, Y., Hollingshead, S. K., Sekine, S., et al. (2011). The Nasal Dendritic Cell-Targeting Flt3 Ligand as a Safe Adjuvant Elicits Effective Protection Against Fatal Pneumococcal Pneumonia. *Infect. Immun.* 79, 2819–2828. doi: 10.1128/IAI.01360-10
- Kimura, A., and Kishimoto, T. (2010). IL-6: Regulator of Treg/Th17 Balance. *Eur. J. Immunol.* 40, 1830–1835. doi: 10.1002/eji.201040391

- Lê Cao, K.-A., Rossouw, D., Robert-Granié, C., and Besse, P. (2008). A Sparse PLS for Variable Selection When Integrating Omics Data. *Stat. Appl. Genet. Mol. Biol.* 7. doi: 10.2202/1544-6115.1390
- Li, S., Roupheal, N., Duraisingham, S., Romero-Steiner, S., Presnell, S., Davis, C., et al. (2014). Molecular Signatures of Antibody Responses Derived From a Systems Biology Study of Five Human Vaccines. *Nat. Immunol.* 15, 195–204. doi: 10.1038/ni.2789
- Love, M. I., Huber, W., and Anders, S. (2014). Moderated Estimation of Fold Change and Dispersion for RNA-Seq Data With DESeq2. *Genome Biol.* 15, 550. doi: 10.1186/s13059-014-0550-8
- Maloy, K. J., and Powrie, F. (2005). Fueling Regulation: IL-2 Keeps CD4+ Treg Cells Fit. *Nat. Immunol.* 6, 1071–1072. doi: 10.1038/ni1105-1071
- Mitsi, E., Carniel, B., Reiné, J., Rylance, J., Zaidi, S., Soares-Schanoski, A., et al. (2020). Nasal Pneumococcal Density Is Associated With Microaspiration and Heightened Human Alveolar Macrophage Responsiveness to Bacterial Pathogens. *Am. J. Respir. Crit. Care Med.* 201, 335–347. doi: 10.1164/rccm.201903-0670OC
- Moffitt, K. L., Gierahn, T. M., Lu, Y., Gouveia, P., Alderson, M., Flechtner, J. B., et al. (2011). T(H)17-Based Vaccine Design for Prevention of Streptococcus Pneumoniae Colonization. *Cell Host Microbe* 9, 158–165. doi: 10.1016/j.chom.2011.01.007
- Oldekamp, S., Pscheidt, S., Kress, E., Soehnlein, O., Jansen, S., Pufe, T., et al. (2014). Lack of Formyl Peptide Receptor 1 and 2 Leads to More Severe Inflammation and Higher Mortality in Mice With of Pneumococcal Meningitis. *Immunology* 143, 447–461. doi: 10.1111/imm.12324
- Paranavitana, C., Zelazowska, E., DaSilva, L., Pittman, P. R., and Nikolich, M. (2010). Th17 Cytokines in Recall Responses Against Francisella Tularensis in Humans. *J. Interferon Cytokine Res.* 30, 471–476. doi: 10.1089/jir.2009.0108
- Pettini, E., Fiorino, F., Cuppone, A. M., Iannelli, F., Medagliani, D., and Pozzi, G. (2015). Interferon- $\gamma$  From Brain Leukocytes Enhances Meningitis by Type 4 Streptococcus Pneumoniae. *Front. Microbiol.* 6. doi: 10.3389/fmicb.2015.01340
- Pichichero, M. E. (2017). Pneumococcal Whole-Cell and Protein-Based Vaccines: Changing the Paradigm. *Expert Rev. Vaccines* 16, 1181–1190. doi: 10.1080/14760584.2017.1393335
- Santoro, F., Donato, A., Lucchesi, S., Sorgi, S., Gerlini, A., Haks, M. C., et al. (2021). Human Transcriptomic Response to the VSV-Vectored Ebola Vaccine. *Vaccines (Basel)* 9, 67. doi: 10.3390/vaccines9020067
- Santoro, F., Pettini, E., Kazmin, D., Ciabattini, A., Fiorino, F., Gilfillan, G. D., et al. (2018). Transcriptomics of the Vaccine Immune Response: Priming With Adjuvant Modulates Recall Innate Responses After Boosting. *Front. Immunol.* 9. doi: 10.3389/fimmu.2018.01248
- Schmeck, B., Zahlen, J., Moog, K., van Laak, V., Huber, S., Hocke, A. C., et al. (2004). Streptococcus Pneumoniae-Induced P38 MAPK-Dependent Phosphorylation of RelA at the Interleukin-8 Promotor. *J. Biol. Chem.* 279, 53241–53247. doi: 10.1074/jbc.M313702200
- Schultz, M. J., Speelman, P., Zaat, S., van Deventer, S. J., and van der Poll, T. (1998). Erythromycin Inhibits Tumor Necrosis Factor Alpha and Interleukin 6 Production Induced by Heat-Killed Streptococcus Pneumoniae in Whole Blood. *Antimicrob. Agents Chemother.* 42, 1605–1609. doi: 10.1128/AAC.42.7.1605
- Shao, J., Zhang, J., Wu, X., Mao, Q., Chen, P., Zhu, F., et al. (2015). Comparing the Primary and Recall Immune Response Induced by a New EV71 Vaccine Using Systems Biology Approaches. *PLoS One* 10, e0140515. doi: 10.1371/journal.pone.0140515
- Singh, R., Gupta, P., Sharma, P. K., Ades, E. W., Hollingshead, S. K., Singh, S., et al. (2014). Prediction and Characterization of Helper T-Cell Epitopes From Pneumococcal Surface Adhesin A. *Immunology* 141, 514–530. doi: 10.1111/imm.12194
- Steinwede, K., Tempelhof, O., Bolte, K., Maus, R., Böhlring, J., Ueberberg, B., et al. (2011). Local Delivery of GM-CSF Protects Mice From Lethal Pneumococcal Pneumonia. *J. Immunol.* 187, 5346–5356. doi: 10.4049/jimmunol.1101413
- Trammell, R. A., and Toth, L. A. (2011). Markers for Predicting Death as an Outcome for Mice Used in Infectious Disease Research. *Comp. Med.* 61, 492–498.
- Weiner, J. N., and Domaszewska, T. (2016). Tmod: An R Package for General and Multivariate Enrichment Analysis. *Peer J Inc. Preprints* 4:e2420v1. doi: 10.7287/peerj.preprints.2420v1
- Weiser, J. N., Ferreira, D. M., and Paton, J. C. (2018). Streptococcus Pneumoniae: Transmission, Colonization and Invasion. *Nat. Rev. Microbiol.* 16, 355–367. doi: 10.1038/s41579-018-0001-8
- Wu, Y., Mao, H., Ling, M.-T., Chow, K.-H., Ho, P.-L., Tu, W., et al. (2011). Successive Influenza Virus Infection and Streptococcus Pneumoniae Stimulation Alter Human Dendritic Cell Function. *BMC Infect. Dis.* 11, 201. doi: 10.1186/1471-2334-11-201
- Yao, F., Coquery, J., and Lê Cao, K.-A. (2012). Independent Principal Component Analysis for Biologically Meaningful Dimension Reduction of Large Biological Data Sets. *BMC Bioinf.* 13, 24. doi: 10.1186/1471-2105-13-24
- Yao, Y., Jeyanathan, M., Haddadi, S., Barra, N. G., Vaseghi-Shanjani, M., Damjanovic, D., et al. (2018). Induction of Autonomous Memory Alveolar Macrophages Requires T Cell Help and Is Critical to Trained Immunity. *Cell* 175, 1634–1650.e17. doi: 10.1016/j.cell.2018.09.042
- Yu, L., Yang, F., Zhang, F., Guo, D., Li, L., Wang, X., et al. (2018). CD69 Enhances Immunosuppressive Function of Regulatory T-Cells and Attenuates Colitis by Prompting IL-10 Production. *Cell Death Dis.* 9, 905. doi: 10.1038/s41419-018-0927-9
- Zhan, Y., and Cheers, C. (1995). Differential Induction of Macrophage-Derived Cytokines by Live and Dead Intracellular Bacteria *In Vitro*. *Infect. Immun.* 63, 720–723. doi: 10.1128/iai.63.2.720-723.1995

**Conflict of Interest:** Authors IM and AG are employed by Microbiotec srl.

The remaining authors declare that the research was conducted in the absence of any commercial or financial relationships that could be construed as a potential conflict of interest.

**Publisher's Note:** All claims expressed in this article are solely those of the authors and do not necessarily represent those of their affiliated organizations, or those of the publisher, the editors and the reviewers. Any product that may be evaluated in this article, or claim that may be made by its manufacturer, is not guaranteed or endorsed by the publisher.

Copyright © 2022 Moscardini, Santoro, Carraro, Gerlini, Fiorino, Germoni, Gholami, Pettini, Medagliani, Iannelli and Pozzi. This is an open-access article distributed under the terms of the Creative Commons Attribution License (CC BY). The use, distribution or reproduction in other forums is permitted, provided the original author(s) and the copyright owner(s) are credited and that the original publication in this journal is cited, in accordance with accepted academic practice. No use, distribution or reproduction is permitted which does not comply with these terms.

# CHAPTER 5

## **Development of a *Streptococcus pneumoniae* mouse model of pneumonia by intra-tracheal infection**

Samaneh Gholami, Francesco Iannelli, Elena Pettini, Fabio Fiorino, Francesco Santoro, Gianni Pozzi

Laboratory of Molecular Microbiology and Biotechnology (LAMMB), Department of Medical Biotechnologies, University of Siena, Siena, Italy

Manuscript in preparation

## **Abstract**

*Streptococcus pneumoniae* (pneumococcus) is a pathogenic organism and the leading cause of bacterial pneumonia. Human is the only natural host of this bacteria, thus host-pathogen interaction is poorly understood, and factors that drive a more severe phenotype are unknown. Experimental findings on Pneumococcal pneumonia in mice are contradictory due to the bacterial strain, dose of bacteria, route of infection as well as the animal models. Here, we established an intratracheal mouse model inducing standardized bacterial pneumonia and characterized the optimal dose and time of pneumonia.

Bacterial pneumonia was induced by intra-tracheal inoculation with *Streptococcus pneumoniae* TIGR4 at different doses. Clinical health score, body weight and temperature measured at different time points after infection. Bacterial counts in lungs and blood and histological changes in the lungs were assessed. Furthermore, we investigated the efficacy of this method to induce pneumonia in mice. Intra-tracheal inoculation resulted in reproducible pneumonia and bacteremia related to the dose of inoculum and demonstrated susceptibility to streptococcal pneumonia developing with a delay of at least 24 h after infection. Higher bacterial counts in mice infected 48 hours after infection suggested the optimal time point to harvest organs to study pneumonia. Pneumonia mortalities were observed in all mice infected by  $10^8$  within 24 hours of infection. We described an intratracheal model of bacterial infection in the lungs with optimal dose and timing that can be utilized for further investigation of disease mechanisms as well as vaccine efficacies.

## **Introduction**

The respiratory tract is extremely well defended from the invasion of pathogenic microorganisms thanks to the presence of chemical and physical barriers that prevent their penetration (Parker et al., 2016). However, some microorganisms have developed mechanisms to overcome these barriers and are responsible for significant morbidity and mortality (O'Brien et al., 2009).

Among the bacterial species capable of causing serious diseases in lower respiratory tract, *Streptococcus pneumoniae* (pneumococcus) is adapted to humans and often colonizes asymptotically. *S.pneumoniae* can cause various kinds of diseases ranging from upper

respiratory tract infections (sinusitis, otitis media) to serious diseases such as pneumonia, however, the mechanism of pathogenicity is not well understood (Henriques-Normark & Tuomanen, n.d.). *S.pneumoniae* is the most common cause of community-acquired pneumonia (Torres et al., n.d.) representing a huge financial and clinical burden worldwide (Feldman & Anderson, 2016), causing approximately 19% of mortality in children under the age of 5 (O'Brien et al., 2009). *Streptococcus pneumoniae* categorized as one of the twelve priority pathogens in 2017 by WHO (*The Top 10 Causes of Death*, n.d.). In order to prevent the spread of antibiotic-resistant strains and the development of invasive pneumococcal disease, vaccination remains the best choice.

Currently available pneumococcal vaccines have some limitations such as poor efficacy in early childhood (polysaccharide vaccine) and reduced serotype coverage (glycoconjugate vaccine) (Lee et al., 2003; K. L. Moffitt & Malley, 2011). The search for new vaccination strategies as well as mechanisms of the disease requires the development of new animal models of infection capable of evaluating their protective efficacy following the challenge (Griffin, 2002; Lee et al., 2003). The characterization of new vaccine candidates includes both the study of the immunogenicity of the vaccine formulation, i.e., its ability to induce a quantifiable humoral and cellular response, such as the measurement of antigen-specific antibody levels, cell populations of innate immunity and of soluble factors induced by vaccination such as the secretion of cytokines and chemokines, and its ability to protect the animal from the onset of infection. Although the presence of anti-capsule antibodies, and in particular with opsonophagocytic activity, was the main factor quantified in immunogenicity studies and probably sufficient to confer protection against invasive *S.pneumoniae* infections, to date it is not completely clear whether they are necessary. and especially if they are the natural protection mechanism that intervenes during *S.pneumoniae* infections (K. L. Moffitt & Malley, 2016). Different models of *S.pneumoniae* infection have been developed, using different routes of inoculation of the pathogen, but only some of these mimics the natural infection that occurs in humans (K. L. Moffitt & Malley, 2011). Another variable factor in animal infection models is the mouse strain used to induce the infection. Only some mouse haplotypes are susceptible to infection induced by *S.pneumoniae* and for many mouse models very high doses are required to induce disease and

thus evaluate the presence / absence of the bacterium or protection from vaccination-induced infection (Kadioglu & Andrew, 2005).

Given these considerations, it is necessary to continue the search for an animal model that allows to mimic natural infection and human pathology as best as possible in order to be able to evaluate, through biomarkers other than those currently used, the disease and protection from the infection produced. from a vaccine or therapy candidate. Between different animal models, mice are the most frequently used model of pneumococcal pneumonia. However, to mimic human pneumonia in mice, the bacterial strain, dose of inoculated bacteria and the method of inoculation should be considered since mice is not its natural host (Borsa et al., 2019; Chiavolini et al., 2008). There are different routes of infection used to study various pneumococcal infections. Among them, Intranasal (IN) and Intratracheal (IT) mostly used to investigate pneumococcal pneumonia (Borsa et al., 2019).

#### **Intranasal infection (IN);**

IN inoculation is a fast and easy procedure, used widely to mimic pneumonia in mice. There are two main IN techniques, Standard aspiration and Aerosol method. In standard aspiration, mice are lightly anesthetized and bacterial suspension is inoculated into the nostril through a pipette tip drop by drop to avoid any bubble formation. Aerosol technique is applied through a nebulizer connected to an exposure chamber. This method was used to study bacterial infection and colonization. By Aerosol method many mice can be inoculated simultaneously (Borsa et al., 2019).

#### **Intratracheal infection (IT);**

The use of the intratracheal infection route allows the bacterial suspension to be conveyed directly into the respiratory tract and into the lungs of mice. This technique has been shown to reproducibly induce infection in the lungs of infected mice in over 99% of cases (Borsa et al., 2019). The intratracheal route of infection offers more precise inoculation of the pathogen directly into the airways. This also has the advantage of being able to use lower concentrations of the pathogen to induce infection. This model is used in numerous studies on drug efficacy, host response to infection, and the role of pneumococcal virulence in disease (Rayamajhi et al., 2011).



Previous studies mainly used tracheal puncture method to inoculate bacteria. The surgery is invasive however the results were promising. Recently a new techniques of IT route called Oro-tracheal/peroral has been established. This method is non-invasive and bacterial suspension inoculates directly via orotracheal route. In this study we examined IT orotracheal challenge to mimic pneumococcal pneumonia in mice. Different groups of mice used to determine the best bacterial dose as well as appropriate timing to develop pneumonia.

## **Material and methods**

### **Animals**

Male C57BL/6n mice were purchased from Charles River (Lecco, Italy) and maintained under specific pathogen-free conditions in the animal facility of the Laboratory of Molecular Microbiology and Biotechnology (LAMMB), Department of Medical Biotechnologies at the University of Siena. Animals were maintained at 20-24 °C, with 55 ± 10% of humidity, with food and water ad libitum, and treated according to national guidelines (Decreto Legislativo 26/2014).

### **Bacterial preparation**

*S.pneumoniae* strain TIGR4 mouse-passaged as described in literature were used (Canvin et al., 1995). Briefly, mice were injected intravenously with 10<sup>7</sup> CFU TIGR4. After 24 hours the mouse was euthanized and liver, spleen and blood aseptically harvested. Meshed organs and blood were plated on tryptic-soy broth (TSB, Becton Dickinson, USA) -1.5% agar (TSA) -5% defibrinated horse blood (Oxoid, UK) and incubated at 37°C, 5% CO<sub>2</sub> over-night. Isolated colonies from liver were cultured on TSA-5% blood plates and confirmed by optochin sensitivity [(using Optochin disks: 6 mm, 5 µg) Thermo Fischer Scientific, USA]. In order to have the high yield bacteria, one or two colonies were inoculated in 10 ml of different media listed in Table 8. The bacterial growth curve and phase measurement were performed by detecting the total biomass of the bacteria culture using optical density measurements at OD = 590nm with a spectrophotometer. The bacterial growth phases were monitored by verifying the bacterial culture every 1-2 hours spectrophotometrically using Thermo-scientific Spectronic200, UV-visible spectrophotometer. The absorbance values were plotted against the different functional growth times in logarithmic scale. Bacterial colony count (CFU) was performed with the multilayer plating method (Iannelli & Pozzi, 2004). was calculated at different ODs through multilayer. The average pneumococcal chain length (Mean chain length: MCL) was evaluated through Gram-staining and microscopic examination at ODs 0.4, 0.6 and 1.0.

Table 8 Media composition used for optimal bacterial growth

Media	Composition	Additives
TSB-GYP	Tryptic Soy Broth (Becton Dickinson)	Glucose 0.2% Yeast extract 0.05% Phosphate 0.016 M
CAT-GP	Bacto Casitone, Yeast extract, Trypton and NaCl	Glucose 0.2% Phosphate 0.016 M
THB	TODD-HEWITT BROTH (OXOID)	--
BHI	BRAIN HEART INFUSION (OXOID)	--
BHI + 5% FBS	BRAIN HEART INFUSION (OXOID)	Fetal Bovin Serum 5%
BHI + 10% FBS	BRAIN HEART INFUSION (OXOID)	Fetal Bovin Serum 10%

### Preparation of inoculum

The day of the infection, mouse-passaged TIGR4 was inoculated 1:50 in TSB-GYP until mid-exponential phase (corresponding to approximately to OD<sub>590</sub>= 0.6). The bacterial culture was centrifuged at 2000x g for 10 minutes and resuspended in an appropriate volume of saline, considering that an OD<sub>590</sub> of 1 corresponded to ≈10<sup>8</sup> CFU/ml. Different doses of bacteria 10<sup>5</sup>, 10<sup>6</sup>, 10<sup>7</sup> and 10<sup>8</sup> CFU/ml in saline with a total volume of 50µl were prepared.

### Animal infection

For intra-tracheal infection, mice were lightly anesthetized with intraperitoneal administration of 11.25 mg/kg tiletamine hydrochloride/zolazepam and 3 mg/kg xylazine and the inoculum. Then mice were placed on the angled wooden platform hanging by its incisors on the wire and gently restrain it in place with a piece of ribbon shown in Figure 12.

With a pair of blunt ended forceps mouth was opened gently pry the tongue pulled out and was hold to the side. Endotracheal tubes were directed to the tracheal through fiber optic illuminator at a 90° angle until opening of the trachea were seen. Inoculum, prepared as described above, in 50µl saline was injected into the tracheal via intubation tube.

The infection dose was verified by plating 10-fold dilutions on blood-agar plates and incubated overnight at 37°C. Mice were checked daily for body temperature, weight, and clinical score for 7 days. Lung, spleen, liver and blood were collected on day1, 2, 3 and 7 post infection.

### **Pathology preparation of the mice lungs**

Mice were anesthetized by an intraperitoneal injection of tiletamine hydrochloride/zolazepam 30 mg/kg and xylazine 8 mg/kg (deep anesthesia) and exsanguinated by severing the abdominal aorta. Mice lungs were excised and fixed intra-tracheally with buffered formalin (5%) at a constant pressure of 20 cm H<sub>2</sub>O for 5 hours then dehydrated. Briefly a micropipette tips (yellow) is cut and placed in a cannula (20 G), the needle should be cut in half, then the cannula inserted into the trachea and fixed with a ligature. Lungs are inflated via the cannula by gentle insertion of formalin. Lungs and trachea are hanged that half of the lungs immersed in formalin for 5 hours. Then trachea and lungs are discarded from the cannula and immersed completely in formalin for another 1 hour. After 1 hour the lungs and trachea are washed with dH<sub>2</sub>O with a gentle pressure to take out extra formalin. Finally, lungs cleared in toluene and embedded under vacuum in paraffin. Multiple 6 µm latero-sagittal lung sections were made and stained with hematoxylin-eosin.

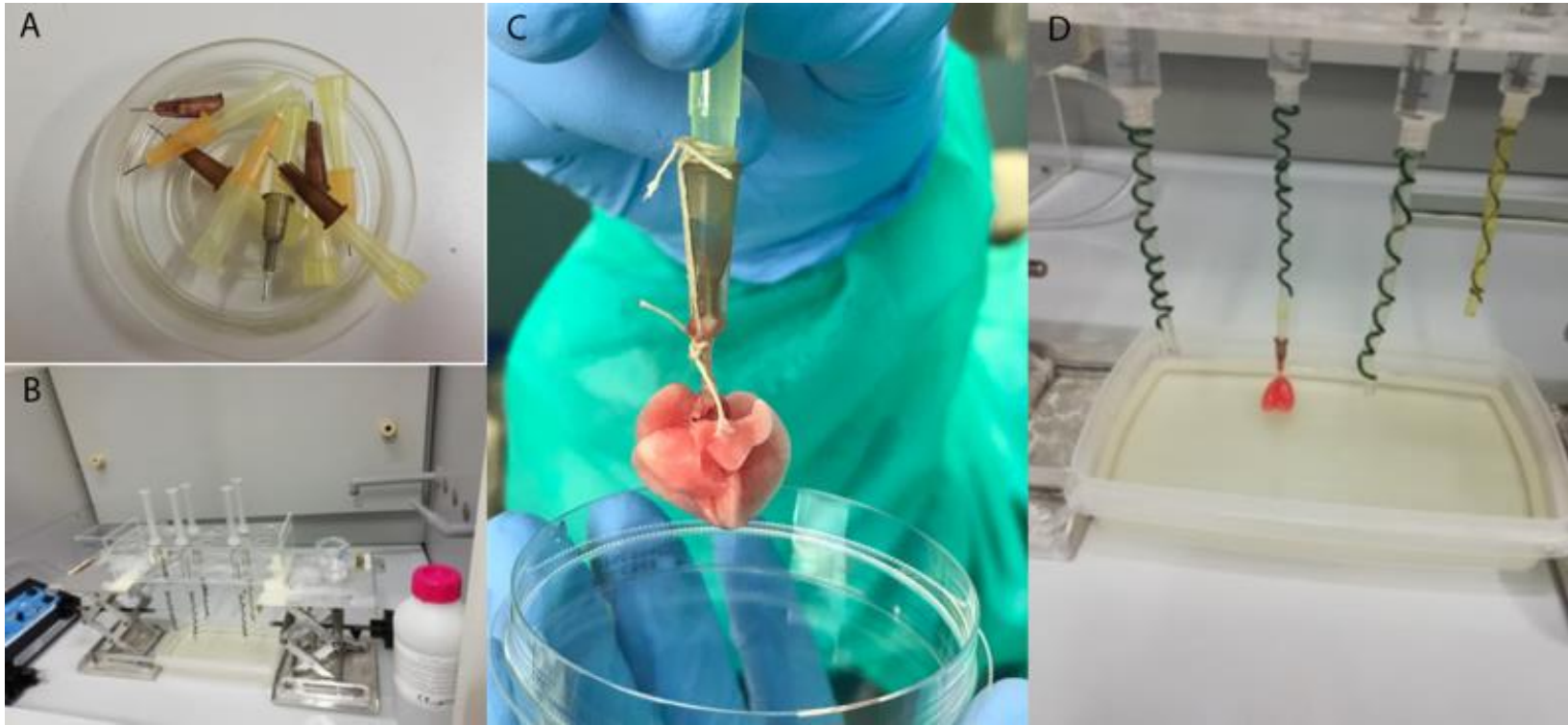


*Figure 12 Pathology preparation procedure. A. Cannula and micropipette tip. B. Apparatus for injecting formalin into lungs. C. Cannula inserted into trachea and fixed with a ligature. D. Lungs are immersed in formalin while the formalin is injected every 10 min for 4 hours*

## Results

### Variation in pneumococcus growth characteristics associated with the composition of media

The growth curves of *Streptococcus pneumoniae* TIGR4 were performed in different media, listed in Table 8. All media pH were precisely optimized based on providing company suggestions around 7.6. These data showed that *S.pneumoniae* grows equally fast in BHI media supplemented with various concentration of BSA followed by THB Figure 13. Mean chain length of bacteria were calculated in three different ODs and plotted on growth curve as shown in Figure 14. Changes in bacterial MCL in these media were not significant (P values > 0.5) however the longer chain was seen in CAT-GP followed by BHI with 10% FBS. Colony counts were also calculated in different time point and plotted versus growth curves shown in Figure 15. As these data showed, although CAT-GP cultures had lower CFU/ml, no significant changes in CFU observed in different media (P values > 0.1). Based on these data we decided to use BHI + 5% FBS and TBS-GYP for further investigation.

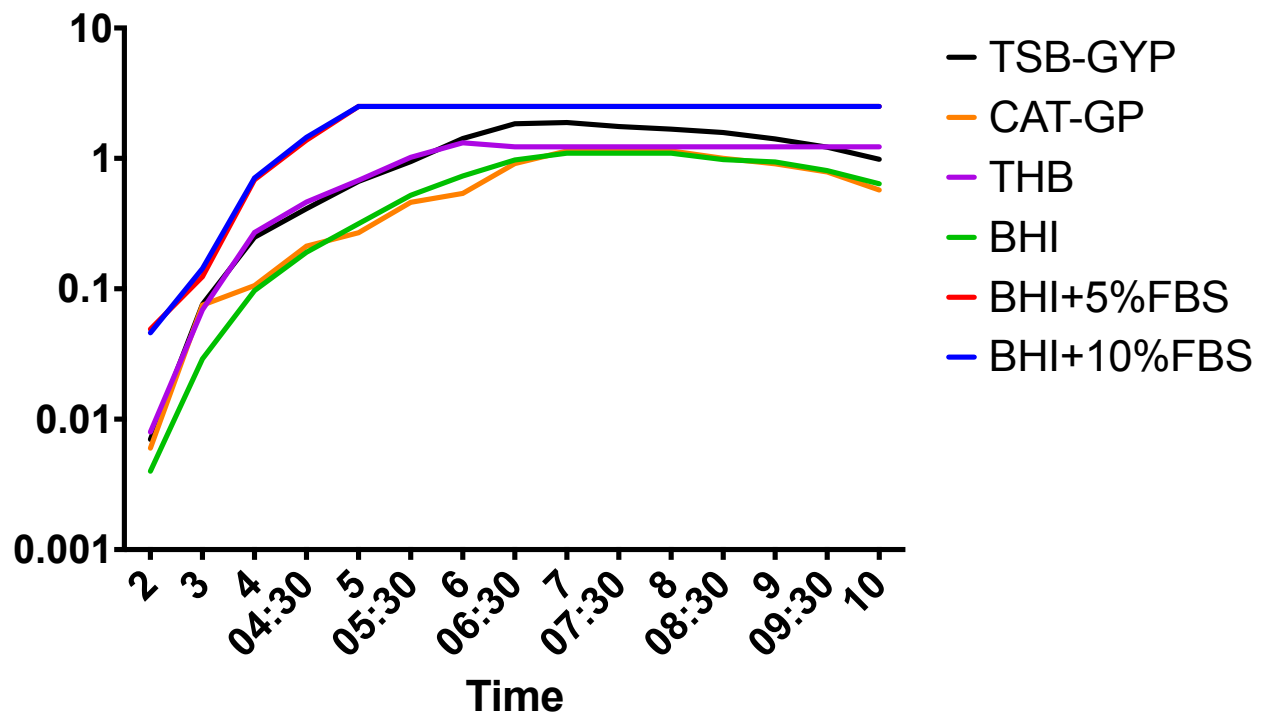


Figure 13 *S.pneumoniae* growth curve on different media listed above

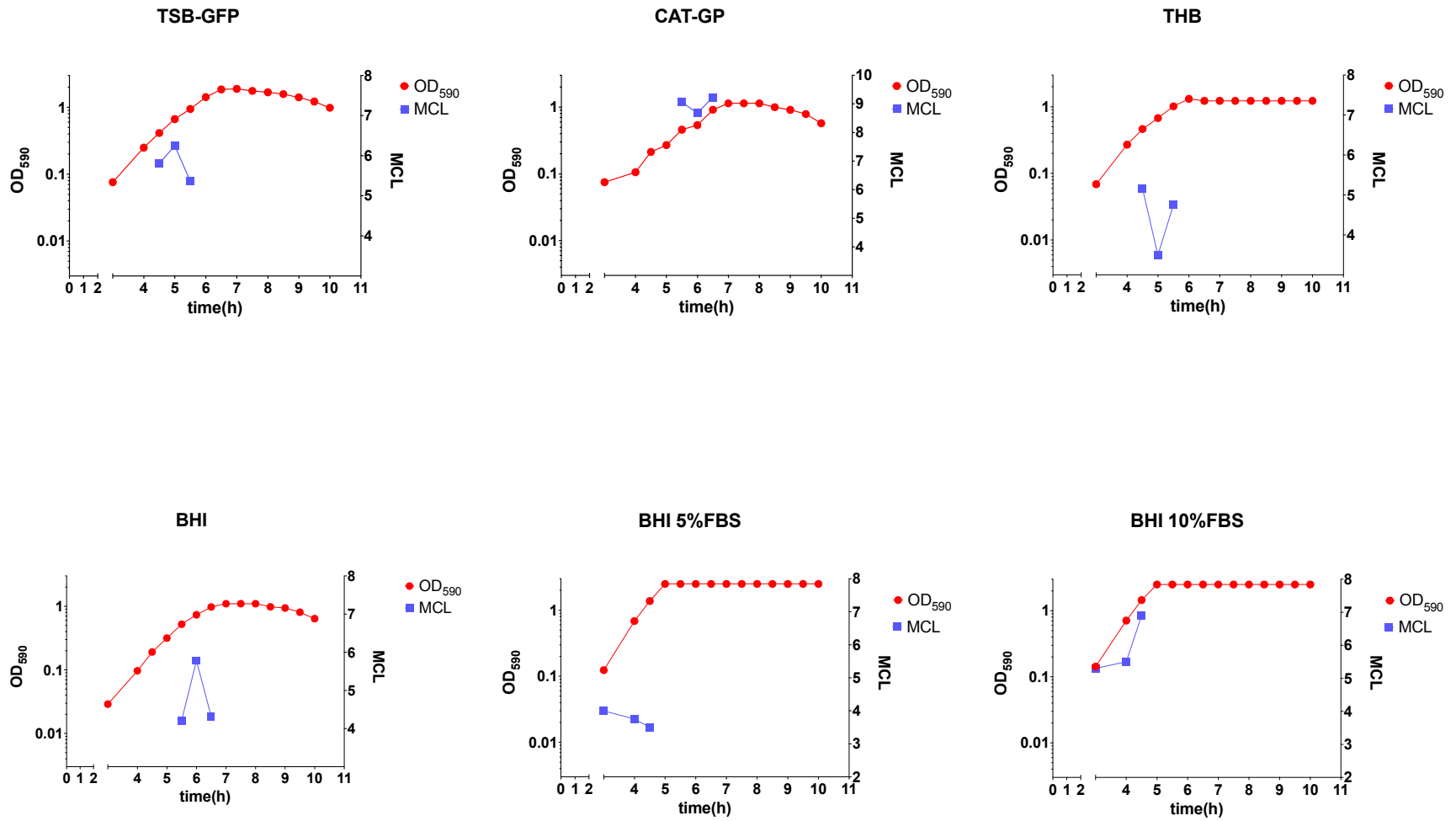


Figure 14 *S.pneumoniae* growth curve and mean chain (MCL) length in different media in 10 hours culture

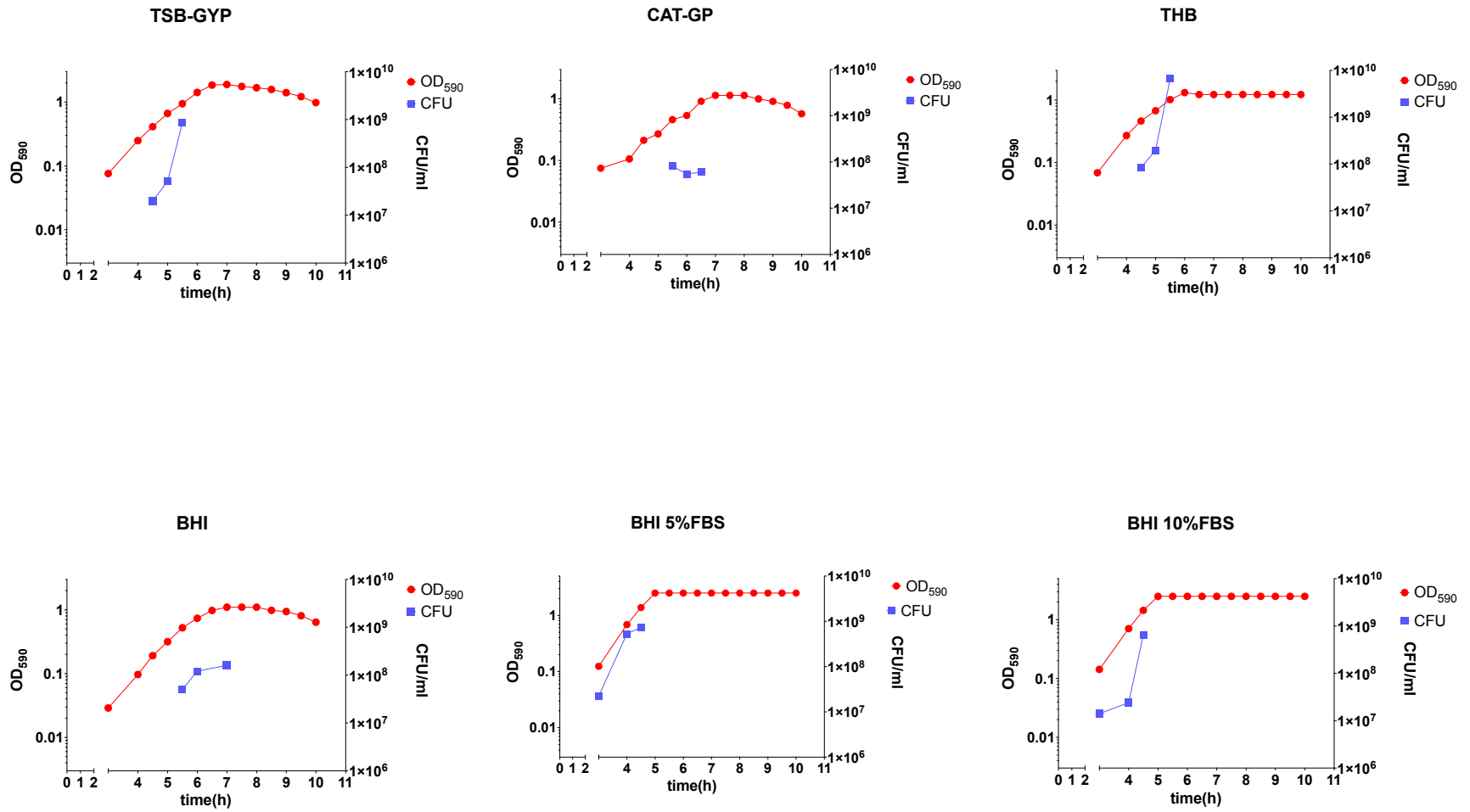


Figure 15 *S.pneumoniae* growth curve and colony count in different media in 10 hours culture



## Evans Blue administration reveals efficacy of intratracheal infection

In order to visualize the administration and final location of the inoculum through intratracheal infection using fiber optic illuminator, which is known as intubation mediated intratracheal administration, Evans blue used. This method showed very precise delivery of inoculum into lungs without affecting other organs as shown in Figure 16. Two doses of Evans Blue solution 20 $\mu$ l and 70 $\mu$ l were injected and result showed in Figure 17. The distribution of Evans Blue solution was not homogenous in lungs; however, the volume of injection as well as the timing should be considered. These mice were harvested at most one hour after injection. Also, higher volume of solution seems to fill the lungs. This observation indicates that to obtain accurate results, the volume of the inoculum should be considered. Thus, we chose 50 $\mu$ l volume of bacterial inoculum to inject into trachea through this method.

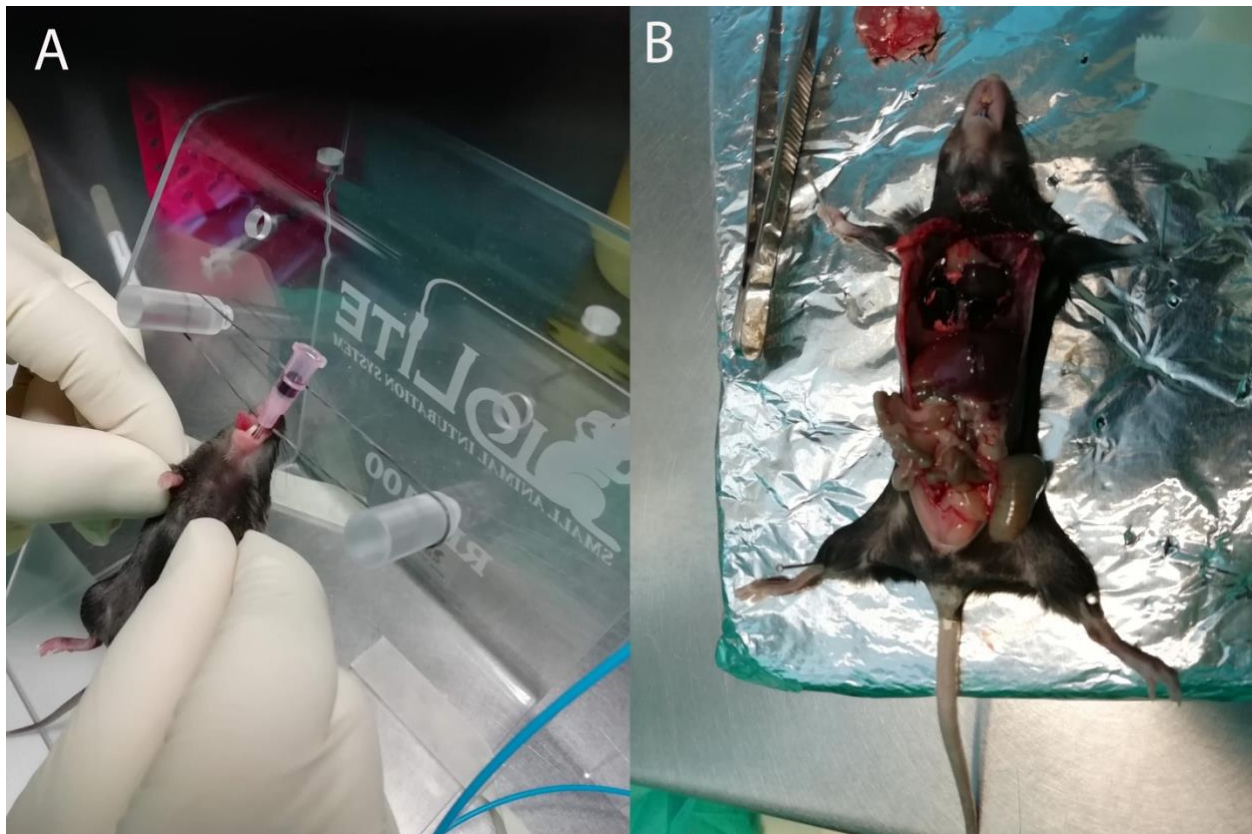


Figure 16 Intratracheal administration of Evans blue solution. A. The mice position during intubation mediated intratracheal administration. B. Intratracheal administration by optic fiber (intubation mediated intratracheal administration) showed that inoculum directed into lungs without affecting other organs.

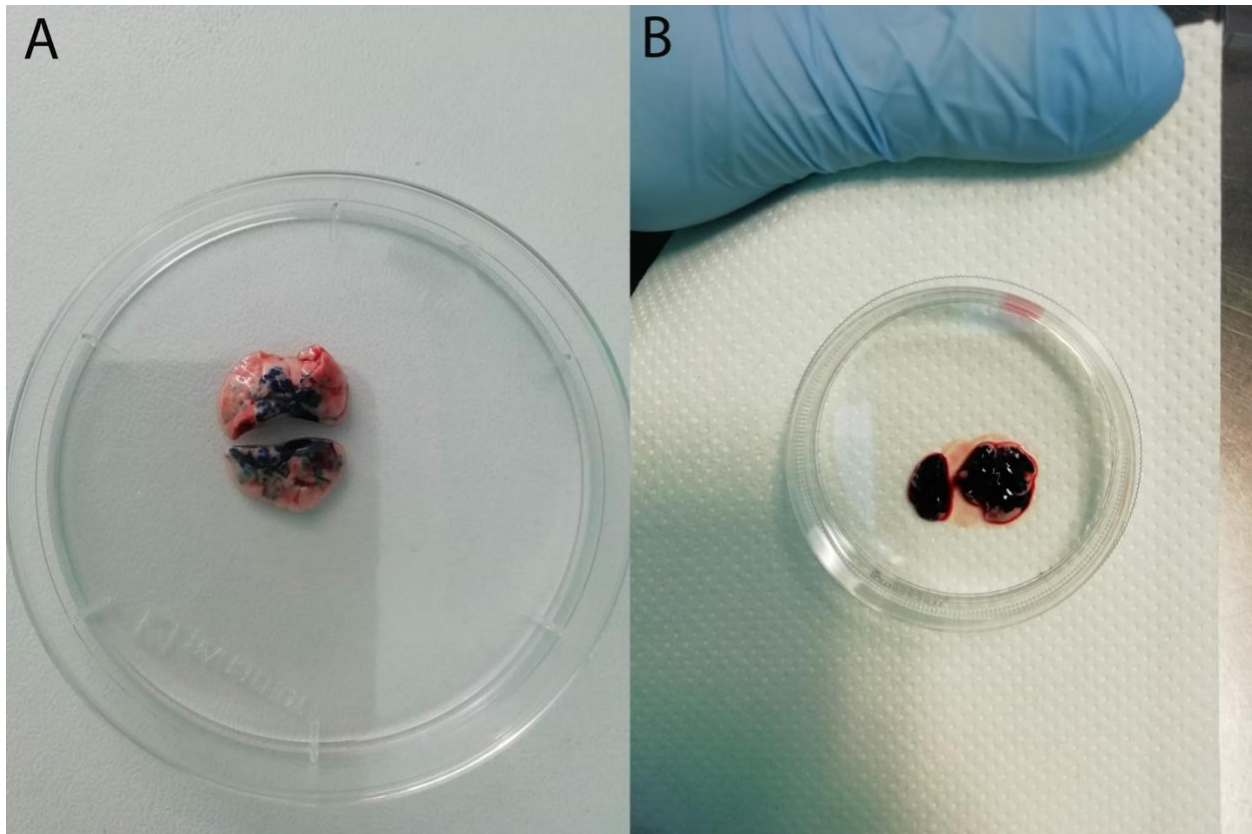


Figure 17 Evans Blue instillation was performed in two volume, A. 25 $\mu$ l and B. 75 $\mu$ l. This staining showed high volume of inoculum can fill lung and affect the results, however very low volume showed disparate distribution.

### **Time course of pneumonia induced by different doses of bacteria shows a higher pneumococcal load at 48 hours after infection**

The bacterial load in different organs such as lung, liver, spleen and blood were calculated by multilayer plating techniques previously described (Iannelli & Pozzi, 2004). As shown in Figure 18, there is a comparable and significant difference in terms of bacterial counts detected after 48 hours post infection in different organs. The injected dose of  $10^7$  bacterial solution showed higher bacterial count in different organs, however, bacterial count changes between  $10^6$  and  $10^7$  doses of bacterial inoculum were not significant. Although bacterial count in blood of animals infected with  $10^7$  CFU/ml of *S.pneumoniae* were slightly positive after one week of infection, bacterial count in blood of animals infected with  $10^5$  and  $10^6$  CFU/ml of inoculum showed complete clearance at this time point.

With  $10^8$  CFU/ml bacterial injection, all mice died within 24 hours post infection and bacterial colony counts were calculated and shown in Figure 19.

The organs weight versus body weight showed slightly bigger lung and liver in  $10^8$  CFU/ml bacterial infected group followed by  $10^7$  CFU/ml bacterial infected, however the results were not significant (data not shown).

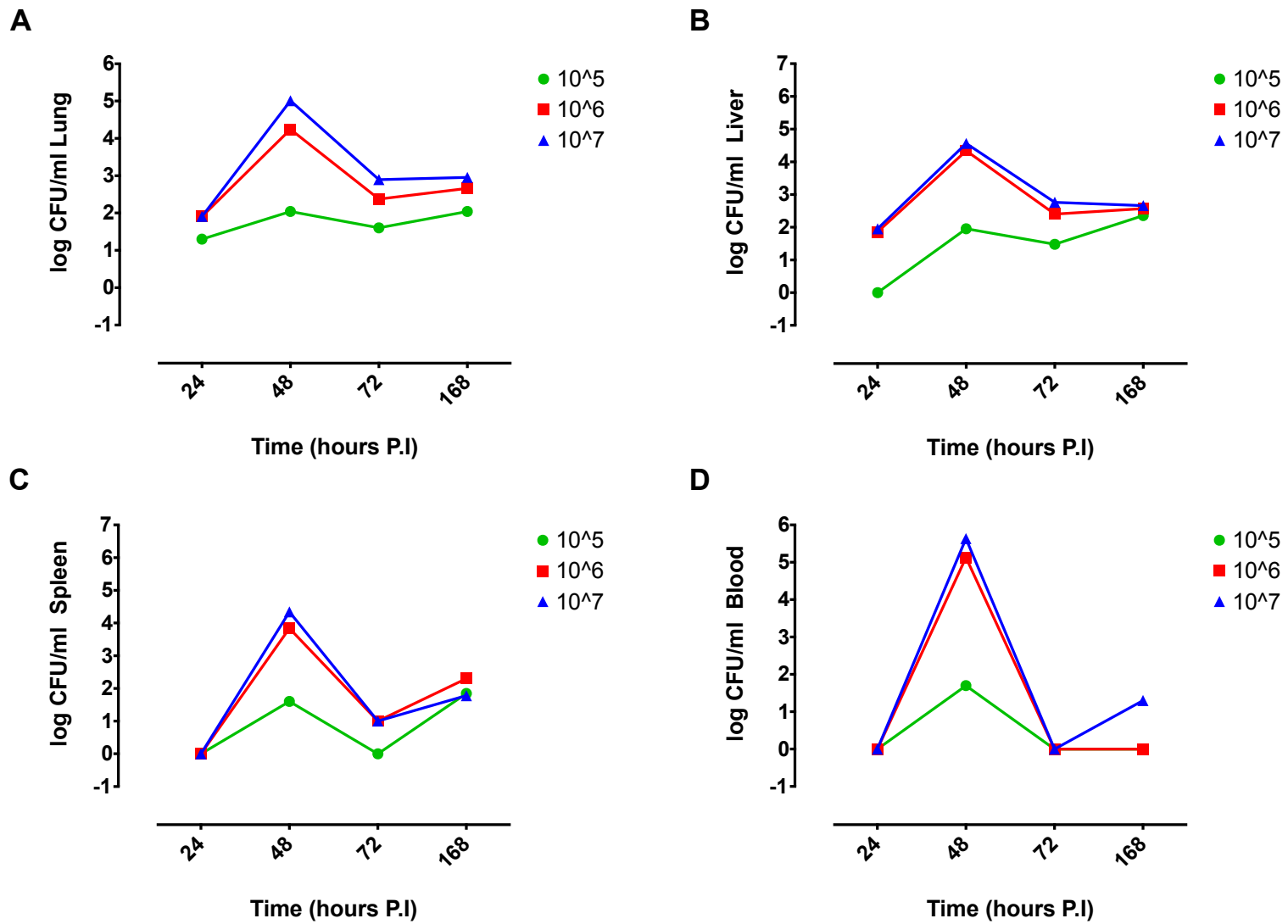


Figure 18 Bacterial colony count in A.Lung, B.Liver, C.Spleen and D.Blood of mice infected with different doses of pneumococcus at 24, 48, 72 and 168 hours after infection

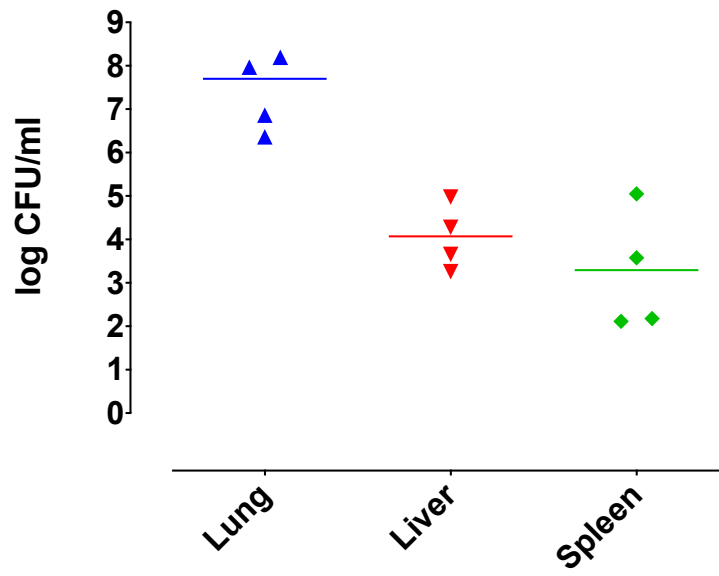


Figure 19 CFU/ml bacterial count in different organs of animals infected by  $10^8$  CFU/ml of bacterial inoculum. All animals in this group died within 24 hours post infection.

**Clinical monitoring of infected mice showed a body weight loss from 24 to 48 hours post infection in all groups**

As far as clinical scores and monitoring concerned, all mice infected with different dose of bacteria by intratracheal methos lost significant body weight at 48 hours, however the body weight loss compensated after one week post infection. There were no significant changes between different groups infected with different bacterial doses Figure 20-A panel. On the other hand, temperature changes also showed significant reduction at 24 and 48 hours post infection in animals infected with  $10^6$  and  $10^7$  CFU/ml of bacteria, however this temperature lost was not corrected after one week post infection. Interestingly no body temperature changes were seen in mice infected with  $10^5$  CFU/ml bacterial solution Figure 20-B panel.

The average clinical scores of animals in different groups are summarized in Table 9. The incresed clinical score with moderate piloerection, slightly reduced motor activity and tachypnea were detected after 72 hours of infection in mice infected with  $10^6$  and  $10^7$  CFU/ml dose of bacteria.

*Table 9 Cilinal score in different groups ranges from 0: Healthy to 5: Death.*

<b>Infection bacterial dose (CFU/ml)</b>	<b>Time course</b>			
	24 hours (p.i)	48 hours (p.i)	72 hours (p.i)	1 week (p.i)
<b><math>10^5</math></b>	0	0	0	0
<b><math>10^6</math></b>	0	1	2	1
<b><math>10^7</math></b>	0	2	3	1
<b><math>10^8</math></b>	5	5	-	-

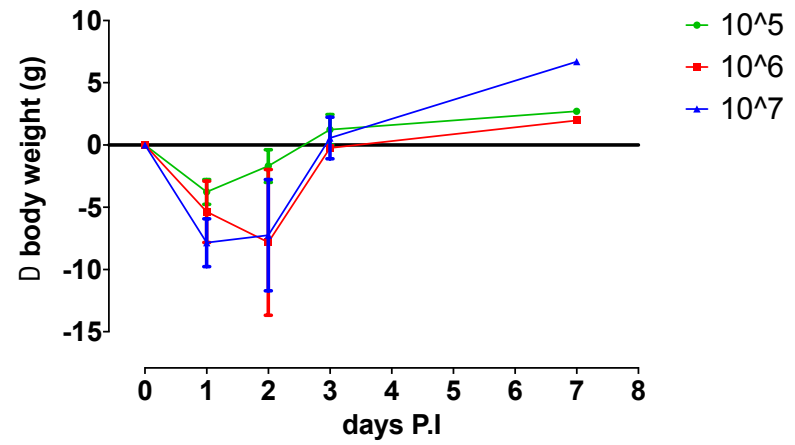
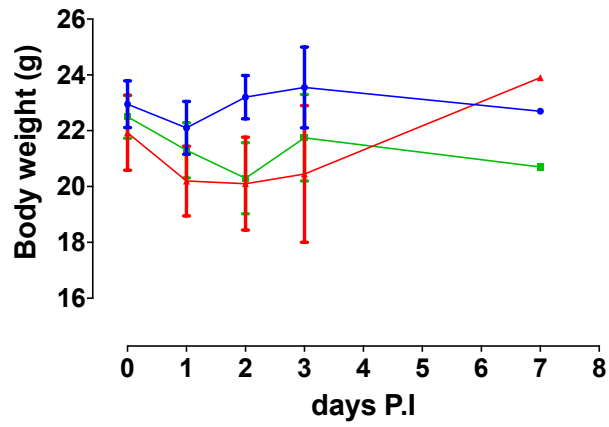
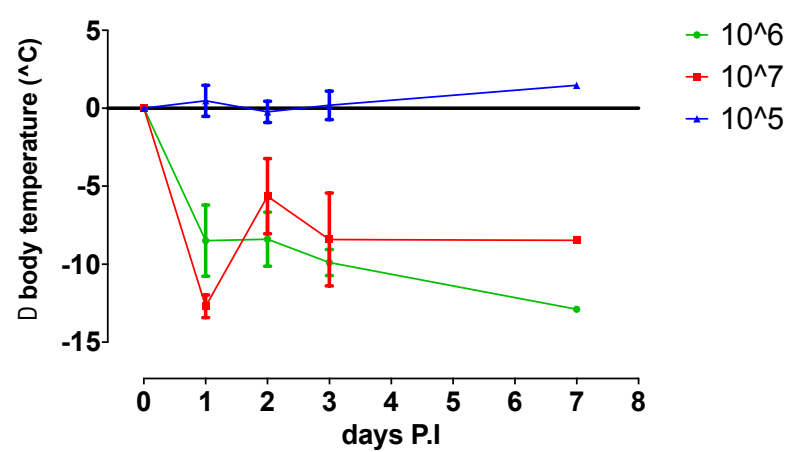
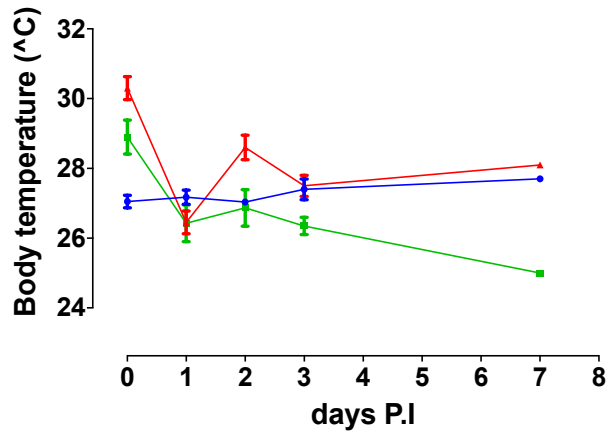
**A****B**

Figure 20 Clinical features assessment. A. Body weight of different groups on the left and delta weight loss on the right. B. body temperature measurement of different groups on the left and delta temperature lost on the right.

## **Histological examination of infected mice lungs at different time point with $10^6$ CFU/ml intratracheal injection revealed different leukocyte infiltration and lung injury**

Histological analysis of lung tissue sections was performed to investigate the histopathology of the infected lung in our mice models. Lungs were removed from the chest avoiding as much as possible mechanical damages and processed as previously described. H&E staining was performed, and sections were studied to detect alterations of the lung parenchyma and leukocyte infiltration. We observed a focal bronchopneumonia with very modest alterations at the alveoli and parenchyma structure with swollen blood vessels starting after 24 hours of infection. These features got worst after 48 and 72 hours of infection. The major alteration was a conspicuous infiltration of cells principally localized in the perivascular and peribranchial areas after 48 hours of infection followed by 72 hours of infection. Figure 10-F, a 40x image showed this infiltration after 48 hours post infection.

This infiltrate was also seen after 1 week post infection in lesser content. Controls sections at all time points showed no infiltration and a normal tissue conformation was observed (Figure 10).



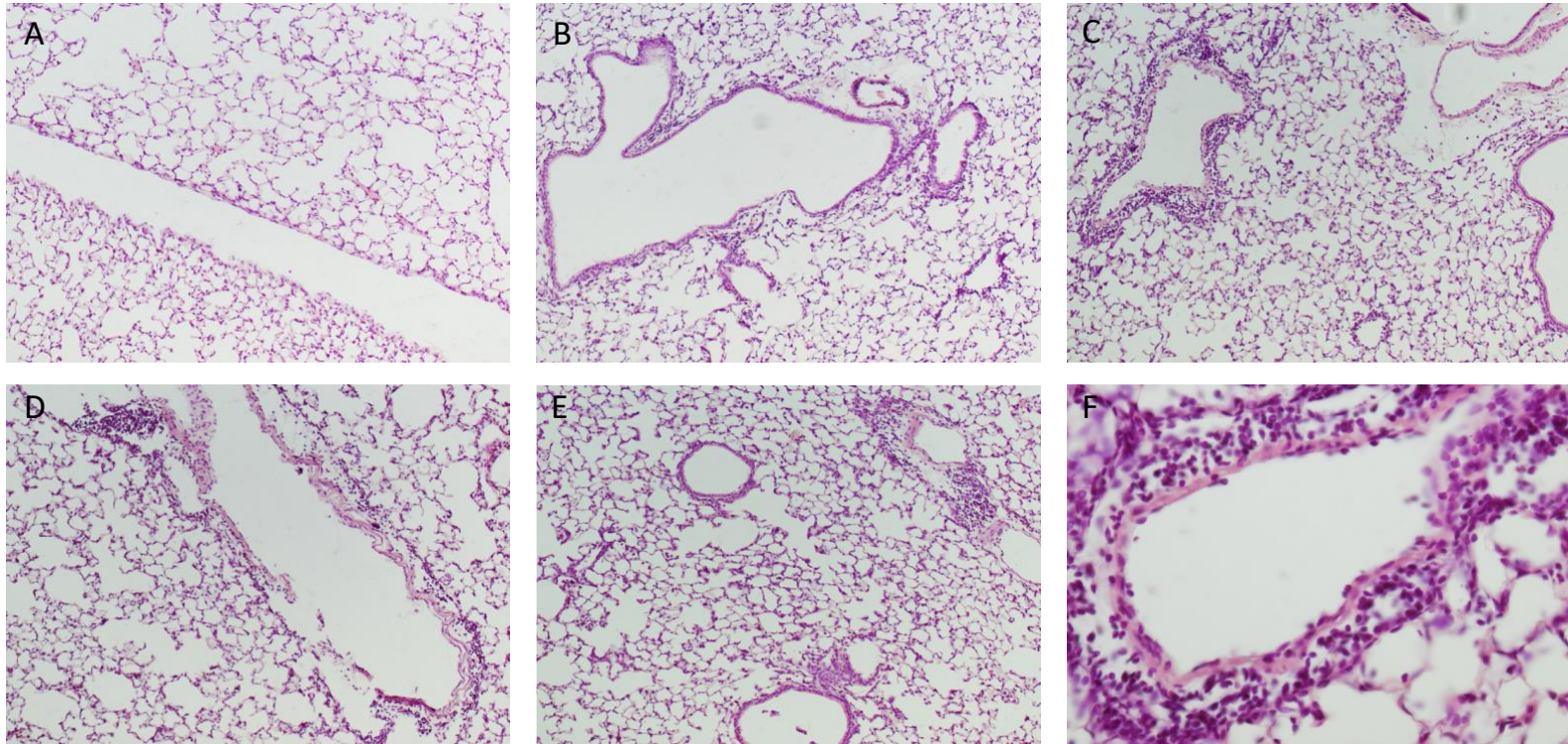


Figure 10 Histopathologic staining of pneumonic murine lungs. Mice were challenged intranasally with  $10^6$  CFUs of *S.pneumoniae* strain TIGR4. Lung sections were fixed in formalin buffer and embedded in paraffin. Sections were stained with hematoxylin and eosin (H&E). 10x images are shown in A. Control mice, B. 24 hours, C. 48 hours, D. 72 hours and E. 1 week post-infection. F. displays 40x image of 48 hours post-infection lungs.

## Discussion

Pneumonia is a leading cause of invasive diseases worldwide and is responsible for the deaths of 1 in 4 children. The most frequent bacterial cause of pneumonia stems from *Streptococcus pneumoniae*. Early invasion of the bacterium into the lungs is often subclinical and is rapidly controlled. During the bacterial invasion, macrophages are among the first host responders in driving an appropriate immune response in the airspace of the lungs. The host-pathogen interactions determine the intensity of disease and pathogenic proteins can cause differential rewiring of the host environment. Different pneumococcal proteins can drive unique host responses and enhanced understanding of how pneumococcus regulates this process may provide insight into new potential antimicrobial targets. Currently, the majority of therapeutic targets focus on the polysaccharide wall and proteins in the cell wall. An understanding disease mechanism as well as host responses will be valuable in different fields of treatments and preventions such as new antibiotics discovery and vaccines efficacy. To achieve this, development of an animal model which can mimic human interactions with bacteria should be crucial. As part of my project, we studied mice models of pneumonia disease caused by *Streptococcus pneumoniae* with different administration routes of infection. Intranasal models showed promising results in our lab and many studies based on this model were conducted. In the previous chapter this model was discussed in detail.

Bacterial counts in lung homogenates were highly dispersed among animals at different time-points after infection; moreover, when mice were infected with different pneumococcal doses, pneumococcal colonies in the lungs were found in mice with doses of  $10^6$  and  $10^7$  CFU/ml bacteria. However, after 1 week post-infection, lung colony count was reduced significantly. The results showed that bacterial colonization in different organs starts 24 hours post-infection and it reached the peak at 48 hours. The reduction of bacterial colony count in different organs after 72 hours to 1-week post-infection suggested the healing process started, however more analysis should be done to have a better understanding. The clinical score of mice health recovered after 1 week and body weight and temperature returned to normal condition. When evaluating the histological damage of lung sections, we found that the most severe infiltration was present at 48 up to 72 hours post-infection, but infiltration was still observable 1 week after infection. This

observation suggests that the infiltrate in the lung tissue persists even beyond the clinical healing phase. Our data also showed infection with  $10^8$  CFU/ml of pneumococcal TIGR4 strain through intratracheal route is lethal for C57Bl/6 mice, all mice died within 24 hours of infection.

Non-invasive intratracheal (Oro-tracheal/peroral) mice models of pneumonia were developed, and results were considering, however it was a pilot study and more investigation should be done. Based on these data intranasal model can be replaced with this new model. The route of infection through oral-tracheal can mimic human disease better with utilizing less concentration of bacteria to induce the infection in mice. However, this method is easy and invasive, still requires more experience. Furthermore host-pathogen interaction, immune responses and vaccine efficacies should be studied by means of this model and should be compared with other pneumonia mice models.

## Bibliography

- Borsa, N., Di Pasquale, M., & Restrepo, M. I. (2019). Animal Models of Pneumococcal pneumonia. *International Journal of Molecular Sciences*, 20(17). <https://doi.org/10.3390/IJMS20174220>
- Canvin, J. R., Marvin, A. P., Sivakumaran, M., Paton, J. C., Boulnois, G. J., Andrew, P. W., & Mitchell, T. J. (1995). The role of pneumolysin and autolysin in the pathology of pneumonia and septicemia in mice infected with a type 2 pneumococcus. *The Journal of Infectious Diseases*, 172(1), 119–123. <https://doi.org/10.1093/INFDIS/172.1.119>
- Chiavolini, D., Pozzi, G., & Ricci, S. (2008). Animal models of Streptococcus pneumoniae disease. *Clinical Microbiology Reviews*, 21(4), 666–685. <https://doi.org/10.1128/CMR.00012-08>
- Feldman, C., & Anderson, R. (2016). Epidemiology, virulence factors and management of the pneumococcus [version 1; referees: 2 approved]. *F1000Research*, 5. <https://doi.org/10.12688/F1000RESEARCH.9283.1/DOI>
- Griffin, J. F. T. (2002). A strategic approach to vaccine development: Animal models, monitoring vaccine efficacy, formulation and delivery. *Advanced Drug Delivery Reviews*, 54(6), 851–861. [https://doi.org/10.1016/S0169-409X\(02\)00072-8](https://doi.org/10.1016/S0169-409X(02)00072-8)
- Henriques-Normark, B., & Tuomanen, E. I. (n.d.). *The Pneumococcus: Epidemiology, Microbiology, and Pathogenesis*. <https://doi.org/10.1101/cshperspect.a010215>
- Iannelli, F., & Pozzi, G. (2004). Method for introducing specific and unmarked mutations into the chromosome of Streptococcus pneumoniae. *Mol Biotechnol*, 26(1), 81–86. <https://doi.org/10.1385/MB:26:1:81>
- Kadioglu, A., & Andrew, P. W. (2005). Susceptibility and resistance to pneumococcal disease in mice. *Briefings in Functional Genomics & Proteomics*, 4(3), 241–247. <https://doi.org/10.1093/BFGP/4.3.241>
- Lee, C. J., Lee, L. H., & Frasch, C. E. (2003). Protective immunity of pneumococcal glycoconjugates. *Critical Reviews in Microbiology*, 29(4), 333–349. <https://doi.org/10.1080/713608018>
- Moffitt, K. L., & Malley, R. (2011). Next generation pneumococcal vaccines. *Current Opinion in Immunology*, 23(3), 407–413. <https://doi.org/10.1016/J.COI.2011.04.002>
- Moffitt, K., & Malley, R. (2016). Rationale and prospects for novel pneumococcal vaccines. *Human*

*Vaccines & Immunotherapeutics*, 12(2), 383–392.

<https://doi.org/10.1080/21645515.2015.1087625>

O'Brien, K. L., Wolfson, L. J., Watt, J. P., Henkle, E., Deloria-Knoll, M., McCall, N., Lee, E., Mulholland, K., Levine, O. S., & Cherian, T. (2009). Burden of disease caused by *Streptococcus pneumoniae* in children younger than 5 years: global estimates. *The Lancet*, 374(9693), 893–902. [https://doi.org/10.1016/S0140-6736\(09\)61204-6](https://doi.org/10.1016/S0140-6736(09)61204-6)

Parker, D., Ahn, D., Cohen, T., & Prince, A. (2016). Innate Immune Signaling Activated by MDR Bacteria in the Airway. *Physiological Reviews*, 96(1), 19.

<https://doi.org/10.1152/PHYSREV.00009.2015>

Rayamajhi, M., Redente, E. F., Condon, T. V., Gonzalez-Juarrero, M., Riches, D. W. H., & Lenz, L. L. (2011). Non-surgical intratracheal instillation of mice with analysis of lungs and lung draining lymph nodes by flow cytometry. *Journal of Visualized Experiments : JoVE*, 51.

<https://doi.org/10.3791/2702>

*The top 10 causes of death*. (n.d.). Retrieved November 2, 2022, from <https://www.who.int/news-room/fact-sheets/detail/the-top-10-causes-of-death>

Torres, A., Blasi, F., Peetermans, W. E., Viegi, G., & Welte, T. (n.d.). *The aetiology and antibiotic management of community-acquired pneumonia in adults in Europe: a literature review*.

<https://doi.org/10.1007/s10096-014-2067-1>

## CHAPTER 6. Conclusions

The importance of physicochemical assessments of bacteria as well as bacterial vectors for vaccine in vaccine design and bacterial manipulation is crucial. These assessments can be done by using simple and easy methods such as measuring isoelectric point and zeta potential. Different modifications of bacterial vectors (recombinant *S.gordonii*) showed different changes in isoelectric point and zeta potential respectively. Not only these modifications correlated with their antigenicity and immunogenicity but also can be predicted based on the modification. For instance, mutation of a positive charge protein on the surface of bacteria, changes the isoelectric points to more negative pH, which is discussed in detail in part one of this thesis. Moreover further investigation should be done to determine if isoelectric point and zeta potential could predict other bacterial behaviour such as attachment and biofilm production.

Another important field of basic science to study disease mechanisms, host-bacterial interaction, antibacterial discoveries and vaccines development is animal study. For pneumococcal pneumonia developing an animal model which can mimic this human disease is fundamental. Pneumonia is a human lower respiratory tract disease caused mainly by *Streptococcus pneumoniae* has been a global burden with high mortality in children and elderly. The only natural host of *S.pneumoniae* is human, thus, optimizing an animal model can improve the knowledge of the disease. Between animals, mice are the best candidate as they are cheap and easy to work with. However the human respiratory tract anatomy is different from mice, by optimizing the infection, mice can develop a disease like pneumonia. The bacterial strain, dose of infection and route of infection should be precisely determined. In the second part of my thesis I focused in mice models of pneumonia, using intranasal and intratracheal route. Although both models showed promising results, further investigation and comparison should be evaluated. For intranasal models we could combine transcriptomic and cytokine assays on mouse splenocytes, to describe the immune response in the days following pneumococcal infection. Cytokine levels suggested the presence of a recall immune response involving both innate and adaptive immunity. This model could study the immune responses involved in pneumococcal infection and possibly monitor vaccine and experimental therapies efficacy in future studies. For intratracheal models we tested different bacterial doses at different time points. Based on our results with intratracheal infection, less dose of bacteria is needed to mimic the pneumonia ( $10^6$ ), compared to intranasal models that usually use higher doses. The

bacterial colony count in different organs, histology of lungs as well as clinical score of infected mice showed promising results that can be utilize as a precise replacement of intranasal induction. This model is very accurately transfer the whole inoculum into the lungs, however this method requires furthur investigatiuon of immune response and also vaccine efficacies should be studied in animal models infected through this intratracheal method.

# APPENDIX. Scientific Curriculum Vitae

## • Education

- October 2019 - present: **PhD student** in the XXXV cycle of doctoral program in Medical Biotechnologies by the Medical Biotechnologies Department of the University of Siena, Italy.  
Main areas of interest: Bacterial vaccine vector, Isoelectric point, Zetapotential, Animal models, Pneumococcal Pneumonia, data analysis.
- October 2017 - July 2019: **Master's Degree** in Medical Biotechnologies (courses held in English), Department of Medical Biotechnologies, University of Siena, Italy.  
Thesis title: “Assessment of the zeta potential measurement to study isoelectric point and surface charge distribution of bacteria”. Mark: 110/110 cum laude and special mention.
- October 2013 - July 2016: **Master's Degree** in Medical Biotechnology and Nanotechnology, Qazvin University of Medical Science, Iran.  
Thesis title: “Cloning, expression, purification and structural analysis of recombinant Human and Mouse Betatrophin”. Mark: 19/20.
- October 2007 - September 2009: **Bachelor's Degree** in Medical laboratory science, Tehran University of Medical Science, Iran.  
Thesis title: “New insight in medical Biotechnology in vaccine field”. Mark: 18/20.

## • Training courses

- 2020, May. “**Metagenomics applied to surveillance of pathogens and antimicrobial resistance**” on-line course Coursera platform, organized by Technical University of Denmark – DTU, Denmark.
- 2020, June. “**Respiratory immunity and COVID**” on-line course organized by IUIS International Union of Immunological Societies, UK.
- 2019, October. “**Diversity Outbred Mice, Inbred, Outbred, Hybrid, Mutant and Transgenic Mice**” on-line course organized by The Jackson Laboratory, USA.
- 2019, October. “**Diversity Outbred Mice, Inbred, Outbred, Hybrid, Mutant and Transgenic Mice**” on-line course organized by The Jackson Laboratory, USA.
- 2019, May. “**R programming (Data science)**” on-line course Coursera platform, organized by John Hopkins University, USA.



- 2015, November. “**Measurement System Analysis (MSA)**” IMQ Academy, Tehran, Iran
- 2013, April. “**Summer school Primer designing, Advanced PCR, Real-Time PCR, Sequence Analysis, Cloning and Genetic engineering, PCR and Gel Electrophoresis**” organized by Pasteur Institute of Iran, Tehran, Iran
- 2012, July. “**Laboratory and Industry Quality Management and Documentary**” organized by Iranian Society of Pathology, Tehran, Iran
- 2011. “**Professional Management**” Tehran Institute of technology, Tehran, Iran

- **Languages**

- **Persian:** native
- **English:** very good knowledge of English language (written and spoken). 2018: B2 English qualification, Centro Linguistico Ateneo (CLA), University of Siena, Italy and IELTS score: 6.5 (Listening:6.5 Reading:6.5 Writing:5.5 Speaking:7.5) 10<sup>th</sup> December 2016

- **List of publications**

1. Immune Memory After Respiratory Infection With *Streptococcus pneumoniae* Is Revealed by in vitro Stimulation of Murine Splenocytes With Inactivated Pneumococcal Whole Cells: Evidence of Early Recall Responses by Transcriptomic Analysis. Moscardini IF, Santoro F, Carraro M, Gerlini A, Fiorino F, Germoni C, **Gholami S**, Pettini E, Medaglini D, Iannelli F, Pozzi G. Front Cell Infect Microbiol. 2022 Jun 20;12:869763. doi: 10.3389/fcimb.2022.869763. PMID: 35795182; PMCID: PMC9251119.
2. Cloning, expression, and spectral analysis of mouse betatrophin. **Gholami S.**, Goodarzvand Chegini,K., Gheibi,N., Mokhtarian,K.,Mohamadi,M. and Falak,R. Med J Islam Repub Iran Dec 2017
3. Cloning, expression, purification and CD analysis of recombinant human Betatrophin. **Gholami S.**, Gheibi N., Falak R., Goodarzvand Chegini K. Reports of Biochemistry & Molecular Biology, Vol.6, No.2, Apr 2018
4. Serodiagnosis of Fascioliasis by Fast Protein Liquid Chromatography-fractionated excretory/secretory antigens. Mokhtarian K., Akhlaghi L., Razmjou L., Meamar A.R., **Gholami S.**, Najafi Samei M., Falak R.. Parasitology Research 2016

- **Conferences**

- 2022, 1-6 November. American Society of Nephrology. Florida, USA. Circulating Endotoxin and Inflammatory Proteins Correlate With Kidney and Hospitalization Outcomes in Critically ill Patients. Sian Piret; Fabliha Fairuz; **Samaneh Gholami**; Sobia N. Khan; Sandeep K. Mallipattu. **Poster**
- 2022, 1-6 November. American Society of Nephrology. Florida, USA. Tubule-Specific Overexpression of Krüppel-Like Factor 6 (KLF6) Is Detrimental After Nephrotoxic Kidney Injury. Sian Piret; Merin Davis; **Samaneh Gholami**; Nehaben A. Gujarati; Bismark Owusu Frimpong; Sandeep K. Mallipattu. **Poster**
- 2015, 20-22 May. 2nd International and 9th National Congress of Parasitology and Parasitic Diseases, Iran. Application of Fasciola hepatica fractionated proteins for serodiagnosis. Mokhtarian K., Akhlaghi L., Falak R., Razmjou E., Meamar A.R., **Gholami S.**, Najafi M. **Poster**
- 2015, 12-14 February. 7th International congress of laboratory and clinic (Infectious disease) and 1st conference of clinical virology, Iran. Comparative immunoblotting assessment of fractionated and crude extract of Fasciola hepatica. Mokhtarian K., Akhlaghi L., Falak R., Razmjou E., Meamar A.R., **Gholami S.**, Najafi M. **Poster**
- 2014, 29<sup>th</sup> April - 2<sup>nd</sup> May. 12th International congress of Immunology and Allergy (ICIA), Tehran, Iran. Assessment of Latent Tuberculosis and Allergy in Patients with Chronic Lower Respiratory Tract Symptoms. **Gholami S.**, Falak R., Mansourzadeh A. **Poster**
- 2013, 12-14 February. 6th International congress of laboratory and clinic, Tehran, Iran. Application of interferon gamma release assay (IGRA) in screening of latent Tuberculosis in the elderly suffering from chronic lower respiratory tract symptoms. **Gholami S.**, Falak R., Mokhtarian K. **Poster**

- **Nucleotide sequences deposited in GenBank:**

- Mouse Betatrophin 549 bp mRNA linear (ROD 04-JUN-2016) was submitted to NCBI database (Gene Bank) under the accession number of KX357380. **Gholami,S.**

Goodarzvand Chegini,K., Gheibi,N., Mokhtarian,K., Mohamadi,M. and Falak,R.  
Cloning, expression and purification of mouse Betatrophin

- **Lecturer in Work Shops:**

- Evaluation of serum specific IgE, 12-14 February 2014, 6Th International Congress of Laboratory & Clinic, Immunology department, IUMS, Tehran, Iran
- Betting on Betatrophin, a new hormone that control beta cell proliferation, Qazvin University of medical Science and Iran university of medical science
- Protein Refolding using smart copolymer, Qazvin University of medical Science